FINAL PROJECT REPORT #00047947

GRANT: DTRT13-G-UTC45
Project Period: 8/1/2014 – 6/30/17

Ultra-high Performance Fiber-Reinforced Concrete (UHPFRC) for Infrastructure Rehabilitation

Volume 1:

Evaluation of Ultra High Strength Concrete (UHSC) in Joints of Bridge Girders

Participating Consortium Member:
Missouri S&T

Authors:
Dr. John J. Myers, Ph.D., P.E., (PI)
Dept. of Civil, Arch. & Environ. Engineering
Missouri S&T
Saipavan Rallabhandi
M.S. Student
Dept. of Civil, Arch. & Environ. Engineering
Missouri S&T

RE-CAST:
REsearch on Concrete Applications for Sustainable Transportation
Tier 1 University Transportation Center

DISCLAIMER

The contents of this report reflect the views of the authors, who are responsible for the facts and the accuracy of the information presented herein. This document is disseminated under the sponsorship of the U.S. Department of Transportation's University Transportation Centers Program, in the interest of information exchange. The U.S. Government assumes no liability for the contents or use thereof.

TECHNICAL REPORT DOCUMENTATION PAGE

1. Report No. RECAST UTC #00047947	**2. Government Accession No.**	**3. Recipient's Catalog No.**
4. Title and Subtitle Ultra-high Performance Fiber-Reinforced Concrete (UHPFRC) for Infrastructure Rehabilitation Volume 1: Evaluation of Ultra High Strength Concrete (UHSC) in Joints of Bridge Girders		**5. Report Date** March 2017 **6. Performing Organization Code:**
7. Author(s) J.J. Myers and S. Rallabhandhi		**8. Performing Organization Report No.** Project #00047947
9. Performing Organization Name and Address RE-CAST – Missouri S&T 500 West 16th Street, 223 Engineering Research Lab Rolla, MO 65409-0710		**10. Work Unit No.** **11. Contract or Grant No.** USDOT: DTRT13-G-UTC45
12. Sponsoring Agency Name and Address Office of the Assistant Secretary for Research and Technology U.S. Department of Transportation 1200 New Jersey Avenue, SE Washington, DC 20590		**13. Type of Report and Period Covered:** Final Report Period: 8/1/2014 – 6/30/17 **14. Sponsoring Agency Code:**
15. Supplementary Notes The investigation was conducted in cooperation with the U. S. Department of Transportation.		

16. Abstract

Joints are often considered as the weak link in a structure and often deterioration of the structure initiates from the joints. Joints transfer the stresses from super-structure to sub-structure and in this process are subjected to large transfer stresses. Not much attention is given to the design of joints as they are positioned in low moment regions and typically a 4 to 6 ksi (28 to 41 MPa) concrete is used to fill the joints. One of the solution to this problem is Ultra-High Strength Concrete (UHSC). In the recent past significant research has been done to use UHSC in deck-level connections and successful results were obtained. UHSC is a relatively new concrete material which not only has high compressive (18 ksi/124 MPa) and tensile strengths (5 ksi/35 MPa) with a very high chemical resistance, and durability. Use of steel fibers in UHSC helps increasing the service life. UHSC was successfully used by New York State and Iowa State Department of Transportations (DoT) in many bridges as various components, and proved to help with Accelerated Bridge Construction (ABC) which makes its use economical and time saving.

This research focused on using UHSC as joint filler material along with High strength self-consolidating concrete (HS-SCC) while studying the effects of using different continuity details and effects of surface preparation of beam in a reinforced concrete section subjected to high-moment loading using 22 test specimens. An investigation of non-prestressed Missouri Department of Transportation (MoDoT) end girder detail using UHSC in the joint was also conducted. UHSC when used in the joints can be a viable solution making joints the stronger link holding the structure together.

17. Key Words Ultra-high strength concrete, joint, bridge girder, infrastructure rehabilitation	**18. Distribution Statement** No restrictions. This document is available to the public.	
19. Security Classification (of this report) Unclassified	**20. Security Classification (of this page)** Unclassified	**21. No of Pages** 160

Form DOT F 1700.7 (8-72) Reproduction of form and completed page is authorized.

Report for

RE-CAST-Research on Concrete Applications for Sustainable Transportation
Tier 1 University Transportation Center (**UTC**)

Grant: DTRT13-G-UTC45

Project 3-B. Ultra-High Performance Fiber Reinforced Concrete for Infrastructure Rehabilitation

Evaluation of Ultra High Strength Concrete (UHSC) in Joints of Bridge Girders

by

Dr. John J. Myers, Ph.D., P.E., (PI)
Saipavan Rallabhandhi

Missouri University of Science and Technology
Department of Civil, Architectural & Environmental Engineering
March 2017

EXECUTIVE SUMMARY

Joints are often considered as the weak link in a structure and often deterioration of the structure initiates from the joints. Joints transfer the stresses from super-structure to sub-structure and in this process are subjected to large transfer stresses. Not much attention is given to the design of joints as they are positioned in low moment regions and typically a 4 to 6 ksi (28 to 41 MPa) concrete is used to fill the joints. One of the solution to this problem is Ultra-High Strength Concrete (UHSC). In the recent past significant research has been done to use UHSC in deck-level connections and successful results were obtained. UHSC is a relatively new concrete material which not only has high compressive (18 ksi/124 MPa) and tensile strengths (5 ksi/35 MPa) with a very high chemical resistance, and durability. Use of steel fibers in UHSC helps increasing the service life. UHSC was successfully used by New York State and Iowa State Department of Transportations (DoT) in many bridges as various components, and proved to help with Accelerated Bridge Construction (ABC) which makes its use economical and time saving.

This research focused on using UHSC as joint filler material along with High strength self-consolidating concrete (HS-SCC) while studying the effects of using different continuity details and effects of surface preparation of beam in a reinforced concrete section subjected to high-moment loading using 22 test specimens. An investigation of non-prestressed Missouri Department of Transportation (MoDoT) end girder detail using UHSC in the joint was also conducted. UHSC when used in the joints can be a viable solution making joints the stronger link holding the structure together.

TABLE OF CONTENTS

LIST OF ILLUSTRATIONS

Page

LIST OF TABLES

Page

1. INTRODUCTION

1.1. INTRODUCTION

Joints are one of the most critical components of bridge elements and are often considered the weakest link in structures. In continuous span structure, joints are often designed where they is less moment or near the inflection points (zero moment). Failure of any structure begins with the failure of connections since they are not designed to withstand the substantial amount of loads to which a structure is subjected to throughout its service life. Joints are responsible for transferring loads from different components of super structure to sub-structure which keeps the chain of load-transfer intact. However not much importance is given to design of these elements which bear such an important role. In pre-cast prestressed bridges, joints are filled with High-strength Self-Consolidating Concrete (HS-SCC) usually 6 to 10 ksi (41 to 69 MPa), while in reinforced cast-in-place (CIP) bridges, joints are often cast with conventional concrete (CC) which are not designed to be very strong (3 to 5 ksi /21 to 35 MPa) or durable.

Ultra-High Strength Concrete (UHSC) is relatively a new material which has been eye of many researchers in the recent past. UHSC might just be the solution to look for in case of joints. UHSC is characterized by high strength, durability, and ductility which are key characteristics for a material required in the joints. Absence of coarser aggregates and SCC like flow-ability makes UHSC an ideal material to be used in connections which makes it easier to pump, avoid segregation and its self-leveling property is helps fill the tight spaces in the joints which often have a closely-knit reinforcement layout. UHSC has been used in bridge elements like girders, decks, columns, and piles, etc., and also in deck level connections (deck-level) in USA, Europe and Japan. This study focused on implementing UHSC in joints subjected to high-moment loading in a bridge structure by using small-scale bridge elements.

The main objective of this research was to use UHSC in joints with different continuity details and evaluate its performance when subjected to a high moment load. The research project was conducted in two phases. The first phase focused on performing a comparative study of UHSC with HS-SCC while using different continuity details in the joints with different surface preparations on the beam-joint interface. The second

phase focused on using UHSC with Missouri Department of Transportation (MoDOT)'s end girder detail with a composite deck-girder system to evaluate the use of UHSC in field-cast operations for MoDOT.

1.2. RESEARCH OBJECTIVES

The main objective of this research was to study the effect of using UHSC in place of HS-SCC or CC in joints. The research consisted of two phases. The first phase focused on using UHSC and HS-SCC with different continuity details in the joint while studying the effectiveness of surface preparation of the beam-joint interface surface where joint was to be casted. The second phase focused more on using a typical MoDOT end girder detail with UHSC in non-prestressed reinforced concrete (RC) section.

1.2.1. Phase One. The first phase of research focused on comparative study of UHSC and HS-SCC with different continuity details in high moment region.
The main objectives are

- To study flexural behavior of two beams connected with 6-in. joint when subjected to high moment in the joint region.
- To evaluate use of different joint fillers. The joint fillers used were
    - UHSC
    - HS-SCC
- To study effect of different continuity details. The joint details used were
    - Straight lap detail: Straight rebars lapped for 6-in. (152 mm) in the connection.
    - Hairpin detail: rebars bent like Hairpin lapped for 3.9-in. (100 mm) in the connection
    - Anchored detail: Anchored rebars lapped for 3.5-in. (89 mm) in the connection.
- To study effect of different surface preparations. The surface preparations used were
    - Smooth/No surface preparation
    - Roughening
    - Sand blasting

1.2.2. Phase Two. The second phase of research focused on using UHSC in non-prestressed MoDOT end girder detail in RC beams. MoDOT has a reinforcing detail it uses in its field projects. UHSC is not yet used by MoDOT in field in structural elements or in connections. The specimen consisted of two beams connected with a 6-in. joint and a deck casted on top, similar to a CIP-deck casted on precast bridge elements erected at the job site.

The main objectives are

- To evaluate use of UHSC in non-prestressed MoDOT end girder detail with CIP deck.
- To evaluate use of UHSC in deck casted along with joint in place of MoDOT B mix which is typically used.

1.3. REPORT ORGANIZATION

This report is organized into seven sections. The first two sections give an introduction to the background and main objectives of the research. The third section discusses the scope of the work that was done, and specimen design process for Phases one & two. The fourth section describes the mix design process and properties of the materials used for this research. The fifth section discusses the experimental program, specimen fabrication, and testing methods, while the sixth and seventh sections give the results and conclusions of the tests performed in Phases one & two, followed by appendices. Each section is laid out by topics in the same order.

2. BACKGROUND

This chapter discusses background information relevant to this study. Joints in bridges are discussed first. Ultra-high performance concrete, its typical advantages over regular concrete are discussed. Previous work done on deck-level UHSC connections is discussed in section 2.3. Typical MoDOT end girder detail is discussed in section 2.4.

2.1. JOINTS IN BRIDGES

Joints in bridges are often considered weak link in a structure as they are subjected to constant flexing from loading, high thermal stresses, freeze/thaw along with corrosion of the rebar itself. Designers are faced with critical decisions as where to place the joint in a continuous structure. Use of precast segments which are cast off site in controlled environment enable proper batching, curing, releasing from forms and careful handling which cannot be done in case of joints. Most of the new or rehabilitation work is done on a tight schedule mostly over the weekend. In these scenarios joints are only cured for small durations and formwork demolded very quickly to enable use of the bridge. In a continuous span, the moment is not constant throughout the length of the spans as moving loads create positive and negative moments. However, considering an ideal uniformly distributed load for long span or segmented construction, designers would place the location of joints such that they are at low or zero moment regions (i.e., inflection points). This is demonstrated in Figure 2.1

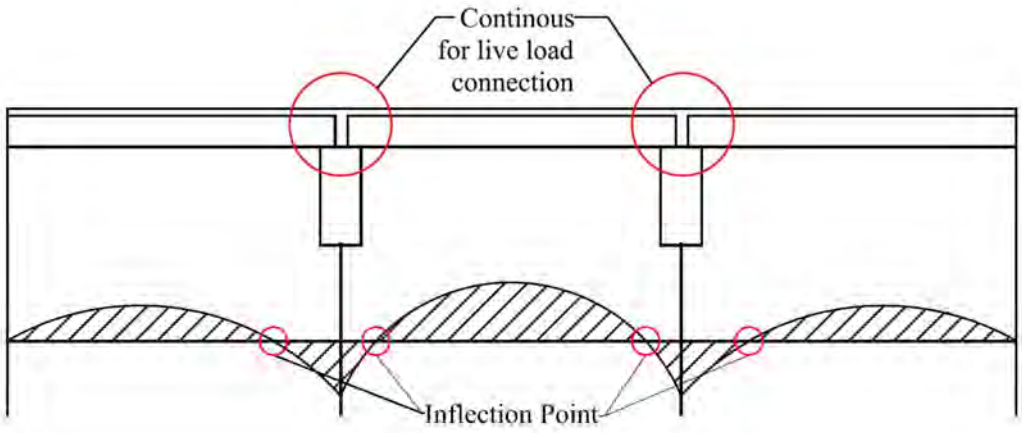

Figure 2.1 Continuous span moment distribution

Joints are designed to be in low moment or negative moment regions. The specimens in Phase one of the research were subjected to a high moment load to study the performance of joints with UHPC in a possible worst case scenario. Phase two specimens were tested to create a negative moment in the connection as the end girder detail used for intermediate bents is typically in negative moment region in a continuous span.

2.2. ULTRA-HIGH PERFORMANCE CONCRETE

ACI 239-UHPC defines UHPC as “concrete that has a minimum specified compressive strength of 150 MPa (22,000 psi) with specified durability, tensile ductility and toughness requirements, fibers are generally included to achieve specified requirements”. UHPC is an advanced cementious material with superior compressive strength, durability, and high tensile strength resulting from internal steel fiber reinforcement. UHPC is characterized by low water to cementious material ratio, high cement content. It has excellent bond development length, freeze and thaw resistance, low porosity and SCC like flow ability. The main aspect of this research was to use UHPC in joint applications. The FHWA publication HRT-11-023, Graybeal (2010) “Behavior of Field-Cast Ultra-High Performance Concrete Bridge Deck Connections under Cyclic and Static Structural Loading” lists the mix design given in Table 2.1 as typical UHPC composition.

Table 2.1 Typical UHPC composition

Material	Amount kg/m^3 (lb./yd^3)
Portland cement	712 (1200)
Fine sand	1020 (1720)
Silica fume	231 (389)
Ground quartz	211 (355)
Superplasticizer	30 (51)
Steel fibers	156 (263)
Water	130 (218)

Conversion 1 kg/m^3 = 1.686 lb./yd^3

The availability of local produced UHPC mixes (non-proprietary) is very limited in the USA. The most widely proprietary and available UHPC concrete is Ductal® by

Lafarge North America, which provides a pre-bagged mix with cementious material, fibers and chemicals required to mix. This has been the most widely used UHPC concrete for research studies at university laboratories and also in several field bridge projects. Table 2.2 list the mechanical properties of JS1000, Ductal® UHPC mix as given on the product data sheet.

Table 2.2 Ductal® JS1000 typical properties

Properties	Design values
Compression	100 MPa (14,500 psi)
Flexural	-
Direct tension	5 MPa (725 psi)
Young's Modulus	44 MPa (6,500 ksi)
Density	2.4 - 2.6 S.G.
Capillary porosity (>10mm)	< 1%
Total porosity	2 - 6 %
Creep coefficient	0.2 - 0.5
Carbonation penetration depth	< 0.5 mm (0.019 in)
Freeze/thaw (after 300 cycles)	100 %
Salt-scaling	< 0.1 g/m^2 (0.00002 lb./ft^2)

Conversion 1 MPa = 145 psi, 1 mm. = 0.04 in., 1 g/m^2 =0.0002 lb./ft^2

Curing of UHPC plays a major role in achieving the required properties. Lafarge recommends to steam cure Ductal at 194° F (90° C) for 48 hours before demolding. Graybeal (2013) researched four ways to cure UHPC to achieve the required material properties. They involved steam curing at 194 °F (90 °C) or 140 °F (60 °C) for 48 hours, starting about 24 hours after casting; steam curing at 194 °F (90 °C), starting after 15 days of standard curing; and curing at laboratory temperatures. It was reported that steam cured specimens reached full compressive strength at 4 days. The research done was aimed to recreate field conditions and curing was done using ambient laboratory environment. The specimens were covered with wet-burlap and cured for 7 days.

High binder content and low water to cement (w/cm) ratio make UHPC mixing longer than Conventional concrete (CC) mixing process making UHPC mixing at batching plants not a viable plan. UHPC mix time ranges between 15-20 minutes. It can be mixed in drum mixer or shear mixers. Graybeal (2013) summarized the importance of

mixer selection used for UHPC as follows, “Nearly any conventional concrete mixer will mix UHPC. However, it must be recognized that UHPC requires increased energy input compared to conventional concrete, so mixing time will be increased. This increased energy input, in combination with the reduced or eliminated coarse aggregate and low water content, necessitates the use of modified procedures to ensure that the UHPC does not overheat during mixing. This concern can be addressed through the use of a high-energy mixer or by lowering the temperatures of the constituents and partially or fully replacing the mix water with ice. These procedures have allowed UHPC to be mixed in conventional pan and drum mixers, including ready-mix trucks”. High shear pan mixer at Missouri S&T was used in this research project.

Many projects in the USA and Canada have implemented using UHPC in field-cast operations. Often small batches of UHPC are made near the site of construction with a high shear mixer as shown in Figure 2.2. UHPC properties enable using narrow, simplified details decreasing the volume of material required, increase ease of construction and the speed of construction.

Figure 2.2 Batching and casting UHPC at site (FHWA, 2016)

A current limitation with UHPC is its high unit cost. A typical UHPC mix is about ten times the cost of a regular conventional concrete mix, which is the primary limiting reason for not implementing UHPC on a large scale. Another limitation could be its batching and placing requirements. UHPC utilizes a high binder content enabling high packing densities which is one of the reasons for high strength. Steel fibers, often about 2% by volume are used with UHPC which is a reason for substantial increase in the cost.

Graybeal (2013) discusses the various methods of developing non-proprietary cost effective UHPC mixes in FHWA report HRT-13-100 stating “Development of Non-proprietary Ultra-High performance concrete for use in the highway bridge sector” using locally available materials. Implementing these methods could enhance the application of UHPC on a wider scale in the industry. For this research study, UHPC with locally available materials was developed by Tier 1 University Transportation Center at Missouri S&T.

2.3. DECK-LEVEL UHPC CONNECTIONS

Using advanced properties of UHPC in connections is not new in concept. The advantages of UHPC is fairly clear, it is strong and durable and therefore could be used to design more compact, stronger and more simplified connections. In fact, use of UHPC dates back to 1995. It was used in connections between slabs and columns at Aalborg University. Ontario’s Ministry of Transportation in Ontario, Canada can be hailed as forerunner in using UHPC significantly in bridges and has done significant research and has many bridge projects deployed where UHPC was used in connection as well as various structural elements like waffle decks, pi girders (Graybeal, 2010). Ductal® has been available for commercial use in North America for more than a decade and has been used in bridge elements and connections. Ductal portfolio (www.ductal-lafarge.com) lists the 49 completed bridge projects which have implemented UHPC in one or more element of construction.

Mackenzie River Twin Bridges project is considered as North America’s largest field-cast UHPC Bridge project in terms of volume used. It consisted of three span continuous bridge with steel girders with precast concrete (PC) deck panels. The transverse connections of the decks and shear pockets under haunches were filled with UHPC. Authors Perry, Krisciunas and Stofko published a PCI Journal in spring of 2014 stating “Mackenzie river twin bridges North America’s largest field-cast UHPC connections project” gives the design and details of this project with advantages of using UHPC in bridge elements. UHPC’s advanced properties help in simplified design, increased speed of construction given that using UHPC, narrow joints could be used which reduces the volume of concrete batching required at the site reducing the time of

traffic hold off. Figure 2.3 and Figure 2.4, extracted from PCI Journal give the simplified details used in this project (Perry et al., 2014).

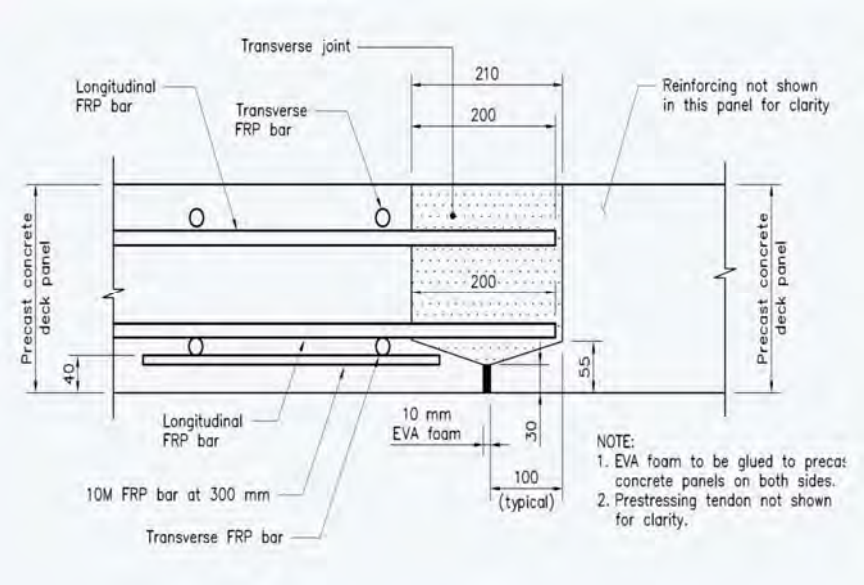

Figure 2.3 Deck level connection used in Mackenzie River twin bridges (adapted from Perry et al., 2014)

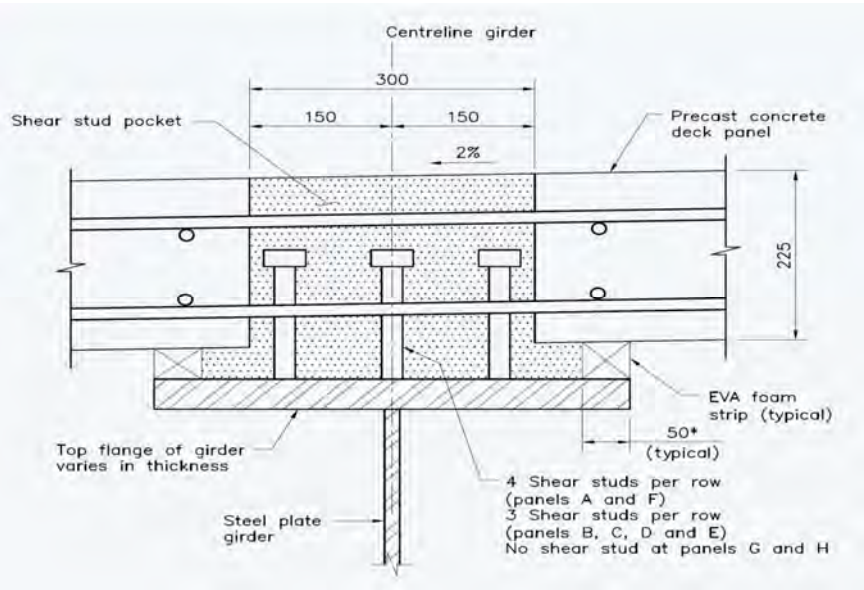

Figure 2.4 Shear pocket connection used in Mackenzie River twin bridges (adapted from Perry et al., 2014)

The Federal Highway Administration (FHWA) has been instrumental in recognizing the use of UHPC and championing the use of UHPC in research and field

projects. FHWA with New York State Department of Transportation (NYSDOT) have deployed many field projects where UHPC has been used for joint fill (Graybeal, 2010). Table 2.3 summarizes the bridges which have implemented UHPC deck connections.by the NYSDOT.

Table 2.3 List of UHPC bridges in U.S (adapted from Graybeal, 2014)

U.S. highway infrastructure with UHPC field cast connections			
Route	Crossing feature	Location	Owner
SR31	Canandaigua outlet	Lyons, N.Y.	NYSDOT
SR23	Otego Creek	Oneonta, N.Y.	NYSDOT
Dahlonega Road	Little Cedar Creek	Ottumwa, Iowa	Iowa DOT
Fingerboard Road	Staten Island Expressway	Staten Island, N.Y.	NYSDOT
SR248	Bennett Creek	Greenwood, N.Y.	NYSDOT
US Route 30	Burnt River and UPRR	Huntington, Ore.	Oregon DOT
US Route 6	Keg Creek	Council Bluffs, Iowa	Iowa DOT
Seven Lakes Drive	Ramapo River	Sloatsburg, N.Y.	NYSDOT
SR 42 (two bridges)	Westkill River	Lexington, N.Y.	NYSDOT
SR 31	Putnam Brook	Weedsport, N.Y.	NYSDOT
I-690 (two bridges)	Peat Street	Syracuse, N.Y.	NYSDOT
I-690 (two bridges)	Crouse Avenue	Syracuse, N.Y.	NYSDOT
US Route 87	BNSF Railroad	Moccasin, Mont.	Montana DOT
I-481	Kirkville Road	Syracuse, N.Y.	NYSDOT
Sr 12	Spring Brook	Greene, N.Y.	NYSDOT
SR 10	Webster Brook	Delhi, N.Y.	NYSDOT
SR 38	Wilson Creek	Newark, N.Y.	NYSDOT
SR 962G	US Route 17	Owego, N.Y.	NYSDOT
SR 907W	US Route 17	Pelham, N.Y.	NYSDOT
SR 2 (two bridges)	SR 9	Colonie, N.Y.	NYSDOT
I-81 (two bridges)	E. Castle St	Syracuse, N.Y.	NYSDOT
I-81 (two bridges)	E. Calthrop Ave.	Syracuse, N.Y.	NYSDOT
I-84 (two bridges)	Dingle Road	Southeast, N.Y.	NYSDOT
I-690 westbound	Onondaga Creek	Syracuse, N.Y.	NYSDOT
I-690	N. Salina St.	Syracuse, N.Y.	NYSDOT

FHWA publication FHWA-HRT-11-023 “Behavior of field-cast deck connections under cyclic and static structural loading” by Graybeal presents the results of testing UHPC connections linking pre-cast deck elements subjected to cyclic loading where different details were used in the joints. The UHPC used in longitudinal and transverse connections simulated the connection between precast deck elements and joints between top flanges of deck-bulb-tee girders. The specimens were subjected to cyclic loading of at least 2 million cycles after which static load was applied until failure of the specimen. Table 2.4 shows the test matrix used, while Figure 2.5 show the test setup, Figure 2.6, Figure 2.7, and Figure 2.8 show different continuity details used in this project and Figure 2.9 show a specimen after failure.

Figure 2.5 Test setup used in FHWA study HRT-11-023

Table 2.4 Test specimens used in FHWA study HRT-11-023

Test specimens			
Name	Orientation	Lap length	Reinforcement
8H	Transverse	90 mm (3.5-in.)	Headed
8E	Transverse	100 mm (3.9-in.)	Hairpin
8G	Transverse	150 mm (5.9-in.)	Straight
8B	Transverse	150 mm (5.9-in.)	Straight
6H	Longitudinal	90 mm (3.5-in.)	Headed
6B	Longitudinal	150 mm (5.9-in.)	Straight

Conversion: 1-in. = 25.4 mm

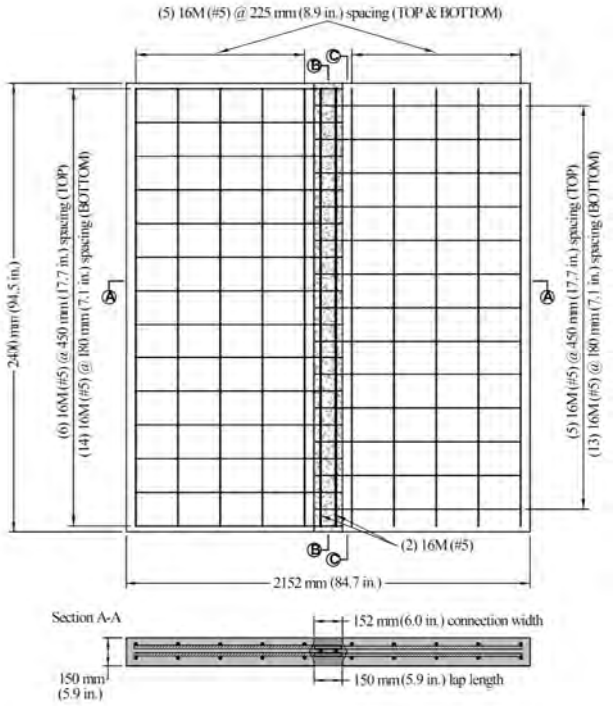

Figure 2.6 Straight detail and panel layout used in FHWA study HRT-11-023

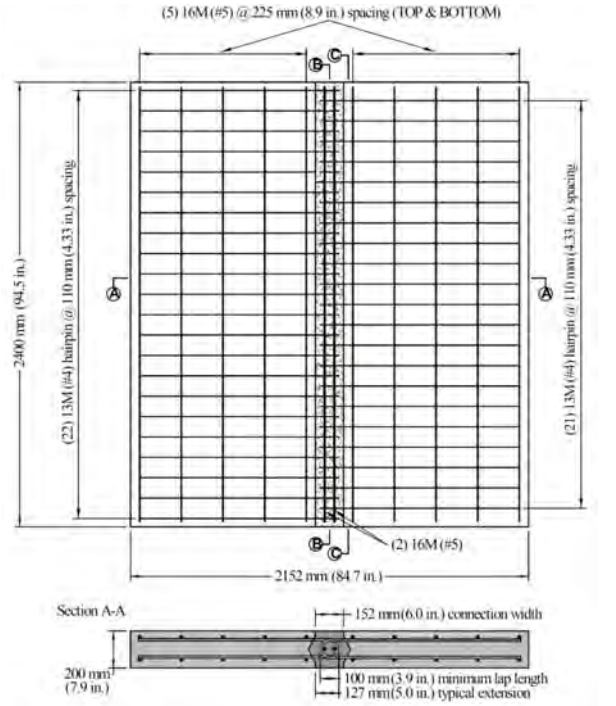

Figure 2.7 Hairpin detail and panel layout used in FHWA study HRT-11-023

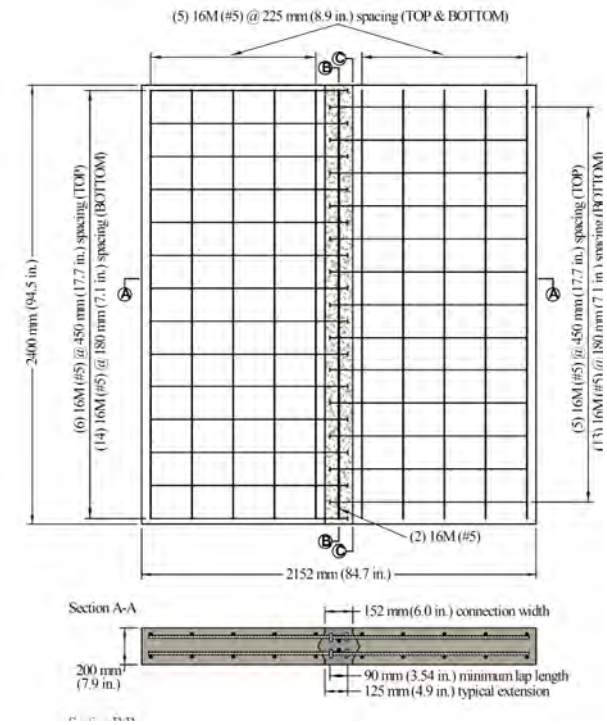

Figure 2.8 Headed detail and panel layout used in FHWA study HRT-11-023

Figure 2.9 Specimen after failure in FHWA study HRT-11-023

The specimens subjected to cyclic loading did not exhibit a failure in the connection. In fact specimens surpassed the performance of a monolithically casted deck. The connections used in the joint did not exhibit any debonding with UHPC. These results indicated UHPC can be successfully used in connections. For this research

investigation, similar specimens were developed and similar connection details were used except studies in beam elements were conducted (discussed in chapter three).

FHWA publication FHWA-HRT-14-084 “Design and construction of field-cast UHPC connections” by Graybeal provides design guidance for connections with UHPC, with case studies and material properties required for UHPC.

2.4. MODOT DETAIL WITH CIP DECK

MoDOT uses a prestressed detail at end of girders for intermediate and end bents. For intermediate bents, the prestressing strands in the bottom of girder are bent upwards after length of at least 3-in. (76 mm) while for end bent they are bent upwards after 6-in. (152 mm). The top strands except two are cut off within 1-in. (25 mm). The two remaining strands are bent in a shop projecting at least 12-in. (305 mm) to create a continuity with the deck casted on top. The typical detail is shown in Figure 2.10, Figure 2.11, Figure 2.12, Figure 2.13, and Figure 2.14.

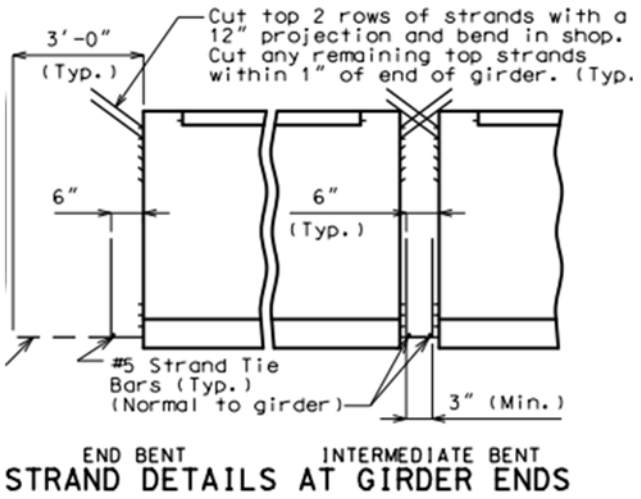

Conversion: 1-in. = 25.4 mm

Figure 2.10 MoDOT end girder detail (adapted from MoDOT Bridge Standard Drawings)

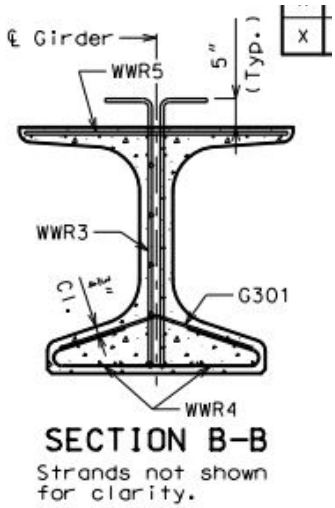

Conversion: 1-in. = 25.4 mm

Figure 2.11 Cross section of end of girder showing rebar layout

For this research, a similar detail was developed for use with non-prestressed section. The research was done for an intermediate bent in a non-prestressed reinforced concrete section. The joint was filled with UHPC and MoDOT. A cast in place (CIP) deck was casted on the beam section with modified MoDOT class B mix (deck mix used by MoDOT in field) and also UHPC to study the effect of using UHPC.

Figure 2.12 Highway-50 bridge intermediate bent with MoDOT end girder detail

Figure 2.13 Girder erected in position for Highway 50 Bridge with MoDOT end girder detail

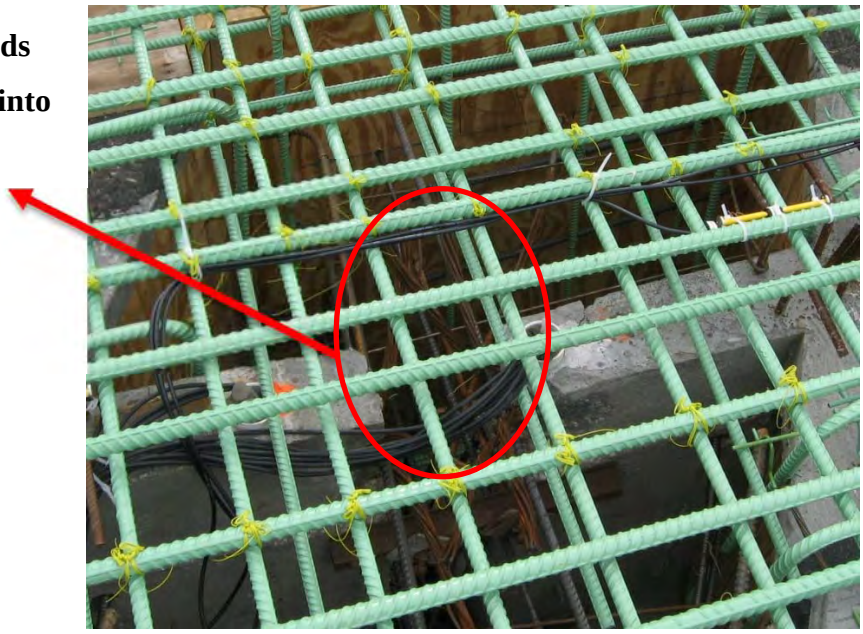

Figure 2.14 Intermediate bent in highway-50 Bridge with top strands highlighted

2.5. UHPC-UHSC

Ultra-high performance concrete has a minimum specified compressive strength of 22 Ksi as defined by ACI239-UHPC committee. The mix design developed was able to achieve the 22 Ksi specified compressive strength. This was achieved by steam curing the UHPC. However, the steam curing was not possible to apply for the test specimens due to size and other restrictions and also the research was trying to replicate the field cast scenario where steam-curing and or heat-curing is not always feasible. To abide with the guidelines of ACI 239, the concrete in this project was called as Ultra-High Strength Concrete (UHSC) instead of UHPC. The UHSC is similar to UHPC in all performance aspects to UHPC expect the compressive strength and the only difference is that the earlier (UHSC) was not steam cured and the later concrete (UHPC) was steam-cured. The Figure shows the difference of steam curing in the strength gain (only).

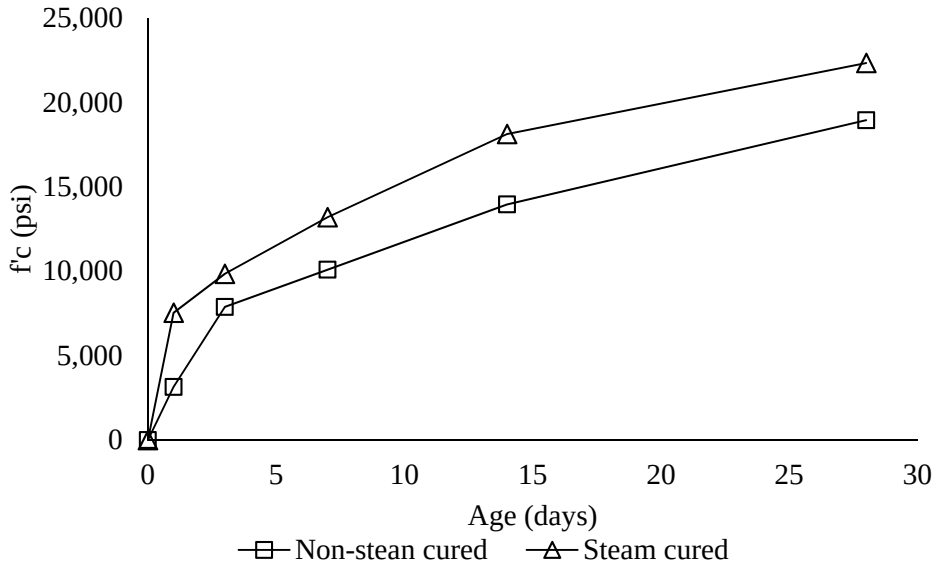

2.15 Steam cured versus non-steam cured UHPC/ UHPC versus UHSC

3. SCOPE OF WORK

The study was conducted to evaluate use of UHSC in joints. The other objective was to evaluate MoDOT end-girder detail with UHSC. This study was conducted in two phases. Phase one focused on evaluating UHSC in joints making a comparative study by using HS-SCC as other joint filler with different continuity details used (Figure 2.6, Figure 2.7, and Figure 2.8) while trying to find the effects of different surface preparations on the beam-joint interface. Phase two focused on using non-prestressed MoDOT end girder detail (Figure 2.10) for connections and evaluating it with UHSC and also modified MoDOT B -Mix.

3.1. PHASE ONE. EVALUATION OF UHSC CONTINUITY DETAILS IN HIGH MOMENT REGION

Phase one's objective was to evaluate use of UHSC in place of HS-SCC with different joint details and surface preparations. In order to do this, a test matrix was developed which consisted of twenty two beams. Based on the type of joint-filler used, there were four controls, nine HS-SCC joint beams, and nine UHSC joint beams.

3.1.1. Specimen Designation. The designation of the test matrix is shown in Figure 3.1 and Table 3.1. The test matrix for Phase one consisted of twenty two beams which were designated by the order of casting, type of filler used, type of surface preparation used and type of continuity detail used in the joint.

For example, the designation shown in Figure 3.1 as specimen B-22-U-S-A represents twenty second specimen in order of casting, which had UHSC as filler, sandblasting as beam-joint surface preparation and anchored rebar detail in the connection. Different connection details had different rebar lap length as listed in Table 3.1. Number of specimens being large, it was possible to cast and test only one replicate of each specimen. Testing more specimens was cost prohibitive for this study.

3.1.2. Member Design. The specimens were designed by research team at Missouri S&T. Graybeal (2010) has done significant research on using different details in joints with UHSC which were subjected to cyclic and static loads and worked successfully. The specimens used in this project were 84-in. (2134 mm) in length with

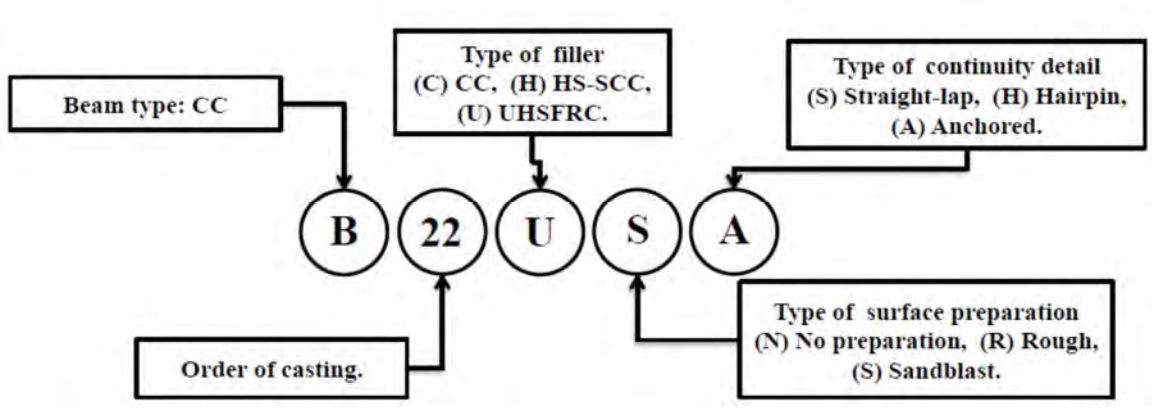

Figure 3.1 Phase one test matrix designation

Table 3.1 Phase one test Matrix

Sl.no.	Nomenclature	Joint filler	Joint detail	Surface preparation	Lap length in. (mm)
1	B-1-C-N-N	No-Joint	Straight	Smooth	0
2	B-2-C-N-S	No-Joint	Straight	Smooth	6.0 (152)
3	B-3-C-N-H	No-Joint	Hairpin	Smooth	3.9 (99)
4	B-4-C-N-A	No-Joint	Anchored	Smooth	3.5 (89)
5	B-5-H-N-S	HS-SCC	Straight	Smooth	6.0 (152)
6	B-6-H-N-H	HS-SCC	Hairpin	Smooth	3.9 (99)
7	B-7-H-N-A	HS-SCC	Anchored	Smooth	3.5 (89)
8	B-8-H-R-S	HS-SCC	Straight	Rough	6.0 (152)
9	B-9-H-R-H	HS-SCC	Hairpin	Rough	3.9 (99)
10	B-10-H-R-A	HS-SCC	Anchored	Rough	3.5 (89)
11	B-11-H-S-S	HS-SCC	Straight	Sand Blasted	6.0 (152)
12	B-12-H-S-H	HS-SCC	Hairpin	Sand Blasted	3.9 (99)
13	B-13-H-S-A	HS-SCC	Anchored	Sand Blasted	3.5 (89)
14	B-14-U-N-S	UHSC	Straight	Smooth	6.0 (152)
15	B-15-U-N-H	UHSC	Hairpin	Smooth	3.9 (99)
16	B-16-U-N-A	UHSC	Anchored	Smooth	3.5 (89)
17	B-17-U-R-S	UHSC	Straight	Rough	6.0 (152)
18	B-18-U-R-H	UHSC	Hairpin	Rough	3.9 (99)
19	B-19-U-R-A	UHSC	Anchored	Rough	3.5 (89)
20	B-20-U-S-S	UHSC	Straight	Sand Blasted	6.0 (152)
21	B-21-U-S-H	UHSC	Hairpin	Sand Blasted	3.9 (99)
22	B-22-U-S-A	UHSC	Anchored	Sand Blasted	3.5 (89)

Conversion: 1-in. = 25.4 mm

rectangular cross-section with a width and depth of 8-in. (203 mm) and 12-in. (305 mm) respectively with a clear cover of 1.5-in. (38 mm). The top and bottom longitudinal

reinforcement consisted of 2 Grade 60 #4 rebar's (see Figure 3.2) with yield strength of 77.5 ksi (534 MPa). Grade 60 #3 rebars (yield stress 74 ksi/510 MPa) were used as stirrups. Each specimen consisted of two beams of 39-in. (990 mm) length connected by a 6-in. (152 mm) joint as shown in Figure 3.3.

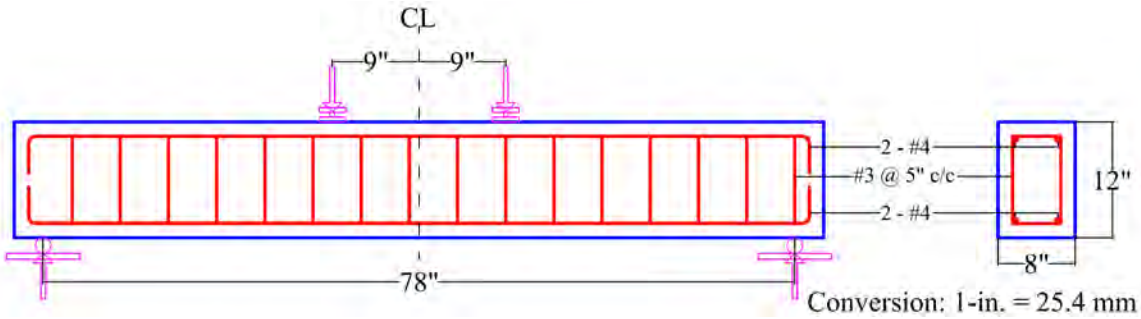

Figure 3.2 Typical specimen cross-section with rebar layout

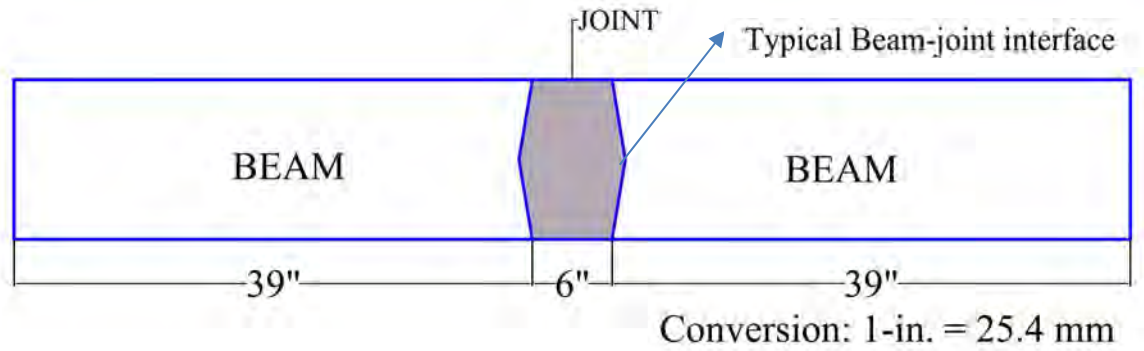

Figure 3.3 Specimen elevation

At the beam-joint interface, a diamond shear key shape was created to provide interlock for the beam and joint (Figure 3.3). Control specimen B-1-C-N-N was cast monolithically which had the rebar detail of a doubly-reinforced beam to serve as primary reference/upper limit for all the specimens. The remaining control specimens were also cast monolithically but had a reinforcement detail as shown in Figure 3.4, Figure 3.5, Figure 3.6 to be used as a secondary reference/lower limit for each detail type. The different rebar details used are described in the following sub-sections.

3.1.2.1 Straight-lap detail. The straight-lap detail was used in previous work done by Graybeal (2010) and is most commonly used in field-cast deck-level connections. The detail consists typically rebars protruding from precast segments and

form a non-contact splice connection (Figure 2.6) and can be spliced for a length based on connection. It is easy to build, maneuver in the field. This detail is also practically feasible in case of prestressed concrete elements. This straight non-contact lap splice detail was modified slightly for the purpose of using it in non-prestressed girder sections. Instead of non-contact splice, the rebars were bent so as to create a lap-splice along the length of the joint (6-in. in this case) as shown in the Figure 3.4.

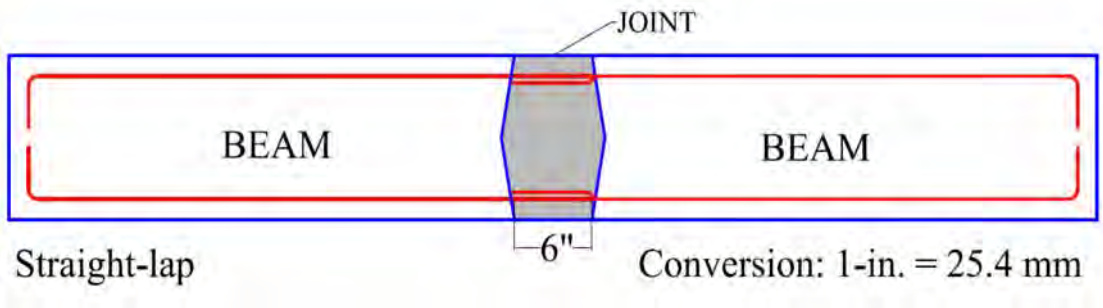

(a)

(b)

(c)

Figure 3.4 Straight-lap detail

3.1.2.2 Hairpin detail. The hairpin detail was a non-contact lap splice layout used in deck-level connections by Graybeal (2010). The layout was also modified (similar to straight lap detail discussed in 3.1.2.1) to be used in girder sections. The rebars were bent like hairpin, shown in Figure 3.5 and were lapped for 3.9-in. (99 mm) (Figure

2.7). This detail will be practical in reinforced concrete sections but not for prestressed-pre-cast elements with prestressing strands and hence not practical for prestressed-precast structures.

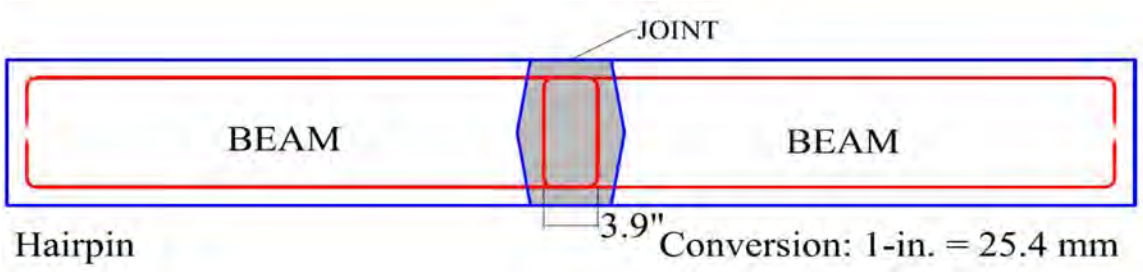

(a)

(b)

(c)

Figure 3.5 Hairpin detail

3.1.2.3 Anchored-rebar detail. This rebar detail was used in research done by Graybeal (2010) (Figure 2.8) and was modified to be used in this study. The rebars were lapped for 3.5-in. length. The headed rebar detail was developed by welding a circular metal disc to weld-able rebar. The weld was tested in tension, none of the rebars failed. The failure was due to yielding of circular disc which buckled rupturing the weld in the process. The detail is shown in Figure 3.6.

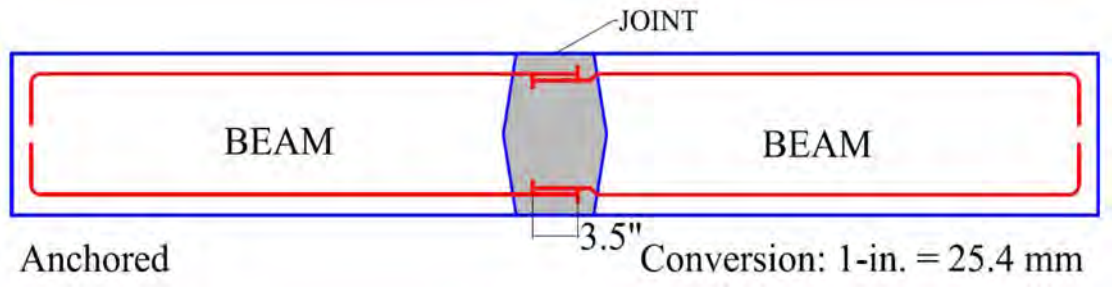

(a)

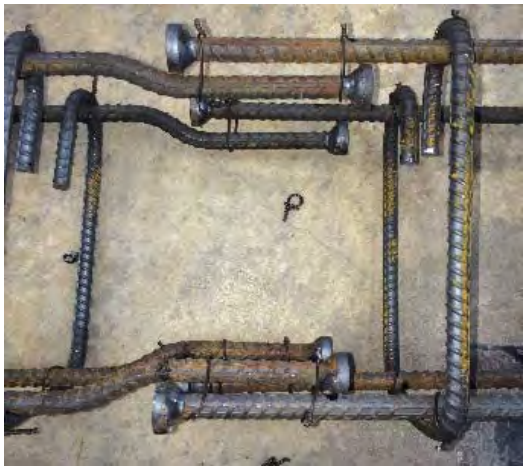

(b)

(c)

Figure 3.6 Anchored rebar detail

3.1.2.4 Surface preparation. Studying the effect of surface preparation was one of the objectives this research project. Sandblasting was used to prepare the surface of concrete. Sandblasting can be used to vary the degree of surface roughness by light cleaning or deep cutting up to ½ inch. Three different surface preparations were studied in this case are discussed briefly as follows

3.1.2.4.1 <u>No surface preparation/smooth.</u> Specimens were de-molded from formwork and the beam-joint interface was left “as is”. This was considered as Smooth/No-surface preparation as shown in Figure 3.7 (a).

3.1.2.4.2 <u>Roughening.</u> The specimens to be roughened were taken to Mines at Missouri S&T and a sandblaster was used to roughen the beam-joint interface. The surface after roughening is as shown in Figure 3.7 (b).

3.1.2.4.3 <u>Sandblasting.</u> The specimens to be sandblasted were taken to mines at Missouri S&T and sandblaster was used to remove the paste until aggregate was visible. The sandblasted specimen surface is shown in Figure 3.7 (c).

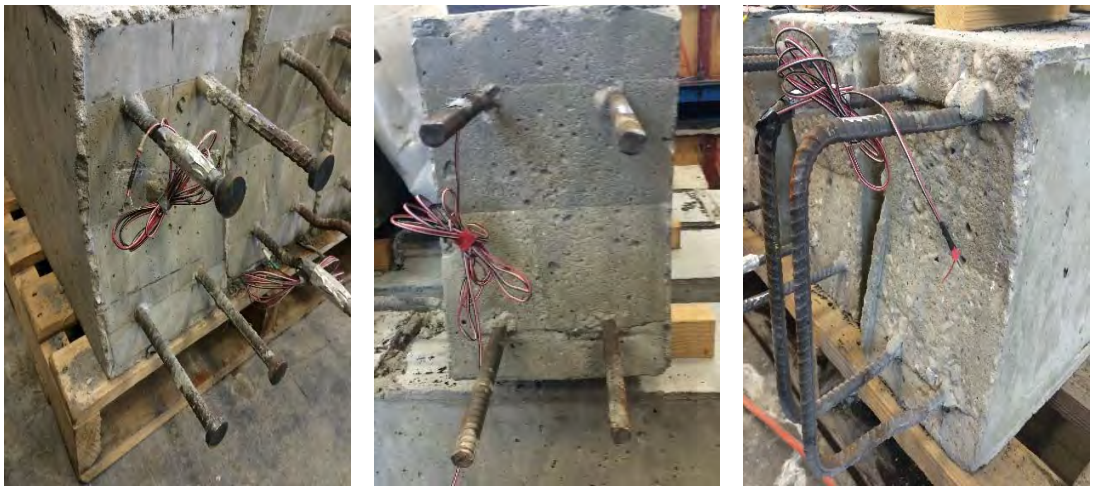

(a) (b) (c)

(d)

Figure 3.7 Figure showing various surface preparations (a) smooth/ no-surface (b) roughening (c) sandblasting (d) technician preparing beam-joint interface at Missouri S&T mines

3.2. PHASE TWO. EVALUATION OF UHSC IN MODOT DETAIL

The main objective of Phase two was to use UHSC in typical MoDOT end girder detail with CIP deck. The research team at Missouri S&T created a test matrix which consisted of five specimens, three controls, one UHSC joint-CC deck specimen and one UHSC joint-deck specimen.

3.2.1. Specimen Designation. The designation of the test matrix is shown in Figure 3.8 and Table 3.2. Phase two test matrix consisted of five specimens. They are designated based on the order of casting, type of joint filler used, type of deck filler used and type of end girder detail used in each specimen.

For example, the designation shown above as specimen B-5-U-U-M represents fifth specimen in order of casting, which had UHSC as joint filler, UHSC as deck filler and MoDOT end girder detail. The test matrix consisted of one beam with continuous reinforcement, and four specimens where MoDOT's end girder detail was used in the connection.

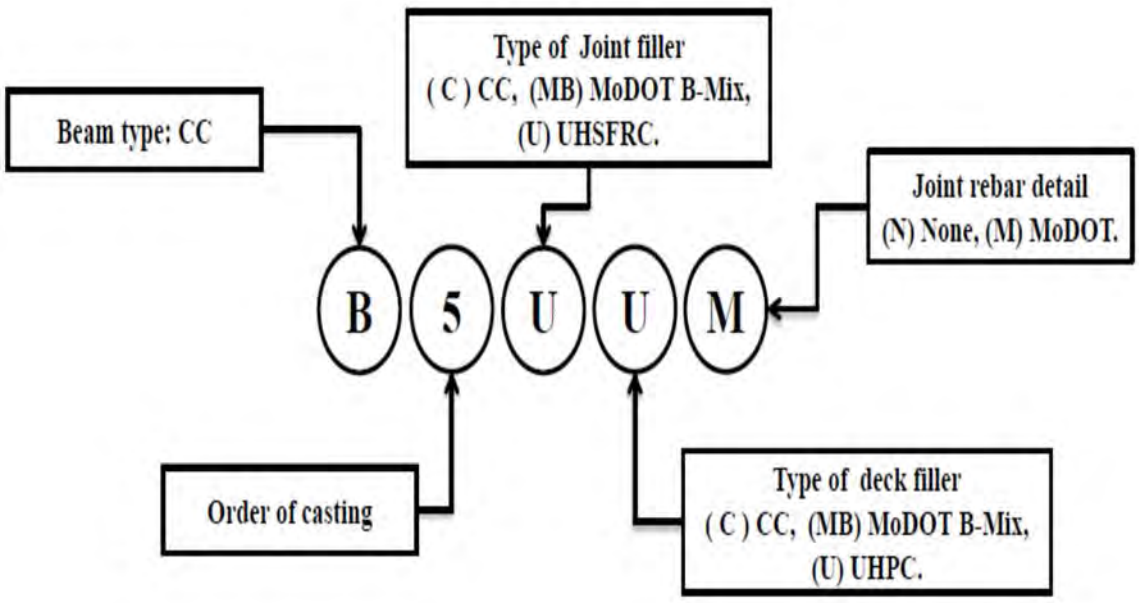

Figure 3.8 Phase two test matrix designation

Table 3.2 Phase two test matrix

Sl.no.	Nomenclature	Beam	Joint type	Deck	Joint detail
1	B-1-C-C-N	CC	CC	CC	None
2	B-2-C-C-M	CC	CC	CC	MoDoT
3	B-3-MB-MB-M	CC	MoDoT B	MoDoT B	MoDoT
4	B-4-U-MB-M	CC	UHSC	MoDoT B	MoDoT
5	B-5-U-U-M	CC	UHSC	UHSC	MoDoT

3.2.2. Member Design. The research team designed a T-section to reproduce a composite section of deck and girder while using MoDOT end girder detail in the connection. Each specimen consisted of two beams of 39-in. (990 mm) length connected by a 6-in. (152 mm) joint and later a deck was cast on top of the beams to create beam-deck composite section. The deck was 4-in. (102 mm) in thickness, while the beams were 8-in. (203 mm) wide and 12-in. (305 mm) deep making the overall depth of cross-section 16-in. (406 mm) as shown in Figure 3.10. The tensile reinforcement consisted of 7 grade 60 #3 rebars (yield stress 74 ksi/510 MPa) and 2 grade 60 # 4 rebars. 2 grade 60 #4 rebars (yield stress 77.5 ksi/534 MPa) were used as compression reinforcement. The shear reinforcement consisted of #3 grade 60 rebars (yield stress 74 ksi/510 MPa) which were bent into modified-U shaped stirrups. The shear reinforcement protruded into the deck (flange) region from the beam (web) so as to create a continuity detail (Figure 3.11). Control specimen B-1-C-C-N's rebar detail was continuous throughout and was cast monolithically. The remaining specimens had a rebar detailing as shown in Figure 3.9. Figure 3.12 (a) shows the prestressed MoDOT end girder detail used in field and Figure 3.12 (b) show the non-prestressed MoDOT detail developed for this research project. Figure 3.13 (a) and (b) show specimens after casting.

Figure 3.9 Reinforcement layout with joint detail

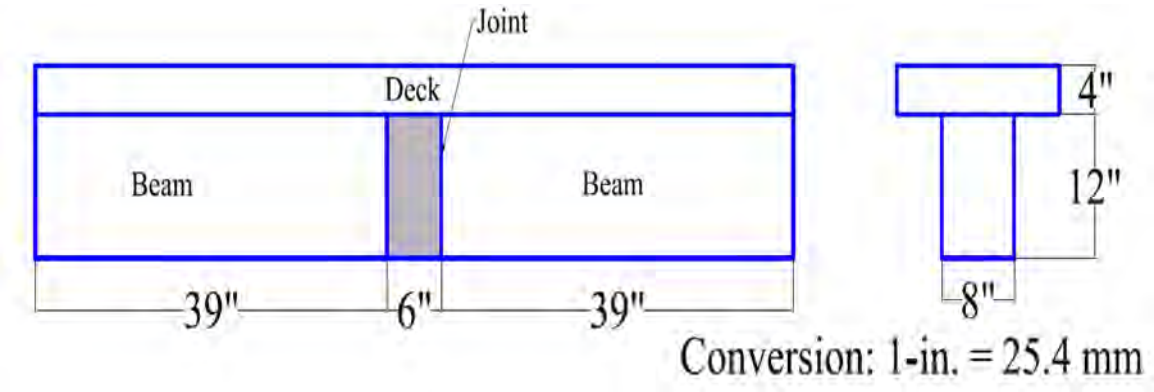

Figure 3.10 T-beam layout with cross-section

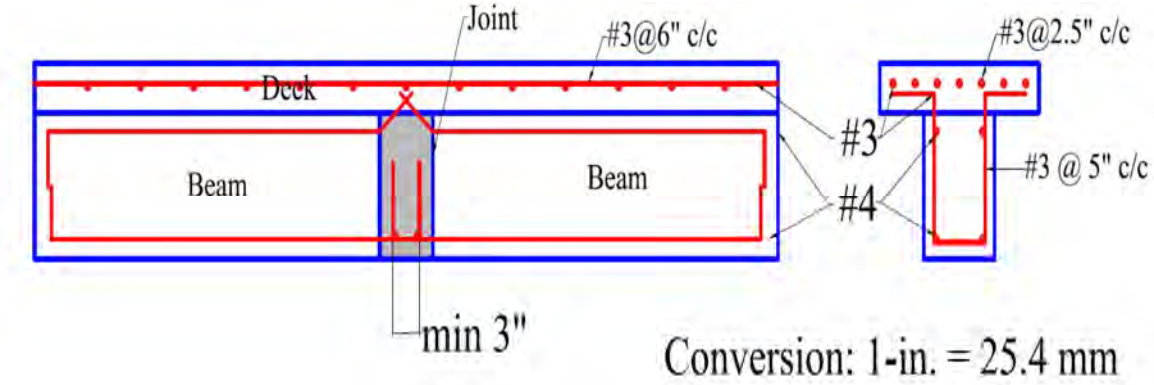

Figure 3.11 Specimen with reinforcement layout (with MoDOT detail) and cross-section

(a) (b)

Figure 3.12 (a) MoDOT end girder detail in Highway-50, (b) non-prestressed Joint detail

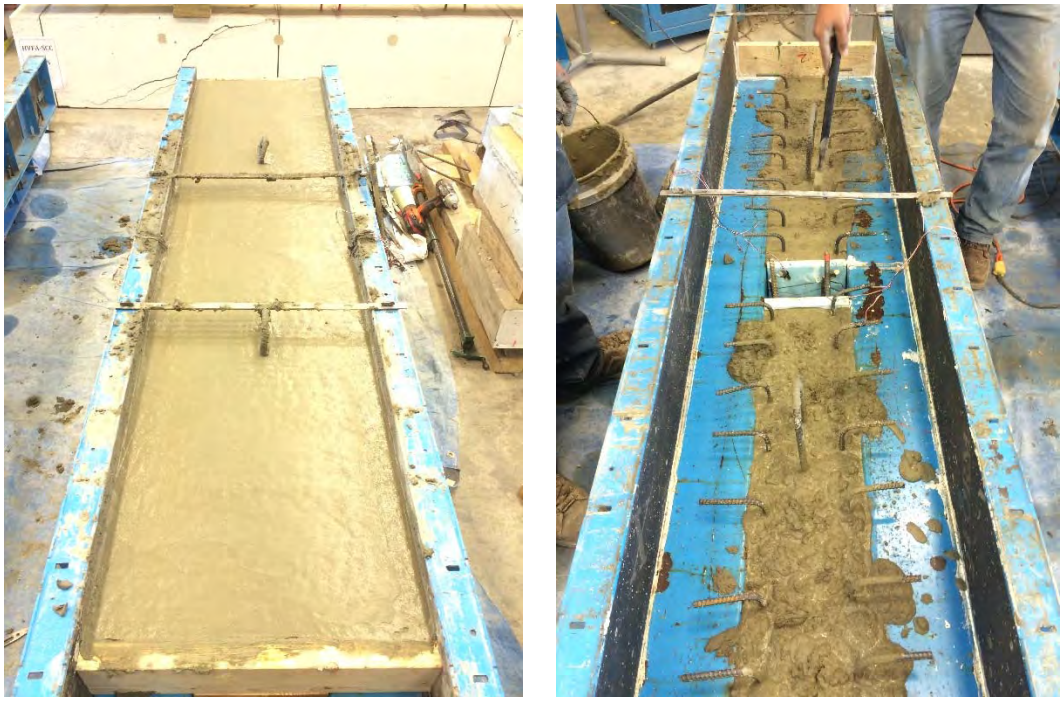

(a) (b)

Figure 3.13 (a) Control specimen (b) specimen with joint

4. MIXTURE DEVELOPMENT

4.1. MATERIALS

One of the objectives of research was to develop mix designs using locally available materials. The materials included Portland cement type I/II and type III, Missouri river sand, masonry sand, 1-in. coarse aggregate, 3/8 inch crushed aggregate, Master Glenium 7500, Steel fibers and Water

4.1.1. Portland Cement. Two types of Portland cement were used in this project. Type I/II and Type III. Type I/II was chosen for CC beams as they represent a precast segment casted in a precast plant. HS-SCC was casted using Type I/II as well. Type III was used for UHSC mix, since Type III has fine particle size and also gives high early strength which is desirable in case of field-cast bridge elements as it reduces the construction-lay off time. The particle size distribution is shown in Figure 4.1.

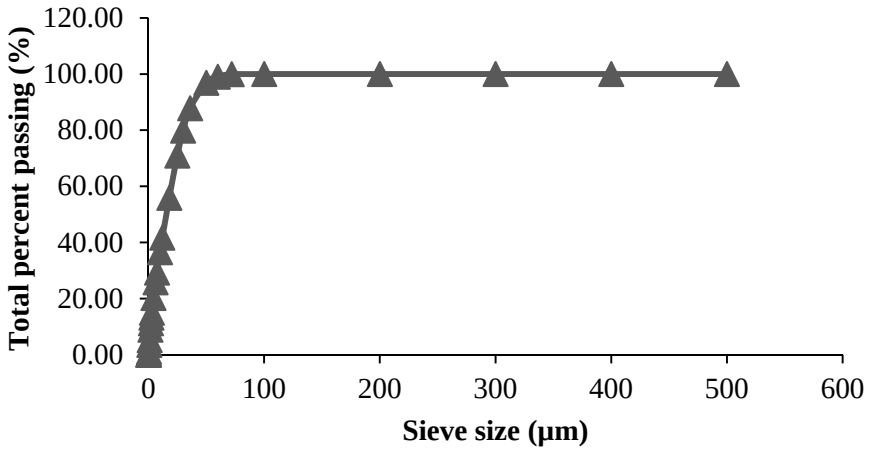

Figure 4.1 Particle size distribution of Type III Cement

4.1.2. Fine Aggregate. Two types of fine aggregate used were Missouri River sand and Masonry sand. Missouri river sand was used in CC, HS-SCC and UHSC mixes. It is locally available in Midwest USA. Using ready mix trucks made it difficult for controlling the quality for CC beams and HS-SCC Joints and resulted in different strengths. It was made sure to use aggregate passing through #4 sieve was used while casting UHSC. Sieving was important in case of UHSC as the size of aggregate used will

influence the particle packing density and hence the strength of the final mix. Masonry sand is also Missouri river sand but finer than #16 sieve size (passing through 1.19mm opening) was exclusively used only in UHSC mix. The two types of sands used are shown in Figure 4.2.

Figure 4.2 Fine aggregate (a) Missouri river sand, (b) masonry sand

4.1.3. Coarse Aggregate. There were two types of coarse aggregate used, 1-in. limestone and 3/8-in. crushed lime stone shown in Figure 4.3. The 1-in. aggregate was used for CC beam casting. 3/8-in. crushed limestone was chosen to be used in HS-SCC joint casting and HS-SCC trial batches to increase paste volume and achieve higher strength mix. UHSC does not have any coarse aggregate in the mix.

Figure 4.3 Coarse aggregate (a) 1-in. limestone (b) 3/8-in. crushed limestone

4.1.4. Silica Fume. The silica fume used was from Elkem Materials ES-900C. It was used in UHSC as a filler material. Due to high fineness and silica content it acts like a pozzolanic material and also has many advantages like increase in bond strength,

cohesiveness, durability and decreases the bleeding, permeability etc. The silica fume used in this project is shown in Figure 4.4.

Figure 4.4 Silica fume

4.1.5. Ground Granulated Blast Furnace Slag (GGBFS). GGBFS used was from Holcim materials and used in UHSC mix. GGBFS reduces the setting speed of concrete enabling to work for extended period of time but doesn't affect the strength gain, increases the workability, chemical resistivity, durability and sustainability as well. The GGFBS used in this project is shown in Figure 4.5.

Figure 4.5 Ground granulated blast furnace slag (GGBFS)

4.1.6. Admixture. Admixture was used in HSCC and UHSC mixes. The product used was Master Glenium 7500 by BASF shown in Figure 4.6. Given the low water-cement ratio mixes, High range water reducer (HRWR) was required to make the mixes more workable. Master Glenium 7500 was chosen based on literature review. Master Glenium 7500 accelerates the strength gain, increases the workability.

Figure 4.6 Master Glenium 7500 (HRWR)

4.1.7. Steel Fibers. The steel fibers used were Bekeart Corporation's Dramix. The fibers were 0.5 inch (13 mm) in length with brass coating (shown in Figure 4.7) and were used in UHSC mix, are responsible for high tensile strength of UHSC mixes. The fibers properties are given in Table 4.1.

Figure 4.7 Dramix Steel fibers

Table 4.1 Fiber properties

	Bekeart Dramix
Fiber Diameter	0.2 mm (0.008 in)
Fiber length	13 mm (0.5 in)
Specific Gravity	7.85
Tensile Strength	2158 MPa (313 ksi)
Coating	Brass

Conversion 1 MPa = 0.145 ksi, 1 mm = 0.04 in.

4.2. MIX DESIGN

This section describes the various mix designs used during phases one & two of study. This project involved use of conventional concrete (CC), high strength self-

consolidating concrete (HS-SCC), ultra-high performance concrete (UHSC), and MoDOT B-mix (MB). The CC was used for beam specimens, while HS-SCC and UHSC were used as joint fill materials during Phase one. The MB was used in Phase two as joint filler and cast-in-place deck mix.

4.2.1. Conventional Concrete (CC). CC was used for fabrication of beams which were later connected with joints. The materials used were Type I/II cement, Missouri river sand, 1-in. concrete stone and water. Two mix designs were used for the beams. For Phase one, there were three castings and ready mix truck was used, hence the three mixes were inconsistent. Mix B1 (Table 4.2) was used to cast the control specimens. Mixes B2 and B3 (Table 4.3) were used to cast beams specimens for HS-SCC and UHSC specimens of Phase one respectively. Mix B3 (Table 4.3) was also used to cast beam specimens for Phase two.

Table 4.2 B1 –Mix design used for control specimens

Material	Amount kg/m^3 (lb./yd^3)
Portland Cement Type I/II	307 (517)
1-in. Concrete Stone	1009 (1700)
Missouri River Sand	839 (1414)
Water	134 (226)
Water/CM	0.43

Conversion 1 kg/m^3 = 1.686 lb./yd^3, 1 l/m^3 = 25.852 oz./yd^3, 1 kg = 2.204 lb.

Table 4.3 B2 & B3 – Mix design used for test specimens

Material	Amount kg/m^3 (lb./yd^3)
Portland Cement Type I/II	364 (614)
1-in. Concrete Stone	1002 (1689)
Missouri River Sand	906 (1527)
Water	120 (202)
Water/CM	0.33

Conversion 1 kg/m^3 = 1.686 lb./yd^3, 1 l/m^3 = 25.852 oz./yd^3, 1 kg = 2.204 lb.

4.2.2. High Strength Self-Consolidating Concrete (HS-SCC). HS-SCC was used as one of the joint fill materials. It was logical to use a HS-SCC for joint fill as it is easy to convey and fill congested locations like the joints where the reinforcement is

really close together. This was one of the reasons to use a smaller size coarse aggregate in this HS-SCC mix. Table 4.4 and Table 4.5 lists the two trial mix designs, HS-SCC-1 and HS-SCC-2 which were developed for HS-SCC study. HS-SCC-1 was used to cast the joint as it had higher paste content and higher strength. The mix was developed for use in bridge girders in Bridge A7957-Route 50 and additional mix properties are presented in report "Self-Consolidating Concrete (SCC) and High-Volume Fly-Ash Concrete (HVFAC) for Infrastructure Elements: Implementation, Myers et al., 2014".

Table 4.4 HSCC-1

Material	Amount kg/m^3 (lb./yd^3)
Portland Cement Type I/II	504 (850)
Missouri River Sand	850 (1433)
3/8-in. crushed stone	795 (1340)
HRWR Master Glenium 7500 (l/m^3)	3.7 (96 oz./ yd^3)
Water	166 (280)
W/CM	0.33

Conversion 1 kg/m^3 = 1.686 lb./yd^3, 1 l/m^3 = 25.852 oz./yd^3, 1 kg = 2.204 lb.

Table 4.5 HSCC-2

Material	Amount kg/m^3 (lb./yd^3)
Portland Cement Type I	504 (850)
Missouri River Sand	823 (1387)
3/8-in. crushed stone	823 (1387)
HRWR Master Glenium 7500 (l/m^3)	3.7 (96 oz./ yd^3)
Water	166 (280)
W/CM	0.33

Conversion 1 kg/m^3 = 1.686 lb./yd^3, 1 l/m^3 = 25.852 oz./yd^3, 1 kg = 2.204 lb.

4.2.3. Ultra-High Strength Concrete (UHSC). UHSC has binder ratio, low water cement ratio, and steels fibers. UHSC has been successfully used in field-cast deck-level connections and can reduce the stress in the connections, improve ductility, and extend service life. UHSC can reach high compressive and tensile strengths and is durable, ductile, chemically resistant, less permeable, and resistant to weathering. The UHSC mixtures used in this project were developed as part of RE-CAST Tier 1

University Transportation Center project 3B at Missouri University of Science and Technology. Locally available materials were studied and a UHSC mix using these materials was developed (Meng et al., 2015). Table 4.6, and Table 4.7 give the trial mixtures U#1 and U#2 developed during this research project. U#1 was used to cast the joint specimens.

Table 4.6 U#1

Material	Amount kg/m^3 (lb./yd^3)
Portland Cement Type III	548 (924)
Silica Fume	41 (70)
GGBFS	535 (902)
Missouri River Sand	708 (1194)
Masonry Sand	310 (523)
HRWR Master Glenium 7500 (l/m^3)	70 (1809 oz./ yd^3)
Steel Fibers	156 (263)
Water	146 (246)
W/CM	0.20*

Conversion 1 kg/m^3 = 1.686 lb./yd^3, 1 l/m^3 = 25.852 oz./yd^3, 1 kg = 2.204 lb.

*The water used in this mix includes the moisture content from fine aggregates and superplasticizer

Table 4.7 U#2

Material	Amount kg/m^3 (lb./yd^3)
Portland Cement Type III	1083 (1826)
Silica Fume	54 (91)
Missouri River Sand	708 (1194)
Masonry Sand	310 (523)
HRWR Master Glenium 7500 (l/m^3)	70 (1809 oz./ yd^3)
Steel Fibers	156 (263)
Water	227 (383)
W/CM	0.20

Conversion 1 kg/m^3 = 1.686 lb./yd^3, 1 l/m^3 = 25.852 oz./yd^3, 1 kg = 2.204 lb.

4.2.4. MoDOT B-Mix (Deck Mix). MoDOT has a mix which it uses for its cast-in-place (CIP) elements like decks, intermediate bents, etc. The mix is called a MoDOT B-mix, as it is known by contractors and ready mix plants, was obtained from

Myers, J.J., et al., “Self-Consolidating Concrete (SCC) and High-Volume Fly Ash (HVFAC) for Infrastructure Elements: Implementation” which is a slightly modified mix. The mix is characterized by low cement content, fly-ash and 1-in. Jefferson City dolomite. Rolla ready mix supplied the mix and specimens were casted in High-bay structures lab at Missouri S&T. the mix design is given in Table 4.8.

Table 4.8 MoDOT B-Mix (MB)

Material	Amount kg/m^3 (lb./yd^3)
Type I Cement	246 (415)
Fly-ash	77 (130)
1-in. Coarse aggregate	1131 (1906)
Missouri River sand	786 (1325)
Air entrainment (l/m^3)	0.5 (13 oz./ yd^3)
Water	133 (224)
W/CM	0.54

Conversion 1 kg/m^3 = 1.686 lb./yd^3, 1 l/m^3 = 25.852 oz./yd^3, 1 kg = 2.204 lb.

5. EXPERIMENTAL PROGRAM

5.1. SPECIMEN FABRICATION

The specimens consisted of controls, UHSC, and HS-SCC-joint beams. First, the four controls were casted, then the beams for UHSC and HS-SCC were casted using ready mix truck. The HS-SCC joints were casted next using ready mix truck as well. The UHSC joints were casted using Pan Mixer in Materials lab and ERL at Missouri S&T.

5.1.1. Phase One Specimen Fabrication. Phase one consisted of twenty two specimens which were four controls, nine HS-SCC and nine UHSC beams. They are discussed in the subsections of 5.1.1

5.1.1.1 Control beams. The four controls consists of one regularly reinforced beam, three beams with continuity detail to be used in the joints i.e., straight, hairpin, anchored detail. These beams were casted together using a 4 ksi (28 MPa) concrete mix design given in Table 4.2. The typical reinforcement layout used was 4 - #4 rebars as longitudinal reinforcement, #3 stirrups at 5-in. (127 mm) center to center spacing as shown in Figure 3.2. Various stages of casting is shown in Figure 5.1 and Figure 5.2

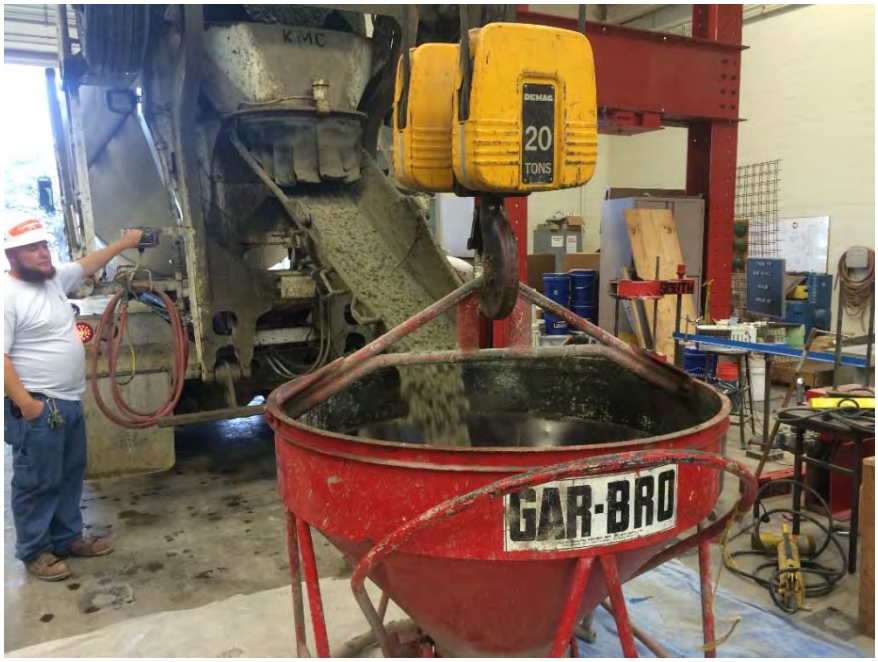

Figure 5.1 Concrete being delivered by a ready mix truck

Figure 5.2 Control specimens after casting

5.1.1.2 Beam specimens for HS-SCC and UHSC. Beams specimens for HS-SCC and UHSC joint beams were cast separately using steel forms, a 6 ksi (41 MPa) CC mix was used, given in Table 4.3. Wooden forms were used as end pieces to create the shear key shape (Figure 5.3). To avoid wooden forms from breaking, concrete was rodded and rubber mallets were used instead of pneumatic vibrators near the wooden sections of the formwork. The casting procedure is shown in Figure 5.4.

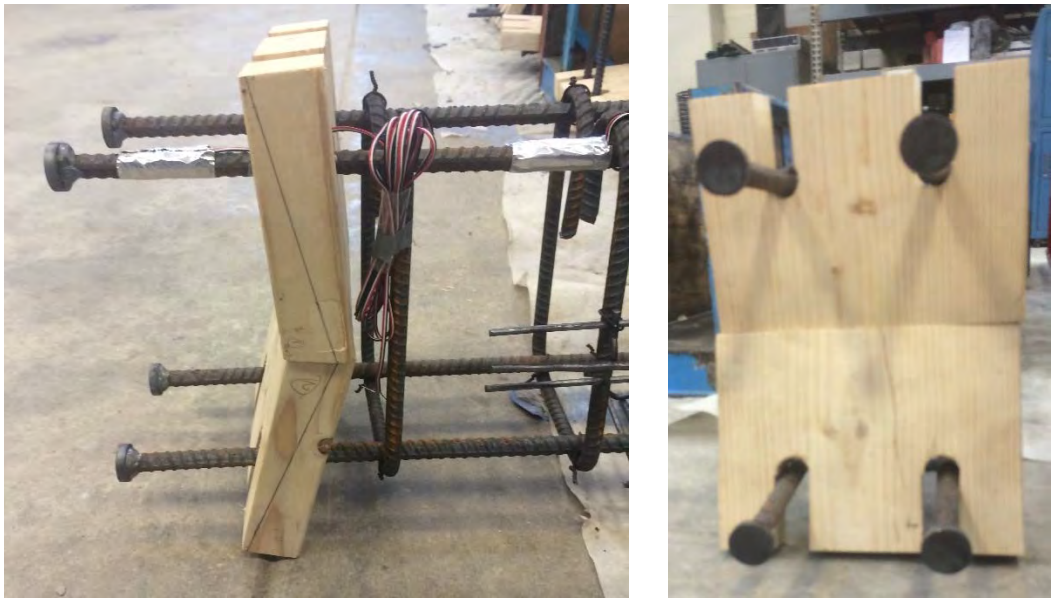

(a) (b)

Figure 5.3 Wooden form built to create shear key shape at beam-joint interface

(a)

(b)

(c)

Figure 5.4 Various stages of casting beam specimens

5.1.1.3 HS-SCC. HS-SCC mix was cast at Missouri S&T using ready mix truck. The mix used is listed in Table 4.4. To cast the joint, plywood forms were made, shown in Figure 5.5. To avoid collapse of the plywood forms due to concrete form pressure, 5-gallon buckets were used to fill the joints instead of a concrete hopper. Rubber mallets were used instead of pneumatic vibrators to make sure the concrete is evenly distributed in the formwork. Couple of hours after casting, wet rags of burlap were used to cover the surface of joints to prevent any moisture loss. The ply-wood forms were then demolded after two days and covered with wet burlap until specimens were seven days old.

(a)

(b)

Figure 5.5 HS-SCC beams before and after casting joints

5.1.1.4 UHSC. UHSC was mixed in materials lab and casted at High-bay at Missouri S&T. The mix design U#1 (Table 4.6) was used. High shear pan mixer was used to mix as UHSC has a water to cementious material ratio of less than 0.2 and regular drum mixers could not mix such a dry mix. The mixing procedure was to add aggregates and mix until they are homogenous, then half of water was added and mixed for 2 minutes. Half of cementious material was then added with half of HRWR and water and mixed until clumps were formed. The remaining material was then added and mixed until fluid UHSC was obtained (Figure 5.6). Steel fibers were then added gradually to avoid formation of clumps and mixed until uniform mix was obtained. Then the pan was dislodged and 5 gallon buckets were used to fill the joints. UHSC is self-leveling, requiring less or no external vibration to ensure proper filling. Due to volume constraints of the mixer available, three UHSC batches were made using same volume to maintain consistency.

(a)

(b)

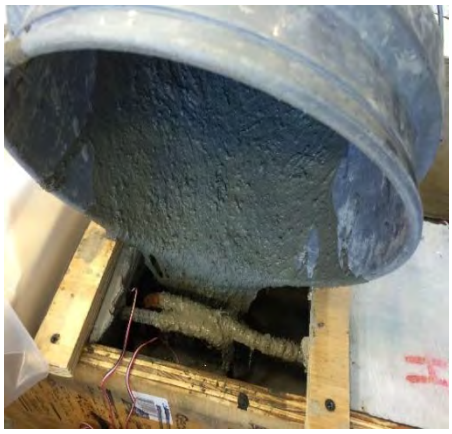

(c)

(d)

(e)

Figure 5.6 Various stages of UHSC batching and casting

5.1.2. Phase Two Specimen Fabrication. The fabrication of Phase two specimens was done at Missouri S&T High-bay lab. The control specimens B-1-C-N-N, B-2-C-C-M were monolithically cast without joints using concrete from Rolla ready mix

using a B3 mix (Table 4.3). The remaining specimens consisted of discontinuous reinforcement with deck on top. The casting was done in following steps. The beam segments for the specimens were cast using the same mix as controls with concrete from ready mix truck. UHSC joint of specimen B-4-U-MB-M was casted using pan mixer at materials lab in MST, then MoDOT B mix was used to cast the deck and joint of specimen B-3-MB-MB-M along with the deck of specimen B-4-U-MB-M. The deck and joint of specimen B-5-U-U-M were then casted at ERL using Enrich mixer. Various stages of casting are shown in Figure 5.7.

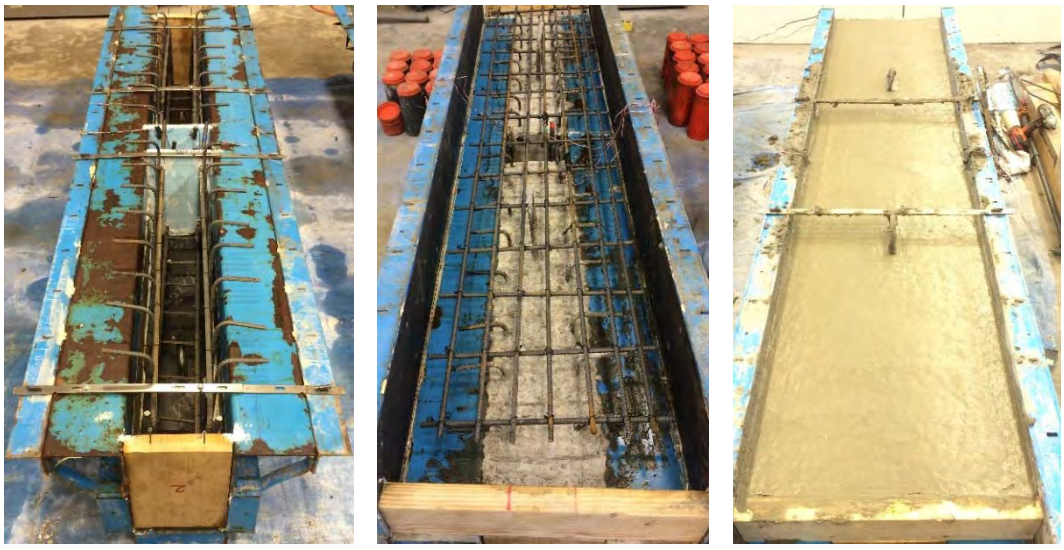

(a) (b) (c)

(d) (e)

Figure 5.7 Various stages of Phase two casting

5.2. DATA ACQUISITION

5.2.1. Actuators. To test the beams, large actuators located at Missouri S&T were used shown in Figure 5.8. These actuators each with a 140 kips load capacity were used to test the specimens during Phases one & two of research.

Figure 5.8 Actuators at High-bay structures lab at Missouri S&T

5.2.2. Deflection. To study the ductile behavior of the specimens, LVDTs were installed as shown in Figure 5.9 and Figure 5.11. Three LVDT's were used. One on the midspan in the joint, other two located at quarter span to study the deflection of the beams with respect to the joint.

Figure 5.9 LVDT at midspan

5.2.3. Strain. Strain gauges were installed on reinforcement to measure the strain in the reinforcement while testing. Strain gauges were installed in various location around the joint to study the behavior of steel in the joint and outside the joint. 2 strain gauges were installed on the tensile reinforcement and two were installed on the compression reinforcement to see if the steel reaches the yield stress value of 0.00207 in/in for a grade 60 steel rebar. The location of the strain gauges is shown in Figure 5.12, and Figure 5.13 and nomenclature explained in Table 5.1. The rebar surface was ground and cleaned to adhere the strain gauge. Then using M Coat-F kit by Vishay measurements, the strain gauges were adhered to the rebar. To protect the gauge, a clay dough type material was used along with rubber pad after which nitrile rubber coating was applied and rested for a few minutes to harden after which metallic tape was adhered over which gorilla tape was applied. These steps are shown in Figure 5.10.

Figure 5.10 Strain gauge installation

Figure 5.11 Data acquisition

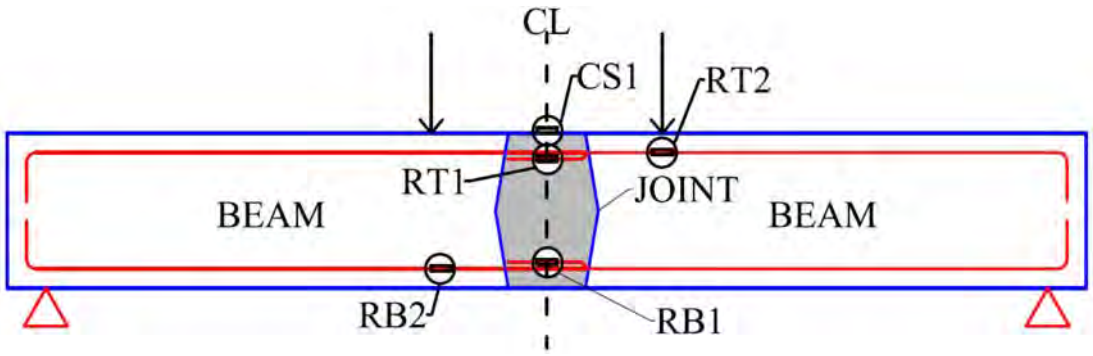

Figure 5.12 Location of strain gauges in Phase one

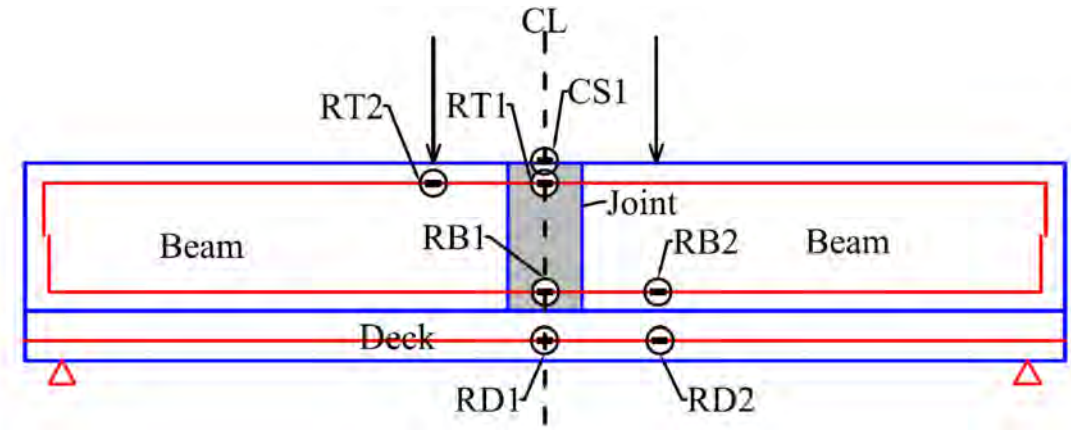

Figure 5.13 Location of strain gauges in Phase two

The plots for peak versus strain are in appendix B at the end of the report.

Table 5.1 Explanation of strain gauge locations

Nomenclature	Strain value	Location of strain gauge
RB1	Strain value reported is corresponding to the peak load in the reinforcement or concrete surface not the peak strain	On tensile reinforcement at midspan
RB2		On tensile reinforcement under the load point
RT1		On compressive reinforcement at midspan
RT2		On compressive reinforcement under the load point
RD1		On deck reinforcement at midspan
RD2		On deck reinforcement under the load point
CS1		On Concrete surface

5.3. FRESH CONCRETE PROPERTIES

The fresh concrete properties evaluated during this research include slump for CC, slump flow, and J-ring for HS-SCC and flow table for UHSC. The procedures for the experiments are briefly described in following sub-sections with deviations (if deviated) mentioned.

5.3.1. Slump Cone. ASTM C143 "Standard Test Method for Slump of Hydraulic-Cement Concrete" was followed while testing. Slump and water content can be used to estimate the strength of the concrete. The slump cone test was used while casting the beams. A typical slump test is shown in Figure 5.14.

For Phase one, three batches of CC casting was done at Missouri S&T for the control specimens, for the beam specimens for HS-SCC joint and another for UHSC joint specimens. For Phase two one batch of casting using CC was done. The results are summarized in Table 5.2.

Table 5.2 Results of Slump cone testing on CC

Specimen		Slump in. (mm)
Phase one	B1	8 (203)
	B2	6 (152)
	B3	6 (152)
Phase two		8 (203)

Conversion 1-in. = 25.4 mm

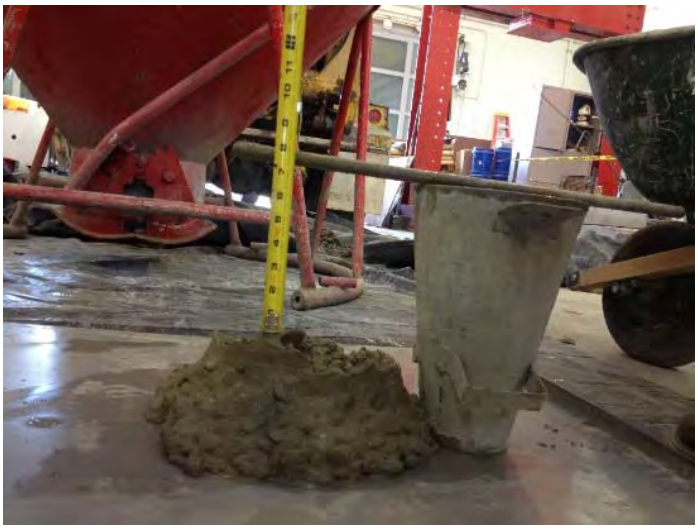

Figure 5.14 Slump cone

5.3.2. Slump Flow. ASTM C1611 “Standard Test Method for Slump Flow of Self-Consolidating Concrete” was followed to test the slump flow of HS-SCC. This method was used to determine the consistency and unconfined flow potential to evaluate the flow-ability of concrete through formwork and segregation in concrete. Slump flow is given in Table 5.3.

5.3.3. J-ring. ASTM C1621 “Standard Test Method for Passing Ability of Self-Consolidating Concrete by J-Ring” was followed to test the passing ability of High Strength Self-Consolidating concrete. This method was used to determine the consistency and unconfined flow potential to evaluate the flow-ability of concrete through formwork when rebars were present. The J-ring flow readings are given in Table 5.3.

Table 5.3 Results of Slump flow and J-ring tests on HS-SCC

Test	Diameter in. (mm)	T50 (secs)
Slump flow	26 (660)	2.2
J ring	27 (685)	2

Conversion 1-in. = 25.4 mm

5.3.4. Flow Table. ASTM C1437 “Standard Test Method for Flow of Hydraulic Cement” was followed to do the flow test on UHSC to ensure the mix was flow able when cast into the joint (test setup shown in Figure 5.15). This experiment similar to slump flow is used to predict the flow behavior of mortar mixes. Three batches of UHSC were mixed during Phase one. Two UHSC mixes were batched during Phase two. All UHSC mixes exceeded the flow table. Mini slump flow test was performed and diameter of slump flow was within range of 7 to 10-in. for UHSC.

Figure 5.15 Flow table

5.4. MECHANICAL PROPERTIES

The mechanical properties evaluated during this research include compressive strength, tensile strength, and modulus of elasticity. The procedures for the experiments are briefly described in following sub-sections with deviations (if deviated) mentioned.

5.4.1. Compressive Strength. ASTM C109 "Standard test method for compressive strength of Hydraulic Cement Mortars (using 2-in. or [50-mm] Cube Specimens)" and ASTM C39 "Standard test method for Compressive Strength of Cylindrical Concrete Specimens" were followed to test the Compressive strength of the cubes and cylinders respectively. 2-in. by 2-in. by 2-in. (50 mm by 50 mm by 50 mm) cubes were casted for UHSC and 4-in. by 8-in. (102 mm by 203 mm) cylinders were casted for CC beams and HS-SCC Joint (Figure 5.16 (a)).

(a) (b)

Figure 5.16 (a) Cube and cylinder specimens (b) end grinder

The cubes were tested for strength at 1 day, 3 days, 7 days, 14 days, 28 days and the day of testing. The cylinders were tested at 3 days, 7 days, 14 days, 28 days and the day of testing. A load rate of 200 lb./s (90.7 kg/s) was used for Cubes, 500 lb./s (227kg/s) was used for cylinders (Figure 5.17). As strength requirement was not met for the capping compound, end grinder (Figure 5.16 (b)) was used for making edges uniform for HS-SCC specimens. The results are given in Table 5.4. For Phase two, cylinders were

casted for CC and MoDOT B mixes and cubes for UHSC were casted to test the strength. The results are given in Table 5.5.

Figure 5.17 Testing cylinder and cube in Tinius Olsen

Table 5.4 Results of Compressive testing of Phase one

Concrete type		f'_c psi (MPa)	
		28 day	Day of test
CC	B1	4123 (28)	4315 (32)
	B2	6383 (44)	6391 (44)
	B3	6731 (46)	7211 (50)
HS-SCC	HS-SCC-1	9353 (64)	9027 (62)
UHSC	U#1	18309 (126)	15772 (109)
		18950 (130)	13758 (95)
		17834 (123)	15165 (105)

Conversion 1 psi = 0.006895 MPa

Table 5.5 Results of compressive strength of Phase two

Compressive strength f'_c psi (MPa)			
Concrete Type	Type	28 day	Day of test
CC	RC	7912 (50)	7901 (54)
	MoDOT	3426 (24)	3291 (23)
UHSC	DECK	16871 (116)	16192 (112)
	JOINT	13801 (95)	13772 (95)

Conversion 1 psi = 0.006895 MPa

5.4.2. Splitting Tensile Strength. The Splitting tensile strength specimens cast were 3-in. by 6-in. (76 mm by 152 mm) for UHSC specimens and 4-in. by 8-in. (102 mm by 203 mm) for Conventional Concrete and HS-SCC. ASTM C496 “Standard test method for Splitting Tensile Strength of Cylindrical Concrete Specimens” was followed to test these specimens. A load rate of 45 lb./s (20.41 kg/s) was applied until failure. This test was conducted on the day of testing using Tinius Olsen (Figure 5.18) at Missouri S&T.

Figure 5.18 Splitting tensile test on UHSC specimen

In Phase one for CC and HS-SCC, 4-in. by 8-in. (102 mm by 203 mm) cylinders were tested for Split tensile strength, while for UHSC 3-in. by 6-in. (76 mm by 152 mm) cylinders were tested the results of which are summarized in Table 5.6.

Table 5.6 Results of split tensile strength of Phase one

Concrete type		Split tensile strength psi (MPa)
		Test day
CC	B1	431 (2.9)
	B2	565 (3.9)
	B3	494 (3.4)
HS-SCC	HS-SCC-1	643 (4.4)
UHSC	U#1	2171 (14.9)
		2395 (16.5)
		1631 (11.2)

Conversion 1 psi = 0.006895 MPa

In Phase two, split tensile strength was tested for CC, UHSC and MoDoT B mix. 4-in. by 8-in. (102 mm by 203 mm) cylinders were tested for CC and MoDoT B mix. 3-in. by 6-in. (76 mm by 152 mm) cylinders were tested for UHSC and are tabulated in Table 5.7.

Table 5.7 Results of split tensile strength of Phase two

Concrete Type	Type	Split tensile strength psi (MPa)
CC	RC	800 (5.5)
	MoDOT	354 (2.4)
UHSC	DECK	2291 (15.8)
	JOINT	1266 (8.7)

Conversion 1 psi = 0.006895 MPa

5.4.3. Modulus of Elasticity. ASTM C469 “Standard Test method for Static Modulus of Elasticity and Poisson’s Ratio of Concrete in Compression” was followed to test the modulus of elasticity of concrete specimens. 4-in. by 8-in. (102 mm by 203 mm) cylinders were cast and test was conducted on the day of testing. A load rate of 440 lb./s (200 kg/s) was applied to the specimen. Tinius Olsen (Figure 5.19) at Missouri S&T was used to do this test and the results of Phase one and two are summarized in Table 5.8, and Table 5.9.

Figure 5.19 Modulus of elasticity testing

Table 5.8 Results of MoE tests Phase one

Concrete type		MoE Mpsi (GPa)
		Test day
CC	B1	4.25 (29.3)
	B2	5.50 (37.9)
	B3	5.50 (37.9)
HS-SCC	HS-SCC-1	5.50 (37.9)
UHSC	U#1	6.35 (43.7)
		8.12 (55.9)
		6.92 (47.7)

Conversion 1 Mpsi = 6.895 GPa

Table 5.9 Results of MOE tests of Phase two

Concrete Type	Type	MOE Mpsi (GPa)
CC	RC	5.35 (36.8)
	MoDOT	3.15 (21.7)
UHSC	DECK	6.47 (44.6)
	JOINT	6.92 (47.7)

Conversion 1 Mpsi = 6.895 GPa

5.5. CURING REGIME

The research was intended to recreate field conditions, so curing methods used in field were used, in this case Burlap. Burlap is a woven fabric made from jute or other natural fibers and when moistened retains moisture for long durations. After the specimens were a few hours old, wet sheets of burlap were used to cover the exposed surface of concrete for three days. During this period, the burlap was moistened on regular basis to avoid drying. For UHSC and HS-SCC specimens, this procedure was carried on for seven days. UHSC needs to be cured properly and its usually recommended to use steam curing, but it is not possible in field scenarios, where usually admixtures are used to help with internal curing. The curing method is shown in Figure 5.20.

For CC specimens and cylinders, the same procedure was applied. The specimens were covered with burlap but the curing regime was continued only for three days. After three days the cylinder and cubes specimens were moved to a different location and stored until the day of testing.

Figure 5.20 Curing using burlap

5.6. TEST SETUP

5.6.1. Phase One. The test setup for Phase one is shown in Figure 5.21. The test setup consisted of two supports and two load points. To create high-moment in the joint region, load points were chosen at 9-in. (229 mm) off the center on both sides of the specimen as shown in Figure 5.21 and Figure 5.22. The supports were placed at 3-in. (76 mm) off the edge of the beam on either sides. A loading rate of 0.002-in./min. (0.05 mm/min.) was applied for the specimens until failure was observed.

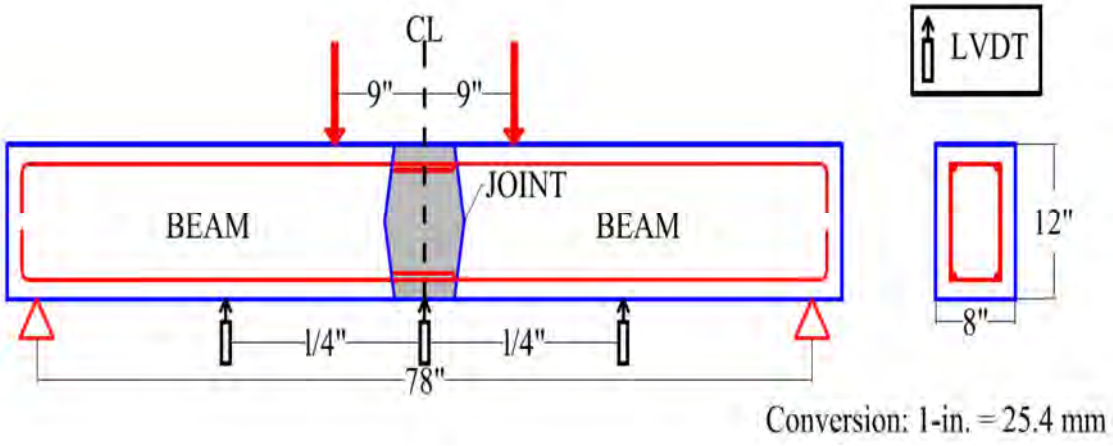

Figure 5.21 Schematic of test setup used in Phase one with cross section

Figure 5.22 Test up for Phase one

5.6.2. Phase Two. The setup used in Phase two was similar to Phase one. The aim of testing was to subject the joint region to a negative moment. To do this, the specimen was flipped upside down and load was applied on the web of T section and deck supported the specimen. Loading points were chosen at 9-in. (229 mm) off the center of the specimen on either side. The supports were placed 3-in. (76 mm) off the edge of the beam on either side. The test setup is shown in Figure 5.23 and Figure 5.24. A loading rate of 0.005-in./min. (0.13 mm/min.) was applied for the specimens until failure was observed.

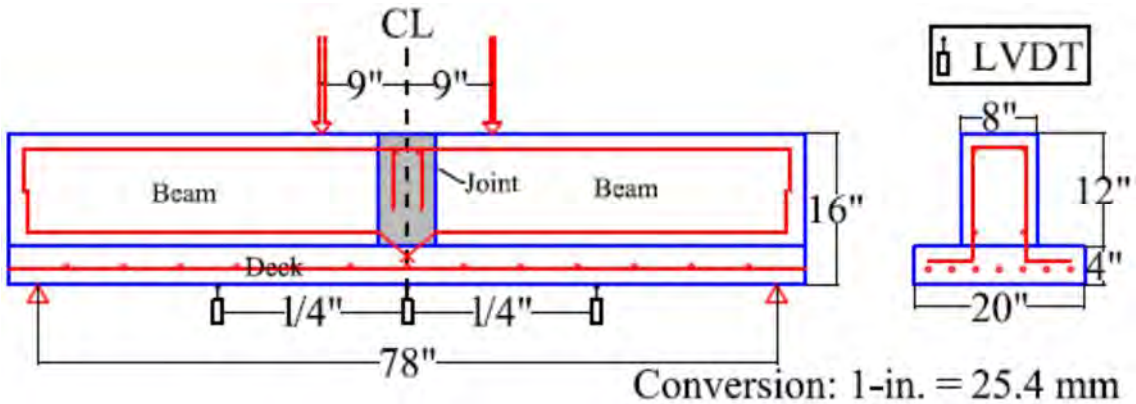

Figure 5.23 Schematic of test setup used in Phase two with cross section

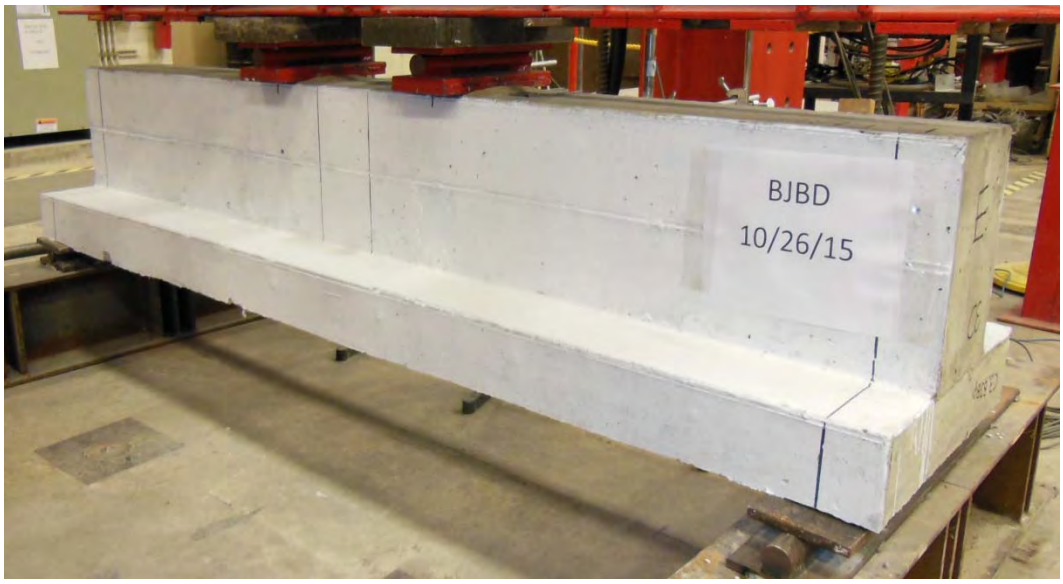

Figure 5.24 Test setup for Phase two

6. RESULTS AND DISCUSSION

This section presents the results and discussions for the two Phases of this research project. Phase one results are presented in sub-sections of Section 6.1 followed by Phase two results in sub-sections of Section 6.2. The individual load versus deflection and load versus strain plots for each specimen are given in appendices A and B respectively.

6.1. PHASE ONE: EVALUATION OF UHSC WITH DIFFERENT CONTINUITY DETAILS WITH CONNECTIONS IN HIGH MOMENT REGION

The objectives of Phase one studies was to evaluate use of UHSC in joints of bridge elements while examining the effect of varied continuity details, and surface preparations. HS-SCC was also used as joint filler to perform a comparative study. The results are organized based on the type of filler material in the joint in the following sections. The flexural and ductile behavior of the specimens were investigated and are discussed at length in the subsections of Section 6.1.

6.1.1. Control Specimens. Table.6.1 summarizes the results obtained via experimental testing for the control specimens. The peak load of the control specimens ranged from 9.0 to 30.6 kips (40 to 136 kN) and peak deflection ranged from 0.5 to 1.4-in. (12.7 to 35.6 mm).

Table.6.1 Summary of results for control specimens

Sl. no.	Specimen	Detail	Peak load kips (kN)	Peak deflection in. (mm)
1	B-1-C-N-N	Continuous	30.6 (136)	1.4 (35.6)
2	B-2-C-N-S	Straight-lap	12.4 (55)	0.5 (12.7)
3	B-3-C-N-H	Hairpin	11.7 (52)	0.5 (12.7)
4	B-4-C-N-A	Anchored	9.0 (40)	0.7 (17.8)

Conversion: 1 kip = 4.45 kN, 1-in. = 25.4 mm

6.1.1.1 Flexural behavior. Figure 6.1 summarizes the peak loads of control specimens. Specimen B-1-C-N-N was cast monolithically without any continuity detail. In this specimen, the mild tensile and compression reinforcement was continuous

throughout the length of the beam. Flexural cracks started in the middle third of specimen eventually extending to the compression zone. It reached a peak load of 30.6 kips (136 kN) and testing was stopped after reaching a peak deflection of 1.4-in (35.6 mm) due to significant crushing of concrete in the compression zone as shown in Figure 6.3. Control specimens B-2-C-N-S, B-3-C-N-H, and B-4-C-N-A were monolithically casted with three continuity details at midspan (straight-lap, hairpin and anchored respectively) to be used as secondary controls. The secondary controls behaved similar to each other (Figure 6.3) characterized by similar cracking patterns and failure by slippage and debonding of the longitudinal reinforcement in the continuity detail. Flexural cracking initiated in the midspan of the specimens. Cracking was localized to the midspan with cracks propagating along the depth of the beam indicating a weak link, which was discontinuity in the rebar detail. Other specimens will evaluate if an alternate joint filler (HS-SCC or UHSC) when used with these continuity details would create the required continuity for improvement in the performance. Steel in the tensile region reached yield strain for the specimen B-1-C-N-N. No significant strain development was seen in other specimens. The strain in the longitudinal reinforcement is tabulated in Table 6.2.

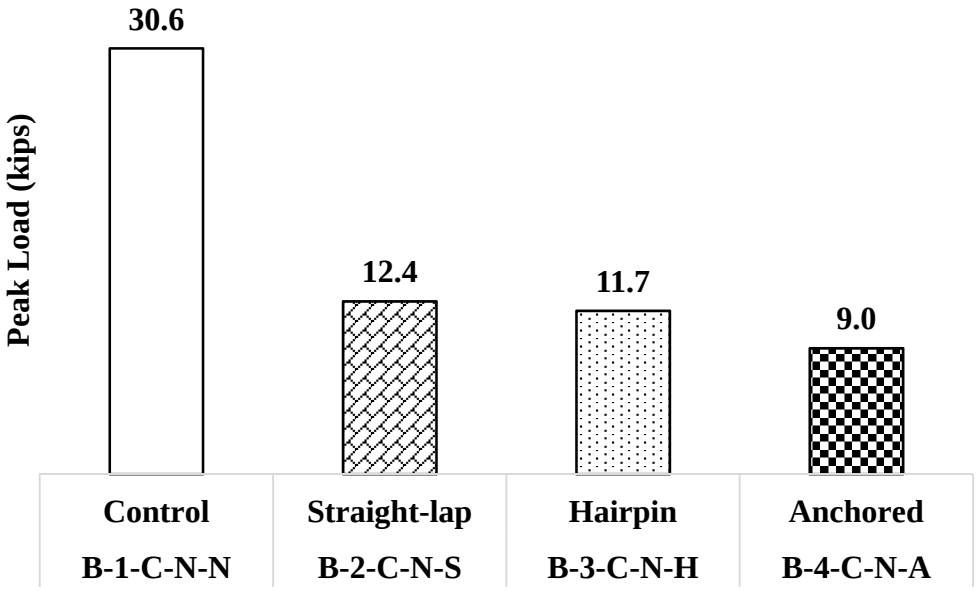

Figure 6.1 Peak loads of control specimens with different rebar detailing

Table 6.2 Strain readings measured on the joint reinforcing bars

Sl.no.	Specimen	RB1 (in. /in.)	RB2 (in. /in.)	RT1 (in. /in.)	RT2 (in. /in.)	Yield strain (in. /in.)
1	B-1-C-N-N	0.00202	0.00248	-0.00171	-0.00289	0.00267
2	B-2-C-N-S	-0.00053	0.00000	0.00000	0.00000	0.00267
3	B-3-C-N-H	0.00000	-0.00013	0.00000	0.00000	0.00267
4	B-4-C-N-A	-0.00010	-0.00012	0.00038	0.00061	0.00207

* Strain locations are discussed in Section 5.2 for reference

6.1.1.2 Ductility index. Load versus deflection plots for the control specimens are illustrated in Figure 6.2. For control specimen B-1-C-N-N, load gain was characterized with an increase in deflection until peak load was attained, after which load dropped gradually with increase in deflection before the loading was stopped due to a concrete crushing failure in the top compression zone. Secondary control specimens were not able to attain a peak load similar to specimen B-1-C-N-N. Load-deformation curves indicated an increase in capacity until peak load after which the load dropped significantly indicating slippage and a debonding type failure in the specimen as shown in Figure 6.3 for the secondary controls. Load-deformation curve for specimen B-1-C-N-N is shown in Figure 6.2 indicated a gradual load drop signifying crushing type failure.

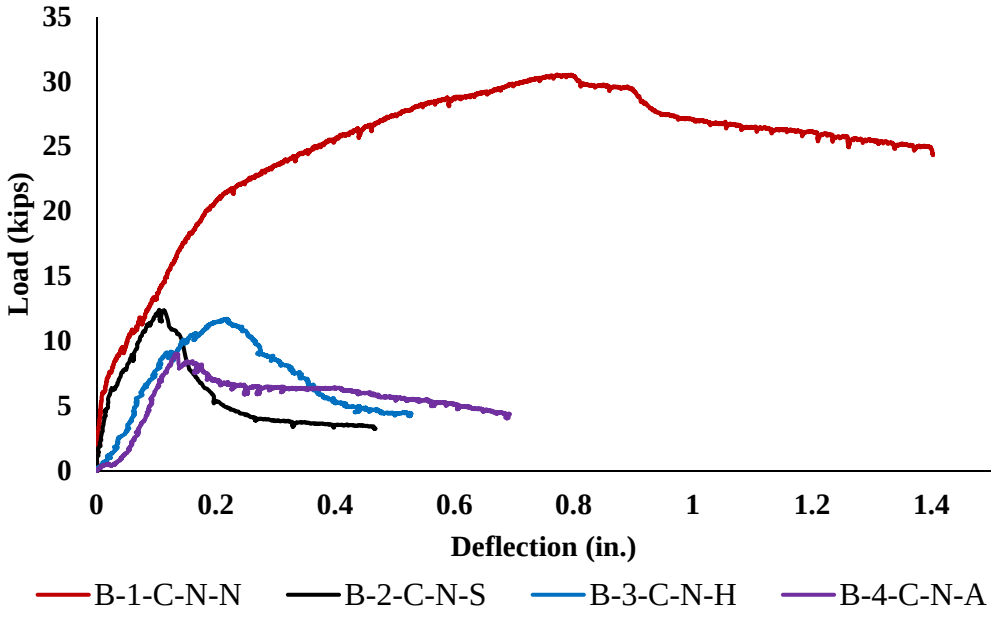

Figure 6.2 Load versus deflection of control specimens

To investigate the deformation ductility of the joint sections and the members as a whole, a Ductility Index (DI) assessment was conducted on the results obtained from load-deflection curves. For all specimens, the area under the curve was calculated by obtaining a 4th degree polynomial equation of the load-deflection curve from an excel spreadsheet and integrated over the limits of each curve (80% of peak load after specimen started failing) using trapezoidal rule. This value yields the area under the curve which when compared with area under the curve of another specimen provides an indication about the relative deflection ductility behavior of the respective specimens. Two DI's were computed to compare the specimens with primary and secondary controls. These were identified as Ductility Index-1 (DI-1) and Ductility Index-2 (DI-2) respectively. DI-1 will be the ratio of area under the curve of a specimen and primary control specimen B-1-C-N-N. DI-2 can be defined as the ratio of area under the curve of a specimen and its respective secondary control. For example, DI-2 of a specimen with straight-lap configuration will be the ratio of its area under the curve and area under the curve of control with straight-lap rebar configuration. A DI value of 1 or greater indicates that the specimen has attained the ductility of the respective control it is being compared to. These DI's are summarized in Table 6.3 for the control specimens.

Table 6.3 Ductility index (DI) results of controls

Sl. no.	Specimen	Detail	Area under curve	DI-1	DI-2
1	B-1-C-N-N	Control	34.63	1.00	-
2	B-2-C-N-S	Straight-lap	2.74	0.08	1.00
3	B-3-C-N-H	Hairpin	3.94	0.11	1.00
4	B-4-C-N-A	Anchored	3.83	0.11	1.00

DI-1: Ductility of specimen with respect to primary control
DI-2: Ductility of specimen with respect to secondary control

Figure 6.3 illustrates the control specimens at failure. When specimen B-1-C-N-N is compared to remaining specimens, it can be clearly seen that none of the specimens were able to create continuity for the beam to sustain the loading. The control specimens B-2-C-N-S, B-3-C-N-H, and B-4-C-N-A failed by slippage caused by the discontinuity of the reinforcement detail in the mid span region. It can be studied if the material to be used

as joint filler used will be able to create the required continuity when compared with control specimens.

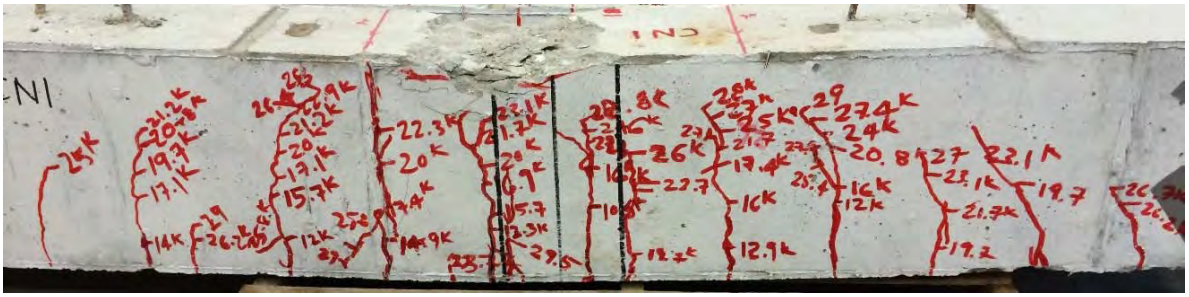

(a) Specimen B-1-C-N-N

(b) Specimen B-2-C-N-S

(c) Specimen B-3-C-N-H

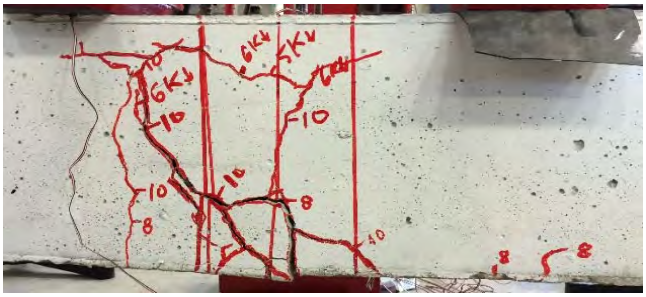

(d) Specimen B-4-C-N-A

Figure 6.3 Control specimens at failure

6.1.2. HS-SCC Specimens. HS-SCC was used as joint filler in nine specimens all of which are presented in this section. The results of experimental testing are discussed in sub-sections of 6.1.2 based on type of continuity detail used in the joint region.

6.1.2.1 Straight-lap. Table 6.4 summarizes the results obtained from HS-SCC joint specimen testing with straight-lap detail. When compared with Control B-1-C-N-N, none of the specimens surpassed its performance in flexure or in ductility. The peak loads ranged from 9.7 to 11.6 kips (43 to 52 kN). The peak deflections ranged from 0.2 to 0.3-in. (5.0 to 7.6 mm). The flexural and ductile behaviors are discussed in the following sub-sections.

Table 6.4 Summary of results for HS-SCC specimens with straight-lap detail

Sl. no.	Specimen	Joint-detail	Surface-prep	Peak load kips (kN)	Peak deflection in. (mm)
1	B-1-C-N-N	Control	Control 1	30.6 (136)	1.4 (35.5)
2	B-2-C-N-S	Straight-lap	Control 2	12.4 (55)	0.5 (12.7)
3	B-5-H-N-S		Smooth	9.7 (43)	0.2 (5.0)
4	B-8-H-R-S		Rough	11.6 (52)	0.3 (7.6)
5	B-11-H-S-S		Sand blasted	9.8 (44)	0.3 (7.6)

Conversion: 1 kip = 4.45 kN, 1-in. = 25.4 mm

6.1.2.1.1 <u>Flexural behavior.</u> Figure 6.4 summarizes the peak loads of HS-SCC specimens with a Straight-lap detail in the connections. Specimen B-8-H-R-S (11.6 kips/52 kN) with a rough surface preparation was the only specimen to attain a peak load similar to the control specimen B-2-C-N-S (12.4 kips/55 kN). In case of other specimens, even though the material (HS-SCC) was more cost effective than UHSC, the detail was not very effective in improving the capacity when used with a HS-SCC joint filler. Slippage and debonding of longitudinal reinforcement in the joint region was mode of failure observed in the HS-SCC specimens, as shown in Figure 6.6, indicating that the bond between joint filler and rebar was a weak link in the detail. It was observed that crack propagation initiated from the beam-joint interface for these specimens accompanied by a sudden load drop due to slip in the joint usually characterized by a horizontal crack in the tensile zone shown in Figure 6.6. This means that HS-SCC used in

the connections was not fully effective in utilizing the full capacity of reinforcement, which led to premature slipping failure in the connection. Specimen B-11-H-R-S's mild steel reached yield strain in compression reinforcement. Specimen B-8-H-R-S's tensile reinforcement reached yield strain. Strain readings are tabulated in Table 6.5.

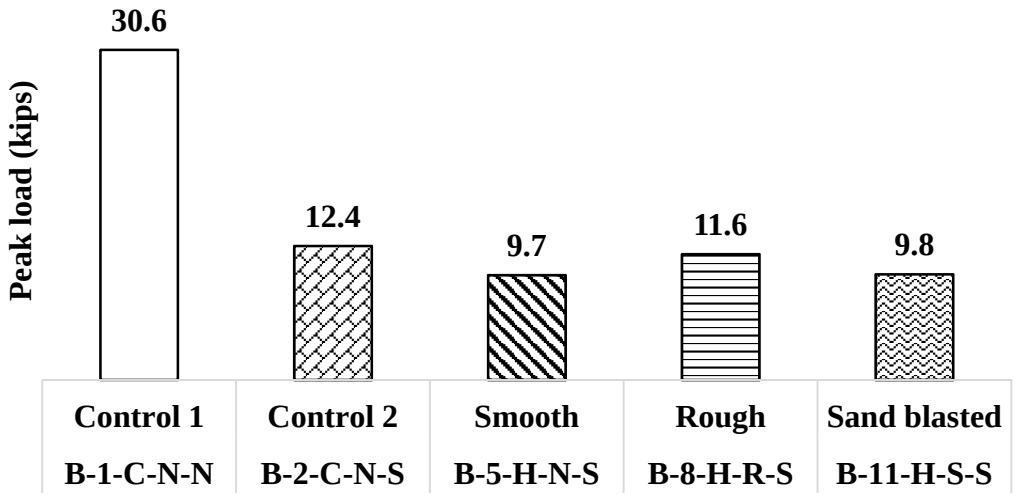

Figure 6.4 Peak loads of HS-SCC specimens with Straight-lap joint detail

Table 6.5 Strain readings measured on the joint reinforcing bars

Sl.no.	Specimen	RB1 (in. /in.)	RB2 (in. /in.)	RT1 (in. /in.)	RT2 (in. /in.)	Yield strain (in. /in.)
1	B-5-H-N-S	0.00070	0.00000	0.00000	0.00000	0.00267
2	B-8-H-R-S	0.00000	0.04000	0.02370	0.02394	0.00267
3	B-11-H-S-S	0.00022	0.00060	0.00001	0.02802	0.00267

* Strain locations are discussed in Section 5.2 for reference

6.1.2.1.2 <u>Ductility index.</u> Ductility of HS-SCC specimens was not significant compared with primary control specimen B-1-C-N-N as illustrated in Figure 6.5. HS-SCC specimens followed a trend similar to specimen B-2-C-N-S in terms of load gain and failure mode which can be seen from the Figure 6.5 and Figure 6.6. It is an indication that HS-SCC was not very effective in creating a continuity to enhance the performance of the section. However, it must be noted that the test specimens are tested to create a high-moment load which is not the usual scenario. HS-SCC can be used in joints where the concentration of loads is very minimal like in bridges in counties.

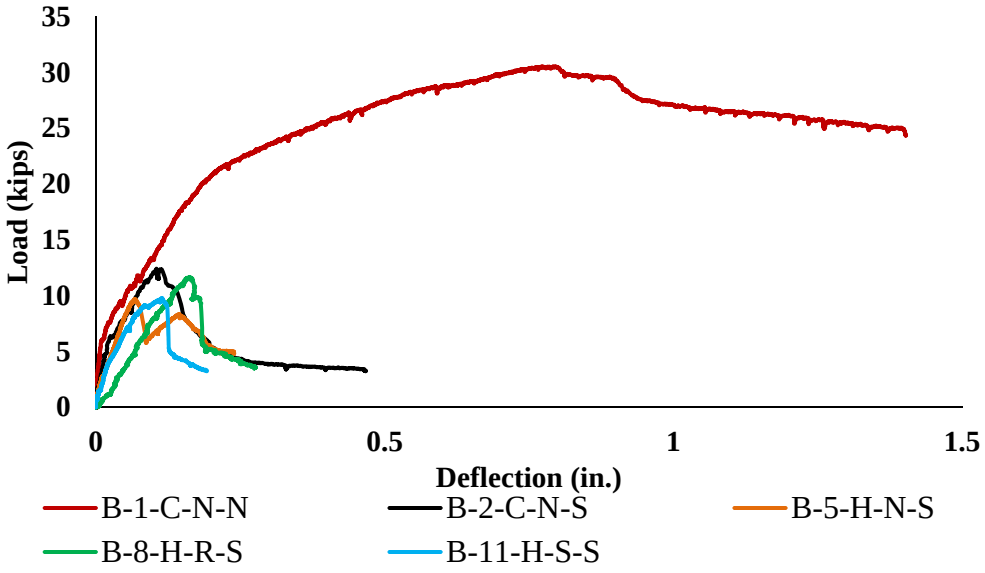

Figure 6.5 Load versus deflection of straight-lap HS-SCC-joint specimens

The results of ductility index study are summarized in Table 6.6. DI-1 values indicate that HS-SCC specimens did not attain ductility similar to specimen B-1-C-N-N indicated by the DI-1 less than 1. It can be inferred from the DI-2 values that HS-SCC specimens were 50% less ductile compared to its secondary control specimen B-2-C-N-S's performance. HS-SCC though high in compressive strength might not be the strongest material to be used in the connection. The poor quality of aggregate and poor bond between HS-SCC and rebar effected the final performance of the joint, which in-turn led to slippage and a debonding failure as seen in Figure 6.6.

Table 6.6 DI results of HS-SCC joint specimens with straight-lap detail

Sl. no.	Specimen	Detail	Area under curve	DI-1	DI-2
1	B-1-C-N-N	Control	34.63	1.00	-
2	B-2-C-N-S	Straight-lap	2.74	0.08	1.00
3	B-5-H-N-S		1.52	0.04	0.56
4	B-8-H-R-S		1.55	0.04	0.57
5	B-11-H-S-S		1.28	0.04	0.47

DI-1: Ductility of specimen with respect to primary control
DI-2: Ductility of specimen with respect to secondary control

(a) Specimen B-5-H-N-S

(b) Specimen B-8-H-R-S

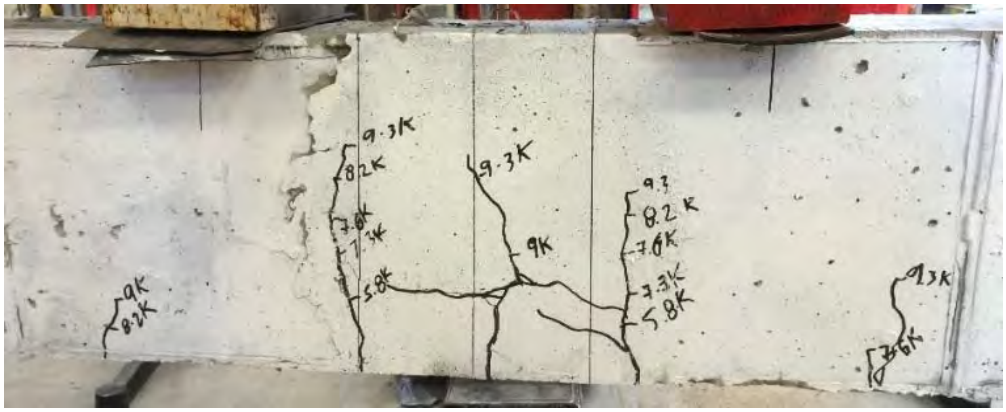

(c) Specimen B-11-H-S-S

Figure 6.6 HS-SCC straight-lap specimens at failure

6.1.2.2 Hairpin. The results obtained from testing HS-SCC specimens with hairpin detail are summarized in Table 6.7. Hairpin detail with HS-SCC peak loads ranged from 12.2 to 14.3 kips (54 to 64 kN) which is an improvement over straight-lap

detail. The peak deflections range from 0.3 to 0.6-in. (7.6 to 15.4 mm). The flexural and ductile behaviors are discussed in following subsections.

Table 6.7 Summary of results for HS-SCC joint specimens with hairpin detail

Sl. no.	Specimen	Detail	Surface prep	Peak load kips (kN)	Peak deflection in. (mm)
1	B-1-C-N-N	Control	Control 1	30.6 (136)	1.4 (35.5)
2	B-3-C-N-H	Hairpin	Control 3	11.7 (52)	0.5 (12.7)
3	B-6-H-N-H		Smooth	13.1 (58)	0.6 (15.2)
4	B-9-H-R-H		Rough	12.2 (54)	0.3 (7.6)
5	B-12-H-S-H		Sand blasted	14.3 (64)	0.4 (10.1)

Conversion: 1 kip = 4.45 kN, 1-in. = 25.4 mm

6.1.2.2.1 <u>Flexural behavior.</u> The peak loads obtained by testing HS-SCC-joint specimens with hairpin detail are illustrated in Figure 6.5. Specimens B-6-H-N-H (13.1 Kips/ 58 kN), B-9-H-R-H (12.2 kips/ 54 kN), and B-12-H-S-H (14.3 kips/ 64 kN) both attained a capacity greater than control specimen B-3-C-N-H (11.7 kips / 52 kN) by 12 %, 4% and 22% respectively. Hairpin detail has more area of reinforcement in the joint compared to other details indicating the reason for slight improvement in capacity over the other two details when used with a HS-SCC joint filler. When compared to specimen B-1-C-N-N, primary control's peak load of 30.6 Kips (136 kN) the hairpin detail was not every effective in improving the capacity when used with a HS-SCC joint filler. Specimen failure initiated with crack propagation from the beam-joint interface. After attaining the peak load, the reinforcement in the joint slipped leading to significant load drop and failure as shown in Figure 6.9. Strain readings are tabulated in Table 6.8. None of the specimens' reinforcement reached yield strains for the hairpin detail. Specimen B-12-H-S-H outperformed the other specimens' peak load behavior.

Table 6.8 Strain readings measured on the joint reinforcing bars

Sl.no.	Specimen	RB1 (in. /in.)	RB2 (in. /in.)	RT1 (in. /in.)	RT2 (in. /in.)	Yield strain (in. /in.)
1	B-6-H-N-H	0.00000	0.00000	0.00031	0.00006	0.00267
2	B-9-H-R-H	0.00211	0.00207	0.00027	-0.00014	0.00267
3	B-12-H-S-H	0.00031	0.00102	-0.00005	0.00000	0.00267

* Strain locations are discussed in Section 5.2 for reference

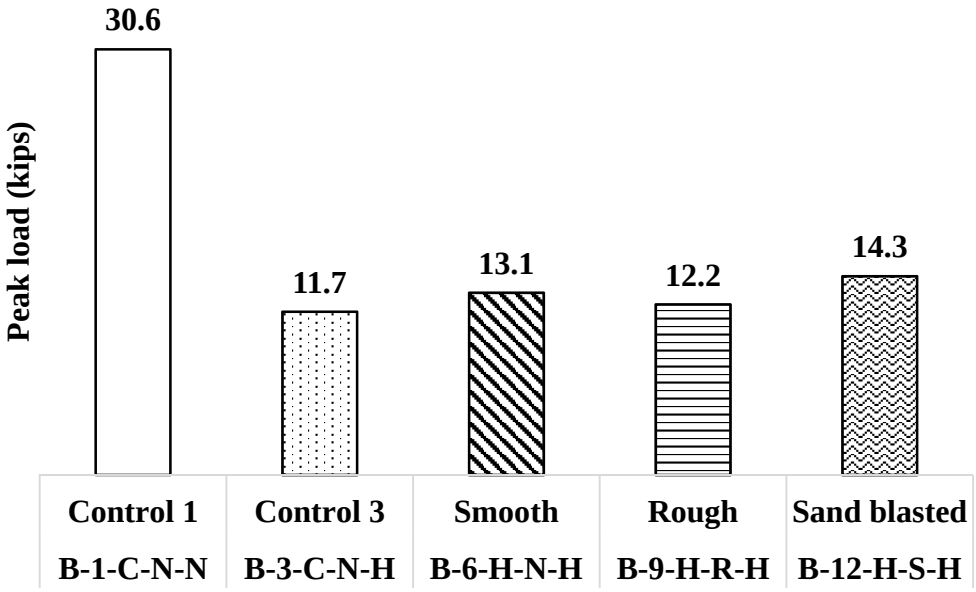

Figure 6.7 Peak loads of HS-SCC specimens with hairpin detail

6.1.2.2.2 <u>Ductility index.</u> Hairpin detail was the best detail to be used with with a HS-SCC joint filler. The load deflection plot shown in Figure 6.8 indicates that specimens with hairpin detail were more ductile than their respective control specimen B-3-C-N-H.

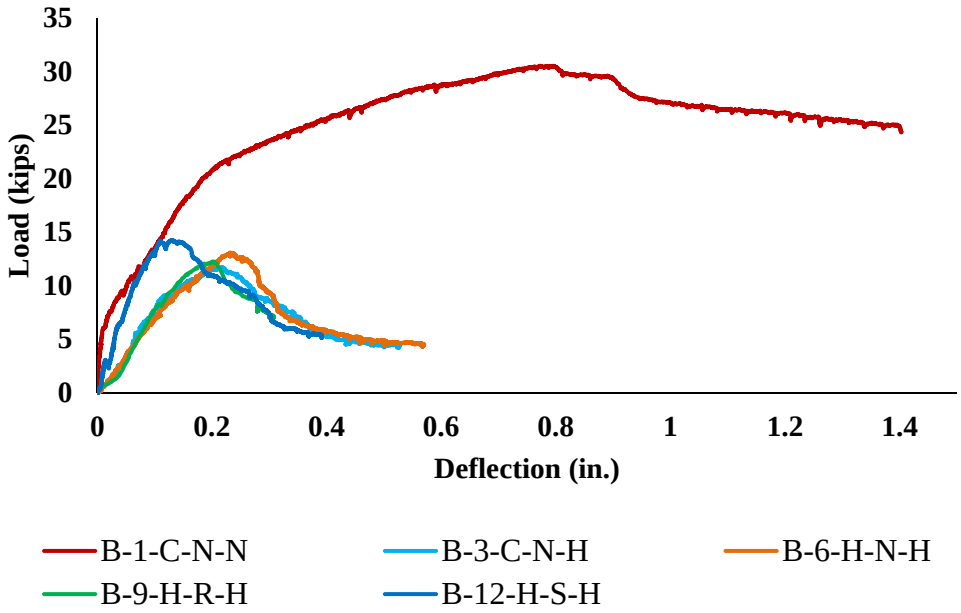

Figure 6.8 Load versus deflection of hairpin HS-SCC-joint specimens

Load gain curves of the specimens followed a very close trend with their secondary control. As for the ductility with respect to primary control B-1-C-N-N, none of the specimens were able to attain similar behavior. It indicates that HS-SCC joint filler with hairpin detail could be used in low moment regions without significant effects.

DI study results are summarized in Table 6.9. DI study indicated that hairpin detail specimens with a HS-SCC joint filler were able to surpass the secondary control performance but not the primary control.

Table 6.9 DI results for HS-SCC joint specimens with hairpin detail

Sl. no.	Specimen	Detail	Area under curve	DI-1	DI-2
1	B-1-C-N-N	Control	34.63	1.00	-
2	B-3-C-N-H	Hairpin	3.94	0.11	1.00
3	B-6-H-N-H		4.03	0.12	1.02
4	B-9-H-R-H		2.43	0.07	0.62
5	B-12-H-S-H		3.69	0.11	0.93

DI-1: Ductility of specimen with respect to primary control
DI-2: Ductility of specimen with respect to secondary control

DI-1 indicates that most of the specimens were only able to reach at least 7% of primary controls ductility. DI-2 values however show that the specimens were able to attain 90% of secondary control ductility. It can also be inferred from DI-2 values that there was no significant effect of surface preparation on beam joint interface as specimen with no surface preparation performed better than sandblasted or roughened surfaces.

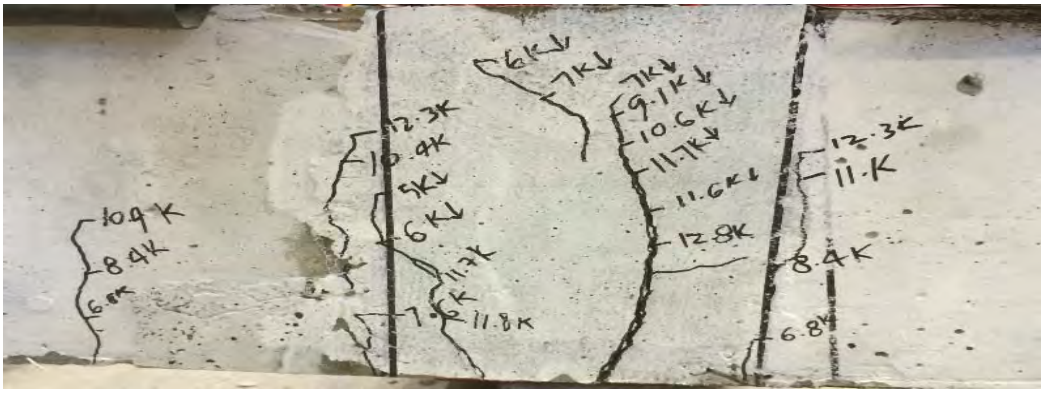

(a) Specimen B-6-H-N-H
Figure 6.9 HS-SCC hairpin specimens at failure

(b) Specimen B-9-H-R-H

(c) Specimen B-12-H-S-H

Figure 6.9 HS-SCC hairpin specimen at failure (cont.)

6.1.2.3 Anchored. Table 6.10 summarizes the results obtained by testing anchored detail with a UHSC filler. Anchored/headed detail peak loads ranged from 6.7 to 7.8 kips (30 to 35 kN). The peak deflections ranged from 0.2 to 0.4-in. (5 to 10 mm).The flexural and ductile behavior of the headed/anchored specimens are discussed in the following subsections.

Table 6.10 Summary of results for HS-SCC joint specimens with anchored detail

Sl. No.	Specimen	Detail	Surface prep	Peak load kips (kN)	Deflection in. (mm)
1	B-1-C-N-N	Control	Control 1	30.6 (136)	1.4 (35.5)
2	B-4-C-N-A	Anchored	Control 4	9.0 (40)	0.7 (17.8)
3	B-7-H-N-A		Smooth	7.1 (32)	0.3 (7.6)
4	B-10-H-R-A		Rough	7.8 (35)	0.2 (5.0)
5	B-13-H-S-A		Sand blasted	6.7 (30)	0.4 (10.1)

Conversion: 1 kip = 4.45 kN, 1-in. = 25.4 mm

6.1.2.3.1 Flexural behavior. The peak loads obtained from testing the anchored detail with a HS-SCC filler are illustrated in Figure 6.10. Specimens attained a peak load of 86% of the control specimen B-4-C-N-A peak load. Straight-lap and hairpin details (discussed in Section 6.1.2) outperformed the anchored detail in terms of peak load capacity by 50% on an average when only roughened specimens are considered. The performance of anchored detail was not very significant when compared to control specimen B-1-C-N-N (30.6 kips/136 kN) peak behavior. Lap-length used anchored detail (3.5-in. /89 mm) was the least when compared to straight-lap (6-in. /152 mm) or hairpin (3.9-in. /99mm), which could be one of the reasons which yielded such low peak loads. Either straight-lap or hairpin detail when used with HS-SCC joint filler were able to attain a peak load similar to secondary control but the anchored detail resulted in lowest peak loads. The crack propagation initiated from typical beam-joint interface leading to failure characterized by horizontal crack indicating slippage. The weak bond between HS-SCC and longitudinal reinforcement resulted in slippage and a debonding type failure in the connection as shown in Figure 6.12. HS-SCC though cost effective, was not the strong material required to sustain high-moment load as illustrated by peak loads for specimens being lower than their respective controls. Tensile reinforcement in specimen B-13-H-S-A reached yield strain, but no significant strains were developed in other specimens. Strain readings are given in Table 6.11.

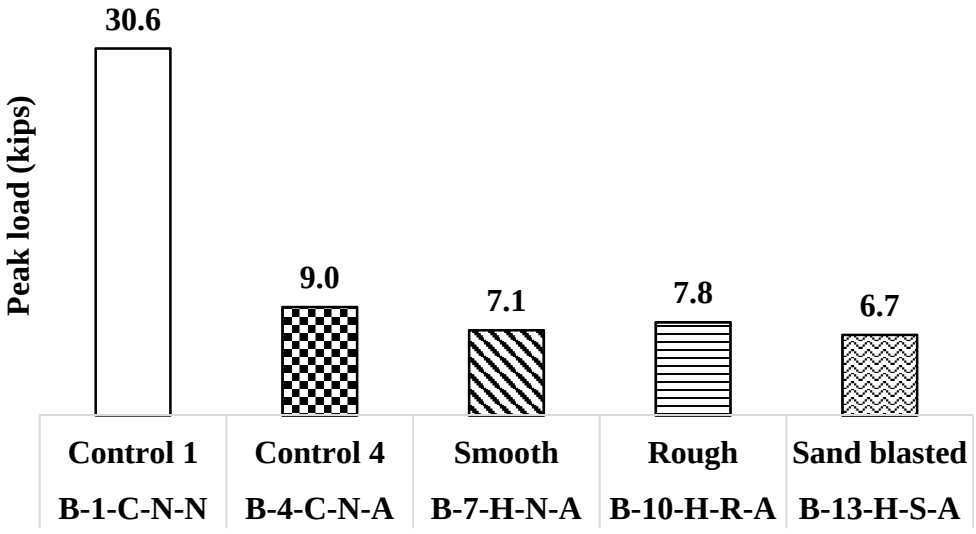

Figure 6.10 Peak loads of HS-SCC specimens with Anchored rebar detail

Table 6.11 Strain readings measured on the joint reinforcing bars

Sl.no.	Specimen	RB1 (in. /in.)	RB2 (in. /in.)	RT1 (in. /in.)	RT2 (in. /in.)	Yield strain (in. /in.)
1	B-7-H-N-A	0.00042	0.00000	0.00000	-0.00022	0.00267
2	B-10-H-R-A	0.00089	0.00117	-0.00059	0.00000	0.00267
3	B-13-H-S-A	0.00170	0.03594	0.00000	0.00019	0.00267

* Strain locations are discussed in Section 5.2 for reference

6.1.2.3.2 <u>Ductility index.</u> The anchored specimens with a HS-SCC joint followed load gain trend very close to their secondary control specimen B-4-C-N-A as shown in Figure 6.11. Anchored detail with HS-SCC was not very effective in improving the ductile behavior of the specimens.

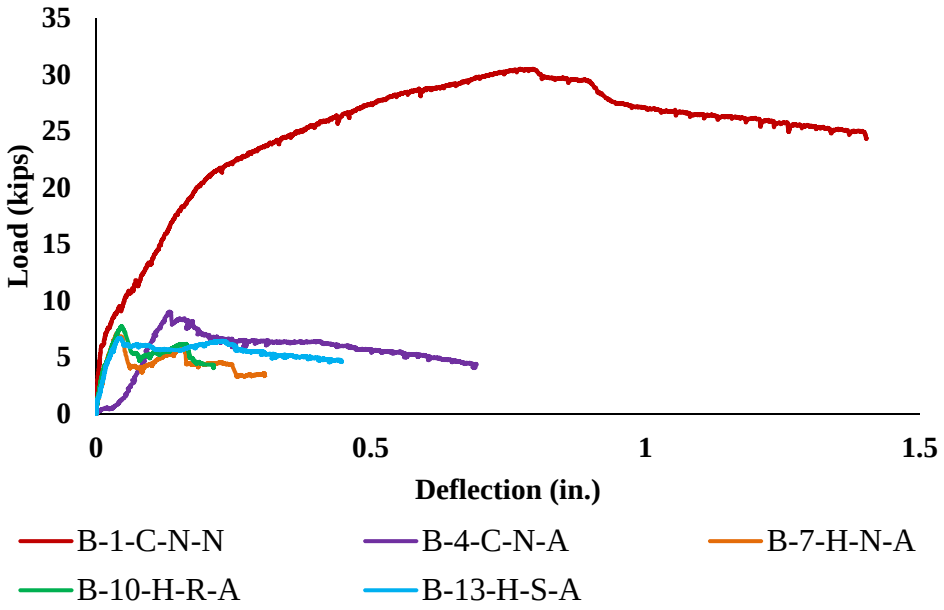

Figure 6.11 Load versus deflection of anchored HS-SCC-joint specimens

DI results are summarized in Table 6.12 indicate that the ductile behavior of anchored detail with UHSC was not significant. DI-1 values indicate that only B-13-H-S-A achieved 7% of primary control specimen B-1-C-N-N's ductility with remaining even lower. DI-2 values indicate that none of the specimens were able to attain a ductile behavior similar to secondary control specimen B-4-C-N-A, with specimen B-13-H-S-A reaching almost 65% of ductility. The ductile behavior of anchored specimens was

similar to straight-lap and hairpin details as indicated by DI values (Table 6.6, and Table 6.9). HS-SCC was not the most effective material in creating the necessary link between the beam segments and failed prematurely leading to weak performance of the specimens.

Table 6.12 DI results for HS-SCC joint specimens with Anchored detail

Sl. no.	Specimen	Detail	Area under curve	DI-1	DI-2
1	B-1-C-N-N	Control	34.63	1.00	-
2	B-4-C-N-A	Anchored	3.83	0.11	1.00
3	B-7-H-N-A		1.28	0.04	0.33
4	B-10-H-R-A		1.42	0.04	0.37
5	B-13-H-S-A		2.47	0.07	0.65

DI-1: Ductility of specimen with respect to primary control
DI-2: Ductility of specimen with respect to secondary control

(a) Specimen B-7-H-N-A

(b) Specimen B-10-H-R-A

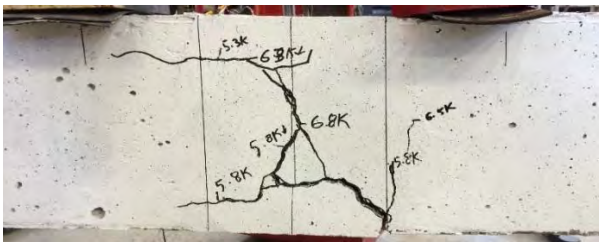

(c) Specimen B-13-H-S-A

Figure 6.12 HS-SCC anchored specimens at failure

6.1.3. UHSC Specimens. UHSC was used as joint filler in nine specimens and the results of testing conducted on them are discussed in the sub sections of Section 6.1.3 based on the type of continuity detail used in the joint region.

6.1.3.1 Straight-lap. Straight-lap detail was used in 3 UHSC specimens the results of which are summarized in Table 6.13. Unlike HS-SCC joint specimens discussed in Section 6.1.2, UHSC specimens surpassed the secondary control by 57% and reached 99% of primary control in terms of peak load performance. The peak loads ranged from 30.2 to 30.4 kips (134 to135 kN). The peak deflections ranged from 1.6 to 1.9-in. (40.6 to 48.2 mm). The flexural and ductile behavior of the specimens are discussed in the following sections.

Table 6.13 Summary of results for UHSC-joint specimens with straight-lap detail

Sl. no.	Specimen	Detail	Surface prep	Peak load kips (kN)	Peak deflection in. (mm)
1	B-1-C-N-N	Control	Control 1	30.6 (136)	1.4 (35.6)
2	B-2-C-N-S	Straight-lap	Control 2	12.4 (55)	0.5 (12.7)
3	B-14-U-N-S		Smooth	30.1 (134)	1.9 (48.3)
4	B-17-U-R-S		Rough	30.4 (135)	1.8 (45.7)
5	B-20-U-S-S		Sand blasted	30.2 (134)	1.6 (40.6)

Conversion: 1 kip = 4.45 kN, 1-in. = 25.4 mm

6.1.3.1.1 <u>Flexural behavior.</u> UHSC joint specimens gave exceptional results when used with straight-lap detail. Figure 6.13 summarizes the peak loads of the specimens. Specimen B-17-U-R-S attained 99% of specimen B-1-C-N-N's 30.6 kips (136 kN) peak load indicates that UHSC can be successfully used within joints subjected to high moment. This substantial increase in capacity can be attributed to UHSC's high tensile strength due to steel fibers. UHSC has been proven to decrease the required embedment length of rebar (Graybeal, 2010). Typical mode of failure observed was by concrete crushing outside the joint in the top compression zone of specimen, which is a complete contrast when compared with the HS-SCC joint specimens which failed due to slipping and debonding of reinforcement in tensile region of the joint. There were indications of slippage with UHSC also (Figure 6.15) but significant amount of crack propagation through UHSC did not occur when compared to HS-SCC. Crack propagation

started from the beam-joint interface at about 6 kips (27 kN). Interesting observation was that at almost 12 to 14 kips (53 to 62 kN) load, beams started cracking (Figure 6.15) engaging the beams until failure by concrete crushing in the top compression zone outside the joint region. For specimen B-17-U-R-S and specimen B-20-U-S-S, the specimen failed after reaching 30.4 and 30.2 kips (135 and 134 kN) respectively by slipping in the continuity detail but there was no indication of any debonding between UHSC and reinforcement in the connection. However, it is to be noted that crushing already started in these specimens before slip initiated. Tensile reinforcement was able to yield in all the specimens which is a very good sign that UHSC could develop significant bond with rebar and use the full capacity of the rebar. Strain readings are given in Table 6.14.

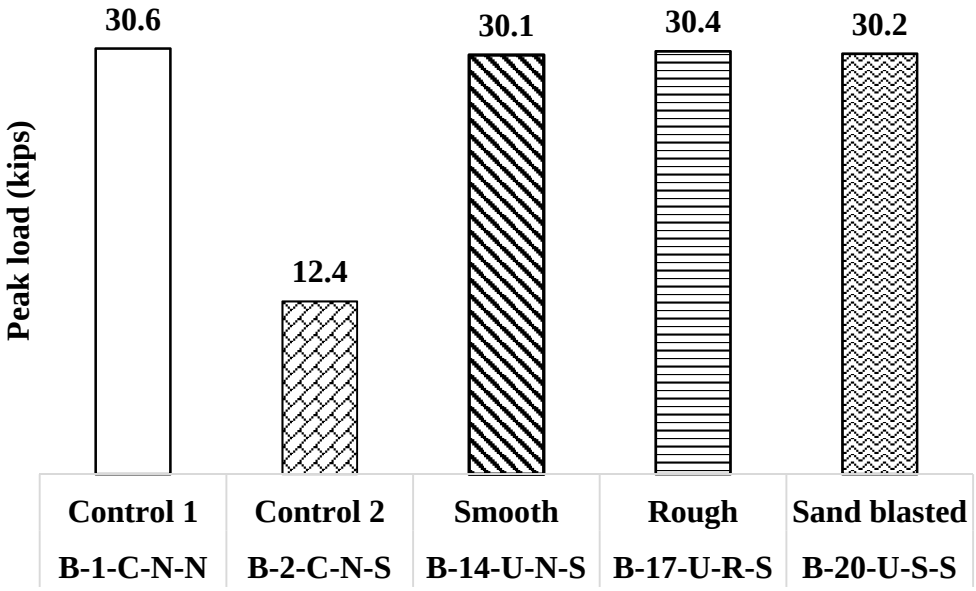

Figure 6.13 Peak loads of UHSC joint specimens with straight-lap detail

Table 6.14 Strain readings measured on the joint reinforcing bars

Sl.no.	Specimen	RB1 (in. /in.)	RB2 (in. /in.)	RT1 (in. /in.)	RT2 (in. /in.)	Yield (in. /in.)
1	B-14-U-N-S	0.00138	-0.04400	0.00085	0.00168	0.00267
2	B-17-U-R-S	0.00206	0.00000	0.00118	0.00000	0.00267
3	B-20-U-S-S	0.00025	0.00357	0.00131	0.00000	0.00267

* Strain locations are discussed in Section 5.2 for reference

6.1.3.1.2 <u>Ductility index.</u> Load versus deflection study indicates that UHSC when used with straight-lap detail in joints, surpassed the deflection of control specimens B-1-C-N-N and B-2-C-N-S as illustrated in Figure 6.14. This is a good indicator as the trend followed by the specimens was very close to the primary control. Specimens B-17-U-R-S and B-20-U-S-S showed a drop in loading but the specimen B-14-U-N-S reached 30.1 kips (134 kN) and still sustained the load without significant drop. This demonstrates that UHSC could not only reach higher loads but also sustain them increasing the structure's serviceability significantly (Figure 6.14). Specimen B-14-U-N-S did not fail by slipping in reinforcement in the joint but due to crushing of concrete in the top compression zone outside the joint region. The test was stopped after there was no significant drop in load after three hours of testing. The specimens B-17-U-R-S and B-20-U-S-S failed by slipping in the connection No debonding was observed in this case.

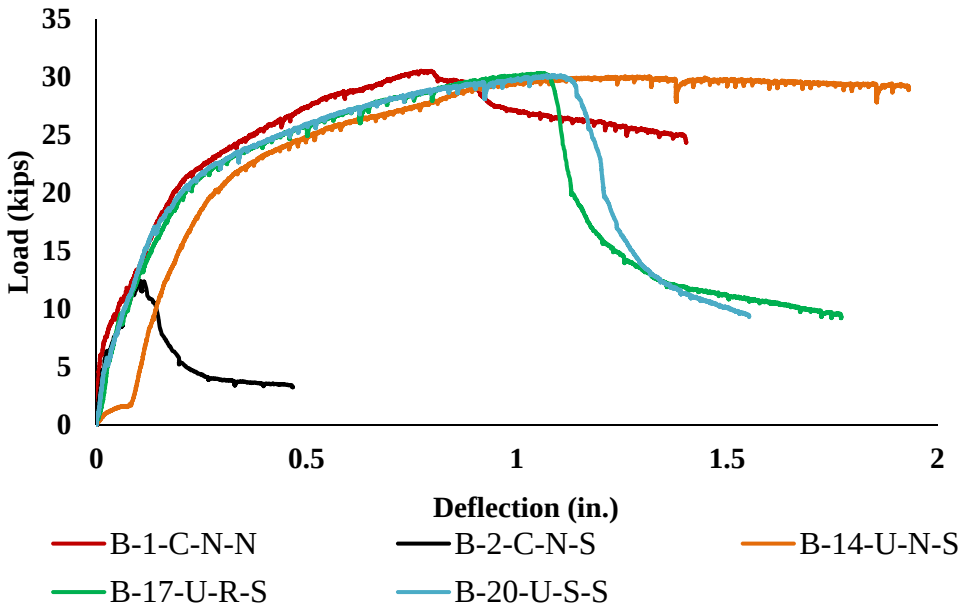

Figure 6.14 Load versus deflection of straight UHSC-joint specimens

Table 6.15 summarizes the results of DI study. It is a positive indication as DI-1 values of UHSC range from 0.98 (~1) to 1.41 (>1) indicating that specimens were able to reach or surpass the ductile behavior of control specimen B-1-C-N-N. It indicates that UHSC is a material which not only increases the flexural but also ductile performance of

the structure. DI-2 values indicate a substantial increase in capacity. UHSC when used in connections improves the ductility of structures by ten folds based on DI-2 values. This can be attributed to the steel fibers used in UHSC, which increase the strength, act as reinforcement increasing the tensile capacity, and avoid formation of micro cracking in the concrete.

Table 6.15 DI results for UHSC-joint specimens with straight-lap detail

Sl. no.	Specimen	Detail	Area under curve	DI-1	DI-2
1	B-1-C-N-N	Control	34.63	1.00	-
2	B-2-C-N-S	Straight-lap	2.74	0.08	1.00
3	B-14-U-N-S		48.72	1.41	17.81
4	B-17-U-R-S		33.87	0.98	12.38
5	B-20-U-S-S		32.38	0.94	11.83

DI-1: Ductility of specimen with respect to primary control
DI-2: Ductility of specimen with respect to secondary control

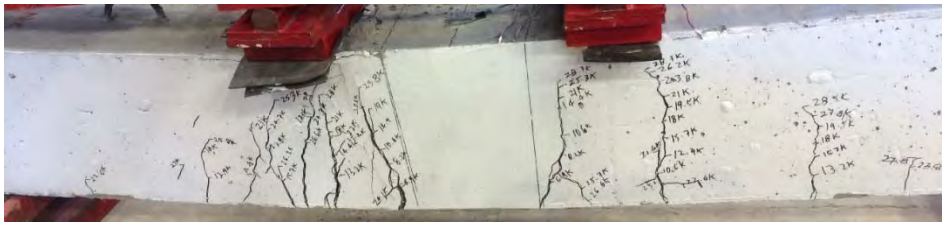

(a) Specimen B-14-U-N-S

(b) Specimen B-17-U-R-S

(c) Specimen B-20-U-S-S

Figure 6.15 UHSC straight-lap specimens at failure

6.1.3.2 Hairpin. Table 6.16 summarizes the results obtained by testing the hairpin detail with a UHSC joint filler with peak loads ranging from 28.8 to 28.9 kips (128.1 to 128.6 kN) and peak deflections ranging from 1.85 to 2.3-in. (47 to 60 mm). The flexural and ductile behaviors are discussed in the following sub-sections.

Table 6.16 Summary of results for UHSC-joint specimens with hairpin detail

Sl. No.	Specimen	Detail	Surface Prep	Peak load kips (kN)	Peak deflection in. (mm)
1	B-1-C-N-N	Control	Control 1	30.6 (136)	1.40 (35.6)
2	B-3-C-N-H	Hairpin	Control 3	11.7 (52)	0.52 (13.2)
3	B-15-U-N-H		Smooth	28.8 (128)	1.85 (47.0)
4	B-18-U-R-H		Rough	28.9 (128)	1.95 (49.5)
5	B-21-U-S-H		Sand blasted	28.9 (128)	2.37 (60.2)

Conversion: 1 kip = 4.45 kN, 1-in. = 25.4 mm

6.1.3.2.1 <u>Flexural behavior.</u> Hairpin detail used with a UHSC joint filler attained peak loads which were only 5% less than control specimen B-1-C-N-N's 30.6 kips (136 kN). The hairpin and straight-lap detail when used with UHSC surpassed the HS-SCC's peak load significantly. It can be seen from Figure 6.16, peak loads of the three specimens varied only by 0.1 kip (0.4 kN) indicating that the effect of surface preparation was not significant with UHSC as joint filler. Flexural crack propagation was similar to control specimen B-1-C-N-N with no significant cracking in UHSC region. The cracking initiated from the typical beam-joint interface but unlike straight-lap detail with UHSC where cracking was observed through joint region (Section 6.1.3.1, Figure 6.15), no significant crack propagation was observed in the UHSC joint region for hairpin detail as shown in Figure 6.18. The loading was stopped after crushing was observed in the top compression zone outside the joint region. Specimen B-21-U-S-H was further loaded manually, even after concrete crushing was observed to look at the behavior of UHSC. It was seen that further loading did not cause an increase in peaked load but resulted in rupture of longitudinal tensile reinforcement at the beam-joint interface (shown in Figure 6.18) indicating that even at high-moment loading, UHSC bond strength was significant enough to create rebar rupture outside the joint. Significant yield strain was observed in the reinforcement of the specimens signifying that UHSC was able

to yield the rebars, rebar rupture was seen specimen B-21-U-S-H. Strain readings are tabulated in Table 6.17.

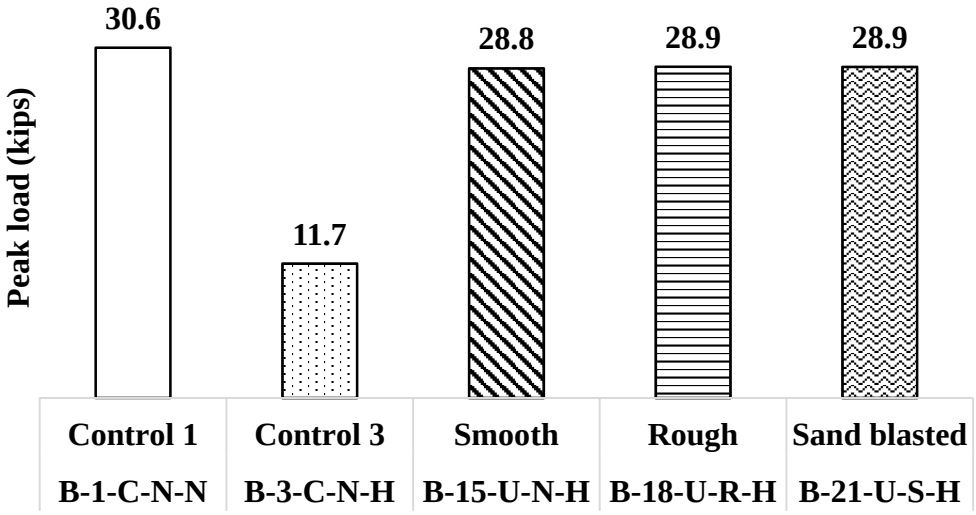

Figure 6.16 Peak loads of UHSC joint specimens with hairpin detail

Table 6.17 Strain readings measured on the joint reinforcing bars

Sl.no.	Specimen	RB1 (in. /in.)	RB2 (in. /in.)	RT1 (in. /in.)	RT2 (in. /in.)	Yield strain (in. /in.)
1	B-15-U-N-H	0.00570	0.00916	0.00036	0.00024	0.00267
2	B-18-U-R-H	0.00038	0.00001	0.00501	0.00493	0.00267
3	B-21-U-S-H	0.00062	0.00097	0.00392	0.00000	0.00267

* Strain locations are discussed in Section 5.2 for reference

6.1.3.2.2 <u>Ductility index.</u> The load versus deflection curve for hairpin detail with a UHSC filler is given in Figure 6.17. The UHSC joint specimens followed a close trend in terms of load gain and failure. As for the ductility, the specimens did not reach a higher load but did attain a greater deflection than the controls. When compared to HS-SCC specimens (Section 6.1.2.2, Figure 6.8), the UHSC specimens with hairpin detail were a lot more ductile. It can be inferred that UHSC can withstand high-moment loads and sustain these loads increasing the serviceability of the structure. From Figure 6.18 (c), and (d) it can be seen that UHSC in the joint was strong enough to withstand the high moment loading and there was no significant damage to the UHSC itself and the bond with reinforcement is sufficiently strong that rebar yielded and ultimately ruptured.

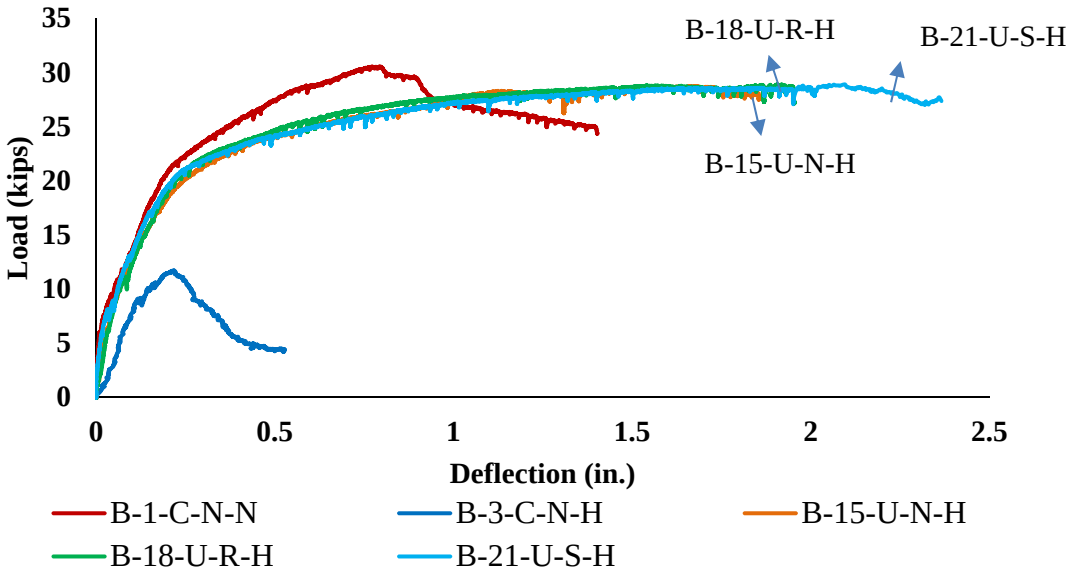

Figure 6.17 Load versus deflection of hairpin UHSC-joint specimens

Ductility index was studied and results are summarized in Table 6.18. The hairpin detail with UHSC joint filler outperformed the control specimen as indicated by DI-1 and DI-2 values. The specimens achieved at least 30% increase in ductility when compared with control specimen B-1-C-N-N ductile behavior. The effect of steel fibers is clearly seen from DI-2 values which show a significant increase in the ductile capacity when compared with secondary control. Straight-lap detail (6-in. /152.4 mm lap length) with UHSC filler when compared to hairpin detail (3.9-in. /99 mm lap length), was not able to attain similar ductility. A modified hairpin detail with UHSC and more lap length (5 to 6-in. /127 to 152 mm) could possibly improve the flexural and ductile performance significantly.

Table 6.18 DI results for UHSC-joint specimens with hairpin detail

Sl. no.	Specimen	Detail	Area under curve	DI-1	DI-2
1	B-1-C-N-N	Control	34.63	1.00	-
2	B-3-C-N-H	Hairpin	3.94	0.11	1.00
3	B-15-U-N-H		45.31	1.31	11.49
4	B-18-U-R-H		48.51	1.40	12.30
5	B-21-U-S-H		59.81	1.73	15.17

DI-1: Ductility of specimen with respect to primary control
DI-2: Ductility of specimen with respect to secondary control

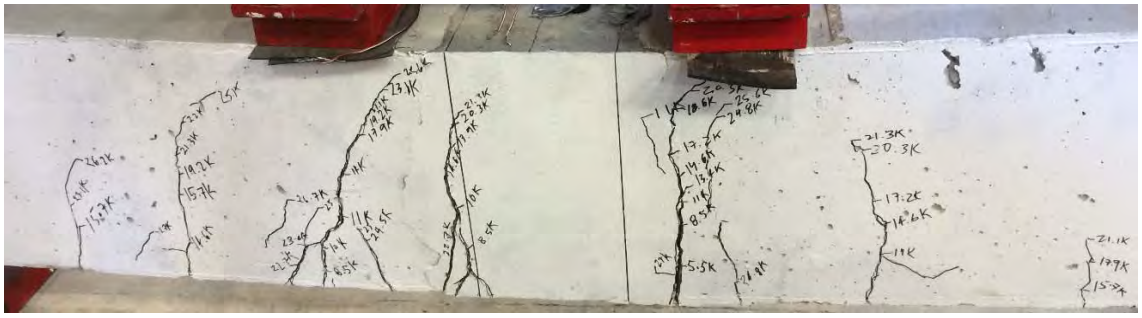

(a) Specimen B-15-U-N-H

(b) Specimen B-18-U-R-H

(c) Specimen B-21-U-S-H

(d) Specimen B-21-U-S-H showing rebar rupture

Figure 6.18 UHSC hairpin specimens at failure

6.1.3.3 Anchored. Anchored detail had the least lap length of all details used in this research, which might be one of the reason for its low peak capacity compared to straight-lap or hairpin detail. The results for peak load ranged from 26 to 28.3 kips (116 to 126 kN). The peak deflections ranged from 0.92 to 1.47-in. (23.4 to 37.3 mm). The results of anchored detail with UHSC joint filler are summarized in Table 6.19.

Table 6.19 Summary of results for UHSC-joint specimens with anchored detail

Sl. no.	Specimen	Detail	Surface prep	Peak load kips (kN)	Peak deflection in. (mm)
1	B-1-C-N-N	Control	Control 1	30.6 (136)	1.40 (35.5)
2	B-4-C-N-A	Anchored	Control 4	9.0 (40)	0.69 (17.5)
3	B-16-U-N-A		Smooth	26.1 (116)	1.47 (37.3)
4	B-19-U-R-A		Rough	26.0 (116)	0.92 (23.4)
5	B-22-U-S-A		Sand blasted	28.3 (126)	1.26 (32.0)

Conversion: 1 kip = 4.45 kN, 1-in. = 25.4 mm

6.1.3.3.1 <u>Flexural behavior.</u> Anchored detail with UHSC performed better than with HS-SCC as joint filler. The peak loads are summarized in Figure 6.19. Specimens with anchored detail and a UHSC joint filler were able to attain 84% of control specimen B-1-C-N-N's peak load which was better than with HS-SCC as joint filler (section 6.1.2.3). Flexural crack propagation initiated at the beam-joint interface engaging the beams with crack propagation eventually extending to the compression zone. It is interesting to note that all the specimens with anchored detailing failed in a similar fashion with slippage in the tensile reinforcement in the joint (Figure 6.3(d), Figure 6.12(c), and Figure 6.21(c)). With HS-SCC joint filler, the beam regions sustained minimal loading as observed from very few or no cracks in the beams. The beam regions with UHSC joint were engaged in loading. Concrete crushing failure was observed in the beam region in the compression zone after which the cracking in the UHSC began. The reinforcement reached yield strain in tensile reinforcement in specimen B-16-U-N-A. Compression reinforcement developed yield strain in specimen B-22-U-S-A. This is a significant finding as UHSC is able to bond with reinforcement and develop the full capacity of steel which is what designers intend to achieve. The strain readings are tabulated in Table 6.20.

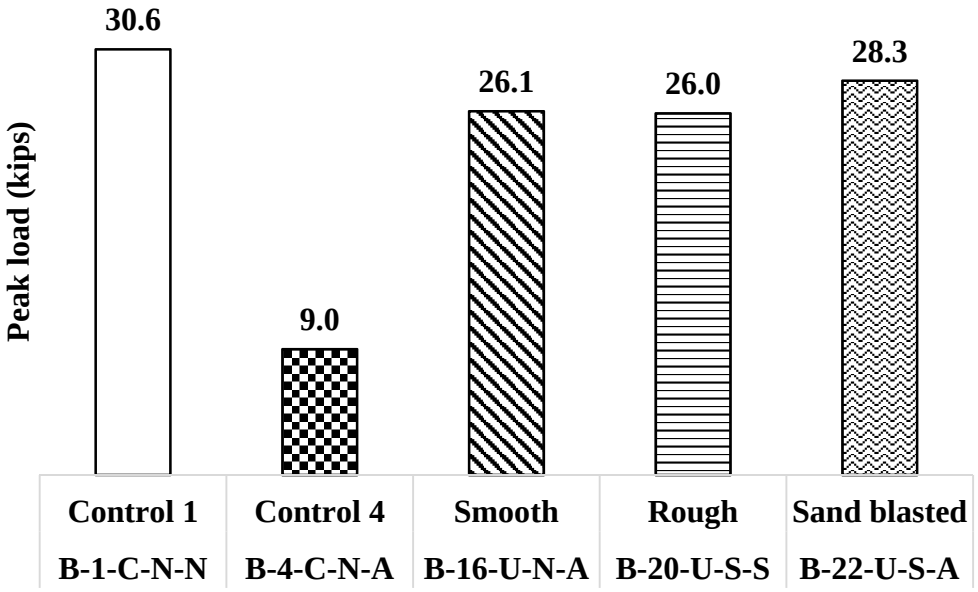

Figure 6.19 Peak loads of UHSC joint specimens with anchored detail

Table 6.20 Strain readings measured on the joint reinforcing bars

Sl.no.	Specimen	RB1 (in. /in.)	RB2 (in. /in.)	RT1 (in. /in.)	RT2 (in. /in.)	Yield strain (in. /in.)
1	B-16-U-N-A	0.00262	0.00000	0.00094	0.00074	0.00267
2	B-19-U-R-A	0.00229	0.00000	0.00048	0.00000	0.00267
3	B-22-U-S-A	0.00217	0.00118	0.00441	0.00974	0.00267

* Strain locations are discussed in Section 5.2 for reference

6.1.3.3.2 <u>Ductility index.</u> The load versus deflection plot of anchored detail with UHSC joint filler are plotted in Figure 6.20. Except specimen B-19-U-R-A, all the remaining specimens were much more ductile than control specimen B-1-C-N-N. When compared to straight-lap or hairpin detail, anchored detail had lesser lap length (3.5-in. /88.9 mm) and still reached 81% of control specimen B-1-C-N-N's ductile behavior. It is interesting to notice that longitudinal reinforcement in the anchored details slipped but no debonding of rebar from UHSC was observed.

The ductility study results are tabulated in Table 6.21 for specimens with anchored detail with a UHSC joint filler. The DI-1 values indicate that when compared with straight-lap or hairpin details (6.1.3.1 and 6.1.3.2) with UHSC were not very significant.

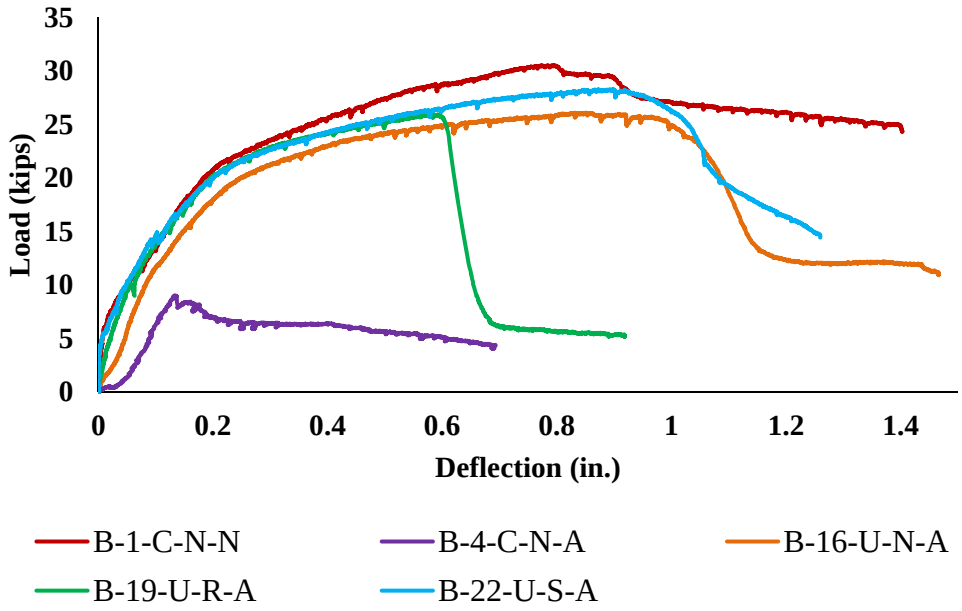

Figure 6.20 Load versus deflection of anchored UHSC-joint specimens

Keeping in mind that anchored detail had the least lap length of all details, it is impressive that with UHSC it was able to attain 81% of specimen B-1-C-N-N's ductility. DI-2 values indicate that with UHSC, there was an increase in ductility by at least 3.7 times and up to 6.3 times. DI-2 values of HS-SCC joint specimens (Table 6.12) indicate anchored detail only reached about 50% of secondary control specimen B-4-C-N-A's ductility meaning UHSC showed an increase of at least 370% which is very significant increase.

Table 6.21 DI results for UHSC-joint specimens with hairpin detail

Sl. no.	Specimen	Detail	Area under curve	DI-1	DI-2
1	B-1-C-N-N	Control	34.63	1.00	-
2	B-4-C-N-A	Anchored	3.83	0.11	1.00
3	B-16-U-N-A		28.05	0.81	7.32
4	B-19-U-R-A		14.31	0.41	3.73
5	B-22-U-S-A		28.02	0.81	7.32

DI-1: Ductility of specimen with respect to primary control
DI-2: Ductility of specimen with respect to secondary control

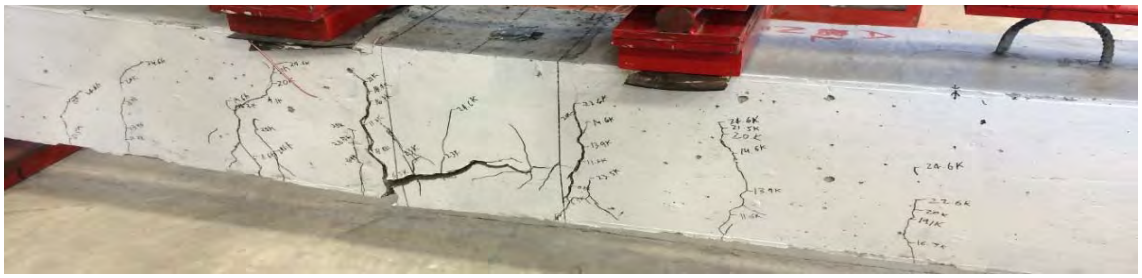

(a) Specimen B-16-U-N-A

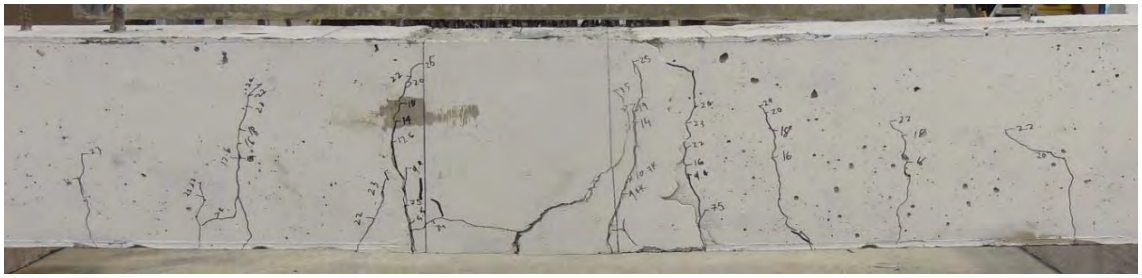

(b) Specimen B-19-U-R-A

(c) Specimen B-22-U-S-A

Figure 6.21 UHSC anchored specimens at failure

6.1.4. Discussion. In this section, discussion of the results of HS-SCC and UHSC joint specimens is done. In terms of capacity, UHSC was the best performing joint filler compared to HS-SCC as seen from the results in Sections 6.1.2 and 6.1.3. It must be noted that the specimens were tested to create high moment in the connection which is not the case in real continuous span scenarios. Though HS-SCC did not reach the load and deflection limits set by control specimen B-1-C-N-N, it still could be used in joints as joints are designed at the inflection points or low moment regions in the span. In case of UHSC, even though it may not be used in high-moment regions it is significant to note that it can sustain high moment and loads, and is also very ductile. One more significant aspect of using UHSC can be seen from Figure . The difference in crack

propagation (as seen in Figure) of specimens B-1-C-N-N, B-8-H-R-S and B-18-U-R-S indicates that UHSC behaves similar to primary control. Though the specimens were connected using a joint filler, with UHSC the beams also carried the load creating a continuity which led to increase in capacity unlike HS-SCC. It can be seen that there are very few or no cracks propagating through UHSC in the joint and the specimen failed due to concrete crushing in the top compression zone type failure in the beam region, similar to control specimen. HS-SCC on the other hand could not create this continuity indicated by slippage and debonding type failure in the joint.

The flexural behavior study concluded that Straight-lap detail with 6-in. /152 mm lap length in the connection, performed the best compared to all other details when used with UHSC. Straight-lap detail has rebar lapped over the length of the connection, which creates more or less a continuous rebar detailing similar to regular longitudinal reinforcement detailing. Also steel fibers used with UHSC increase the tensile capacity of concrete significantly, which might be one of the reasons for increase in flexural capacity of UHSC connections when compared to HS-SCC connections. While in HS-SCC connections, hairpin detail could be considered better as it was the only detail that surpassed the behavior of secondary control specimen B-3-C-N-H but not the primary control, B-1-C-N-N.

The DI study conducted indicates that hairpin detail was much more ductile than straight-lap or anchored detail. Hairpin detail has more surface area of reinforcement in the joint which with a material like UHSC could increase the bond strength increases ductility. Increasing the lap length of hairpin detail might also lead to increase in flexural and ductile behaviors. It was also observed that UHSC was a better material compared to HS-SCC to be used to improve the ductility of any structure. The DI-2 values indicated that UHSC could improve the ductile behavior of specimens by at least 100% while with HS-SCC specimens only a 10% increase was observed (discussed in sub-sections of 6.1.2 and 6.1.3).

The longitudinal reinforcement in the tensile region of the control specimen B-1-C-N-N reached yield stress (Table 6.2). In case of HS-SCC specimens, no significant yield stresses were developed, seen from the tables in the results section (Table 6.5, Table 6.8, and Table 6.11). Significant observation was that with UHSC, the reinforcement

reached yield strains at least in one rebar in the tensile and compression regions (Table 6.14, Table 6.17, and Table 6.20). This indicated that UHSC can bond with steel rebars and develop the full yield capacity of the steel reinforcement which is one of the main design criteria.

The effect of surface preparation can be considered insignificant, though roughening the beam surface in most of the cases improved the capacity but not by a huge amount. Further studies are needed in this area as only not enough test specimens were observed to make such conclusions.

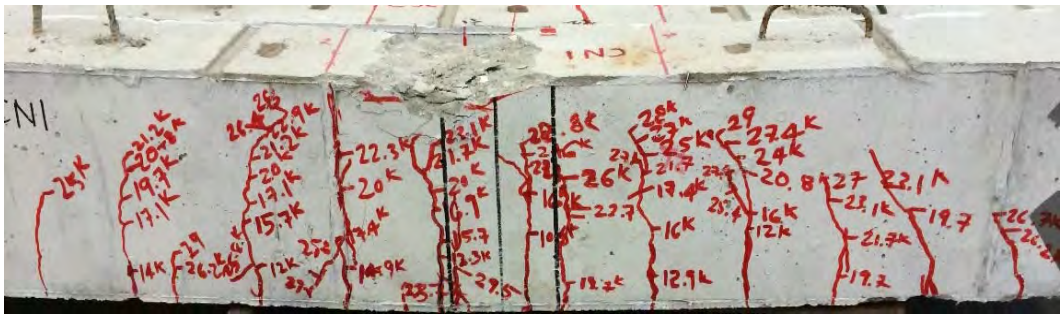

(a)Control specimen B-1-C-N-N at failure

Figure 6.22 Specimens at failure

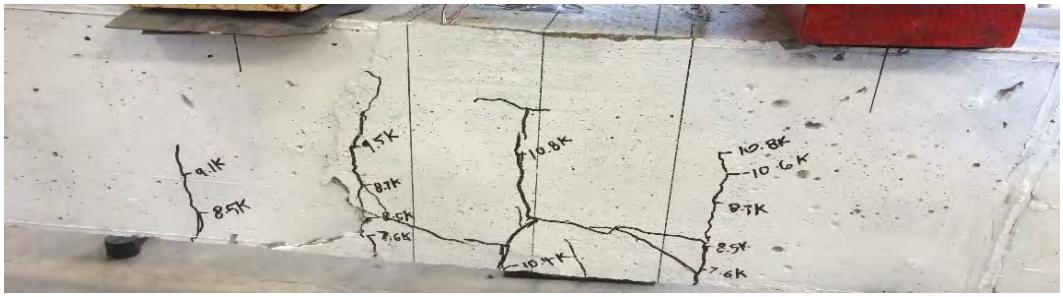

(b) HS-SCC specimen B-8-H-R-S at failure

(c) UHSC specimen B-18-U-R-S at failure
Figure 6.22 Specimens at failure (cont.)

6.2. PHASE TWO: EVALUATION OF MODOT DETAIL WITH UHSC

Phase two focused on using UHSC within a non-prestressed MoDOT end girder detail. The results of testing conducted on Phase two are presented in this section. The flexural and ductile behavior are discussed in this section.

6.2.1. Results. The testing conducted on the T-beam specimens gave some Interesting results. The results are summarized in Table 6.22. There were three controls specimens and two test specimens. Control specimen B-1-C-C-N is the primary control with continuous reinforcement. Specimen B-2-C-C-M is the secondary control cast monolithically with MoDOT detail. Specimen B-3-MB-MB-M is tertiary control with MoDOT detail and MoDOT B-mix in the joint and deck. These serve as three limits to compare UHSC deck and joint specimens. Specimen B-4-U-MB-M has MoDOT deck and UHSC joint while specimen B-5-U-U-M has UHSC deck and joint. The peak load results ranged from 64 to 99 kips (285 to 441 kN). Peak deflections ranged from 1.2 to 3.8-in. (30.5 to 96.5 mm).

Table 6.22 Summary of Phase two test results

Sl. no.	Nomenclature	Joint filler	Deck filler	Joint detail	Peak load kips (kN)	Peak deflection in. (mm)
1	B-1-C-C-N	CC	CC	None	85 (378)	3.8 (96.5)
2	B-2-C-C-M	CC	CC	MoDoT	74 (330)	2.3 (58.4)
3	B-3-MB-MB-M	MoDoT B	MoDoT B	MoDoT	64 (285)	2.3 (58.4)
4	B-4-U-MB-M	UHSC	MoDoT B	MoDoT	72 (320)	2.9 (73.7)
5	B-5-U-U-M	UHSC	UHSC	MoDoT	99 (441)	1.2 (30.5)

Conversion: 1 kip = 4.45 kN, 1-in. = 25.4 mm

Controls specimens B-1-C-C-N and B-2-C-C-M reached peak loads of 85 and 74 kips (378 and 330 kN) respectively. Primary control specimen was characterized by flexural shear cracks which resulted in failure by concrete crushing in top compression zone. No significant drop in load was observed for specimen B-1-C-N-N and loading was stopped when loading arms of the actuator reached maximum push limit. The MoDOT detail used in specimen B-2-C-C-M resulted in crushing of concrete in the midspan because of discontinuity leading to concrete crushing failure after reaching the peak load.

Specimen B-4-U-MB-M with UHSC joint and B mix deck reached a peak load 72 kips (320 kN), 84% of control specimen B-1-C-C-N's peak load capacity. The peak loads are illustrated in Figure 6.23. The crack propagation started from the deck with cracks extending to the compression zone quickly. The beam region started slipping with crack completely separating the beam and UHSC. Significant crushing of concrete was observed in the compression zone of concrete accompanied by concrete spalling off from deck (Figure 6.24). Specimen B-4-U-MB-M surpassed the peak load of the specimen B-3-MB-MB-M and came very close to specimen B-2-C-C-M's peak load capacity. The low cement deck mix was not very strong leading to concrete spalling off and failure of specimen.

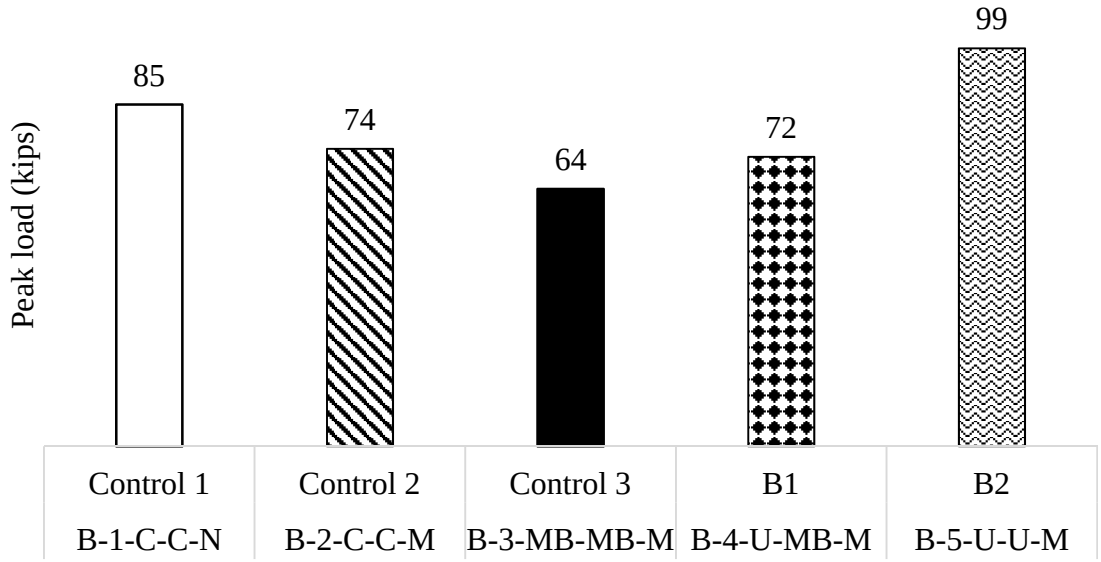

Figure 6.23 Peak load results of Phase 2

Specimen B-5-U-U-M with UHSC deck and joint reached a peak load of 99 kips (441 kN) a 16% increase in capacity with respect to specimen B-1-C-N-N. Specimen B-5-U-U-M failed with rebar rupture in the deck region. Sudden drop in load with explosive sound while testing indicated rebar rupture failure. The difference in failure from specimen B-4-U-MB-M can be seen from Figure 6.24. Specimen B-5-U-U-M surpassed the peak load of the two other controls. The reinforcement in tensile region of control specimens were able to reach yield strain. It was observed that the specimens, B-4-U-MB-M and B-5-U-U-M's reinforcement also reached yield strain in the tensile region. No significant strain was developed in B-3-MB-MB-M because of the weak joint started failing sooner than the rebar yielded. It is significant finding is that rebar ruptured in the tensile zone of B-5-U-U-M indicating UHSC bond with rebar is strong and failure was because of steel yielding and not concrete failure. The strain readings are given in Table 6.23

The load versus deflection plots for Phase two are given in Figure 6.25. Even though specimen B-5-U-U-M attained the largest peak load, in terms of ductility specimen B-4-U-MB-M was the best. Specimen B-4-U-MB-M followed a load gain trend very close to control specimen B-2-C-C-M. The test specimen B-5-U-U-M only reached 70% of specimen B-3-MB-MB-M's ductility, while specimen B-4-U-MB-M surpassed

the ductile behavior of B-3-MB-MB-M behavior indicating UHSC in joints is excellent in increasing the ductility of connections.

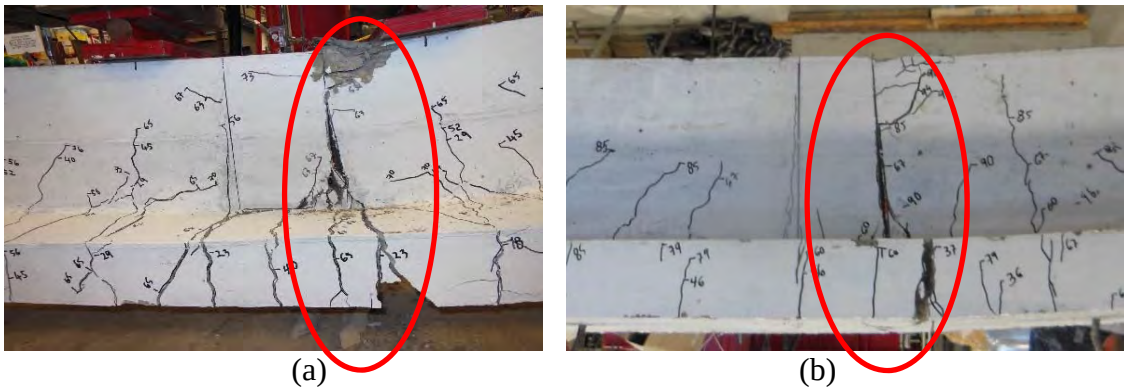

(a) (b)

Figure 6.24 Failure mode (a) B-4-U-MB-M (b) B-5-U-U-M

Table 6.23 Strain readings measured on the joint reinforcing bars

Specimen	RB1 (in. /in.)	RB2 (in. /in.)	RT1 (in. /in.)	RT2 (in. /in.)	Yield strain (in. /in.)
B-1-C-C-N	0.00000	0.00000	0.00000	0.00000	0.00267
B-2-C-C-M	-0.01001	0.00000	-0.00107	0.00000	0.00267
B-3-MB-MB-M	0.00386	0.00088	-0.00012	-0.00039	0.00267
B-4-U-MB-M	-0.00086	-0.00086	0.00045	0.00000	0.00267
B-5-U-U-M	-0.00187	0.00000	-0.00011	0.00000	0.00267

* Strain locations are discussed in Section 5.2 for reference

Table 6.23 Strain readings measured on the joint reinforcing bars (cont.)

Specimen	RD1 (in. /in.)	RD2 (in. /in.)	Yield strain (in. /in.)
B-1-C-C-N	0.00207	0.00000	0.00255
B-2-C-C-M	0.00000	0.00000	0.00255
B-3-MB-MB-M	0.00231	0.00000	0.00255
B-4-U-MB-M	0.00462	0.00026	0.00255
B-5-U-U-M	0.00562	-0.0015	0.00255

* Strain locations are discussed in Section 5.2 for reference

DI study results are summarized in Table 6.24. The results are interesting as specimen B-5-U-U-M, though reached highest peak load was not the most ductile as indicated by DI-1 value of 0.7. Specimen B-4-U-MB-MB with the UHSC joint performed

the best indicated by DI-1 value of 1.6. From DI-1 values of specimens B-3-MB-MB-M and B-4-U-MB-M, it can be inferred that by using UHSC in the connection, the ductility increased by about 60% which is a very positive finding. It can be said that, UHSC when used in end girder detail of a non-prestressed girder with CC CIP deck could improve the ductility of the structure by at least 50%. Crack propagation through UHSC joint region was not observed, which resulted in concrete spalling off from deck (Figure 6.26 (e)) and significant crushing in compression zone of beam indicating that if UHSC is used, the joint will not be the weak link in the structural member.

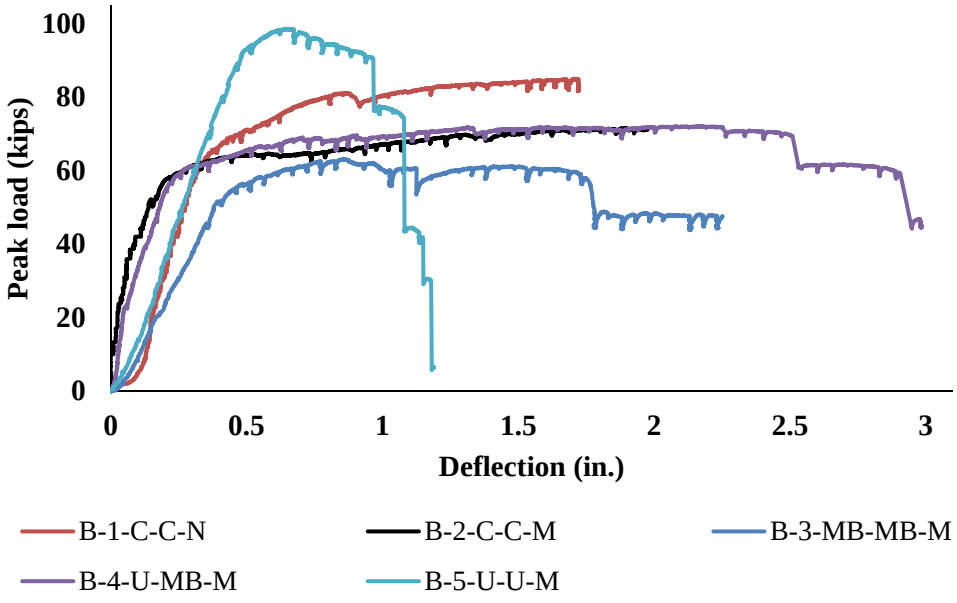

Figure 6.25 Load versus deflection plots for Phase two

Table 6.24 DI study results of Phase two

Sl.no.	Nomenclature	Area under curve	DI-1	DI-2	DI-3
1	B-1-C-C-N	119.2	1.0	-	-
2	B-2-C-C-M	126.5	1.1	1.0	-
3	B-3-MB-MB-M	112.8	0.9	0.9	1.0
4	B-4-U-MB-M	186.5	1.6	1.5	1.7
5	B-5-U-U-M	79.8	0.7	0.6	0.7

DI-1: Ductility of specimen with respect to primary control
DI-2: Ductility of specimen with respect to secondary control
DI-3: Ductility of specimen with respect to tertiary control

6.2.2. Discussion. The significant findings of this Phase of research were that, UHSC can increase the peak load, ductility and long-term durability performance of joint, following yielding of the steel in the joint, a secondary brittle failure was observed. This was observed in the case of specimen B-5-U-U-M (Figure 6.26 (e)) where there was no significant cracking in the specimen yet attained a high peak load, which after yielding of the steel resulted in a sudden failure with ultimate rupture in the rebar. But when used in connections, UHSC gave the best performance along with MoDOT B mix deck which outperformed the controls in ductility and reached 90% of specimen B-1-C-N-N's peak load. It is a very positive indicator that UHSC in connections outperformed the controls even in the worst case scenario of high moment which makes it a good solution for connections. It is a significant observation that UHSC when used with MoDOT connection detail and MoDOT B mix (specimen B-4-U-MB-M, Figure 6.26 (d)) was able to surpass that performance of primary control ductile behavior by 60%.

(a) Specimen B-1-C-N-N

(b) Specimen B-2-C-C-M

Figure 6.26 Test Specimens at failure

(c) Specimen B-3-MB-MB-M

(d) Specimen B-4-U-MB-M

(e) Specimen B-5-U-U-M

Figure 6.26 Test Specimens at failure (cont.)

7. CONCLUSIONS

This section summarizes the conclusions that were observed from this research project.

7.1. PHASE ONE

The main objective of Phase one of this research study was to evaluate use of UHSC and HS-SCC in high moment continuity detail regions with different rebar configurations and surface preparations, this was done by putting together a test matrix which consisted of twenty two test specimens described in Section 3.1 of this report. The following conclusions can be made based on the results obtained

- HS-SCC when used in connections, was not the most desirable or efficient type of joint filler to be used as control specimens with a continuity detail (secondary controls) outperformed HS-SCC specimens except when used with hairpin detail.
- The hairpin detail when used with HS-SCC as a joint filler yielded the best performance in terms of the continuity details to be used with HS-SCC as joint filler material.
- HS-SCC specimens in terms of ductility were unable to yield desirable results when compared to the primary control specimen.
- UHSC when used in continuity details, outperformed HS-SCC's performance in terms of flexural and ductile behavior.
- The straight-lap detail when used with UHSC yielded the best flexural performance of all the test specimens including HS-SCC.
- In terms of ductility, UHSC with the hairpin detail outperformed the other specimens.
- No significant effect was observed from different surface preparations of the beam-joint interface. However, a very slight improvement in flexural capacity was observed when the beam-joint interface was roughened.
- Connections, although they may not be utilized in high-moment regions in typical applications, with use of UHSC can sustain the high moment successfully with proper design, detailing and execution.

In conclusion, UHSC was highly successful in creating continuity even when subjected to a high moment loading region. It signifies that UHSC could successfully be used in joints outside of inflection point regions.

7.2. PHASE TWO

UHSC's advanced material properties when used with joints could improve the performance of structure significantly. The testing conducted on test specimens with a non-prestressed MoDOT style end girder detail gave favorable results in this aspect.

- UHSC used with a non-prestressed mild steel MoDOT end girder detail surpassed the ductile behavior of the control specimen, but couldn't surpass the peak load as the deck used was a modified MoDOT B mix which was not very strong(3.2 ksi/23 MPa) or durable compared to UHSC(16.2 ksi/112 MPa) or the control(7.9 ksi/54 MPa).
- UHSC when used as a deck filler attained the highest peak load for all specimens investigated. It may be noted that a sudden failure was observed in the form of rebar rupture in the deck region well after yielding of the reinforcement.
- Significant cracking was not observed in the UHSC joint region in both beams and failure was due to crushing of concrete in the beam specimens under the load points.

8. FUTURE WORK AND RECOMMENDATIONS

This section summarizes the some of the future work that could be done and some recommendations.

8.1. RECOMMENDATIONS

- UHSC worked very well in the connections subjected to high-moment loading and was able to achieve a behavior similar to the control specimens.
- Simple continuity detail like straight-lap detail worked best. This would be more economical as the detail eliminates longer durations of cage preparation.
- Using simple continuity detail also eliminates the need of using highly skilled technicians, will be easier to manufacture and erect and also manipulate during construction.
- Surface preparation does help with increasing the bond capacity of UHSC with beam surface, hence roughening with an amplitude of 0.25 inch is recommended.

8.2. FUTURE WORK

- Further research needs to be conducted with UHSC in high-shear regions to better study the effect of surface preparation of the beam-joint interface.
- Research on connections in high-moment and high-shear regions needs to be done as most connections will be located near supports which are high shear regions.
- Shear study involving UHSC shear pull off specimens could better predict the shear behavior of UHSC.
- One of the joint fillers used during this research was HS-SCC. Future research could study the effect of using steel fibers with HS-SCC and study the performance.
- Research using prestressed steel reinforcement with UHSC in connections with MoDOT end girder detail could better establish the effectiveness of using UHSC in connections and could lead to new paths in bridge design.

APPENDIX A.
LOAD VERSUS DEFLECTION CURVES

This appendix lists the Load versus deflection plots of each specimen individually. The setup consisted of three LVDT's. One on the midspan in the joints, two other LVDTs were located at a distance of quarter length of the span from the midpoint of the specimen. The LVDTs were designated as Midspan which was located on the midspan, Quarter span, east and Quarter span, west based on the geographic location of test setup with respect to High-bay structures lab at Missouri University of Science and Technology. LVDTs were placed in similar location during both Phases of the project illustrated in Figure A.1.

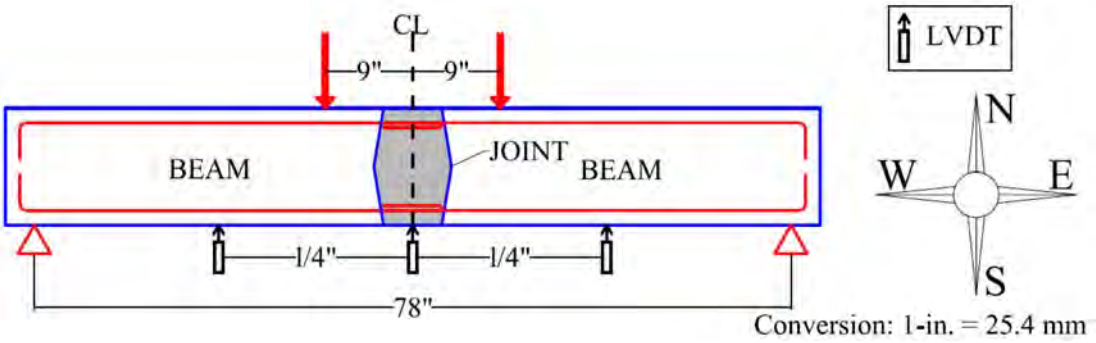

Figure A. 1 Test setup used

Figure A. 2 Location of LVDTs

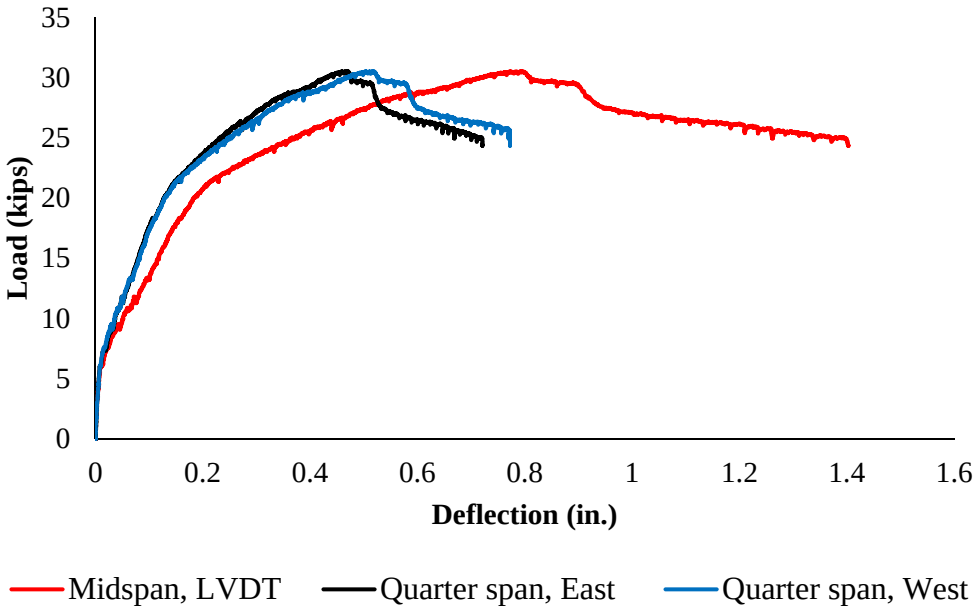

Figure A. 3 Load versus deflection for specimen B-1-C-N-N

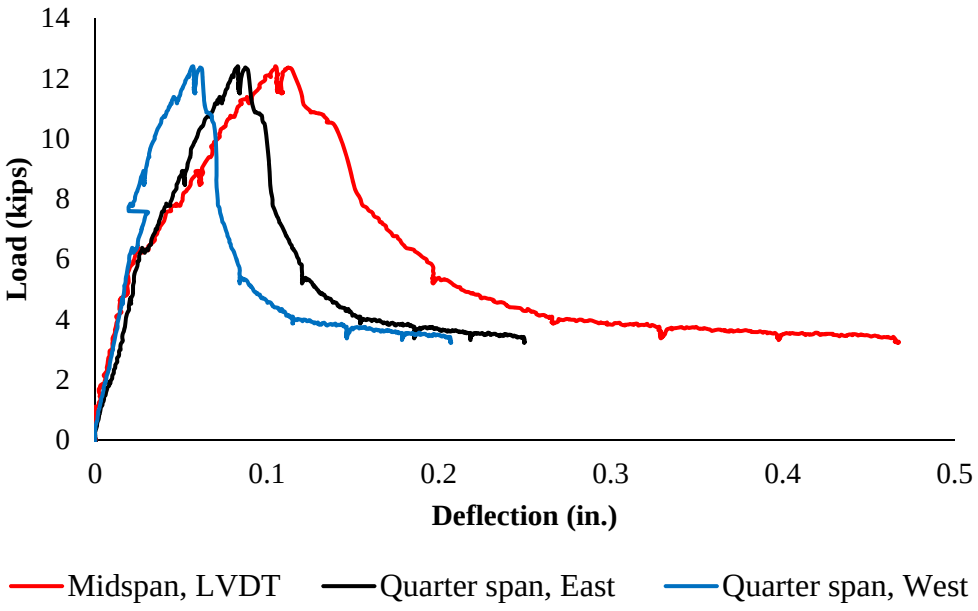

Figure A. 4 Load versus deflection for specimen B-2-C-N-S

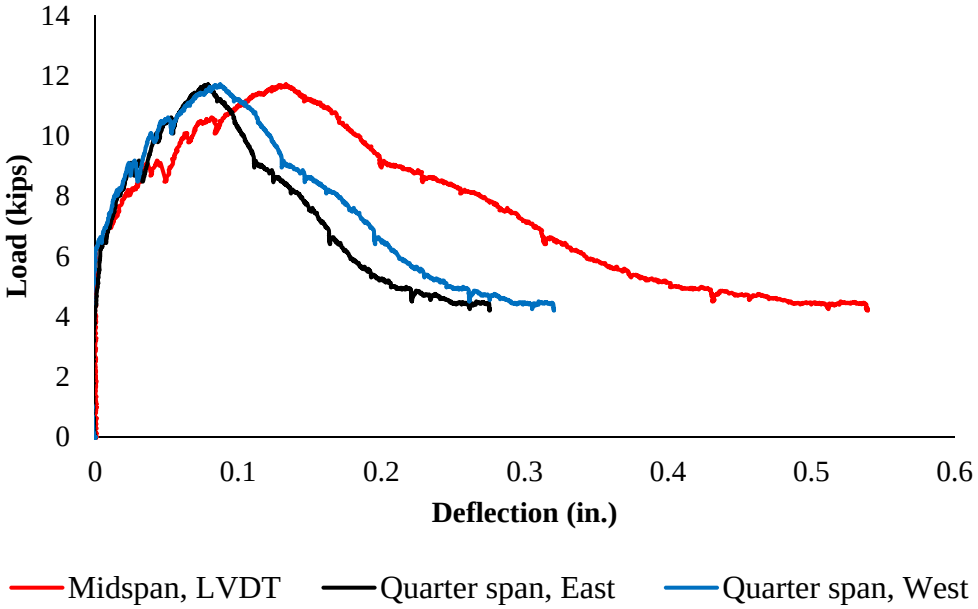

Figure A. 5 Load versus deflection for specimen B-3-C-N-H

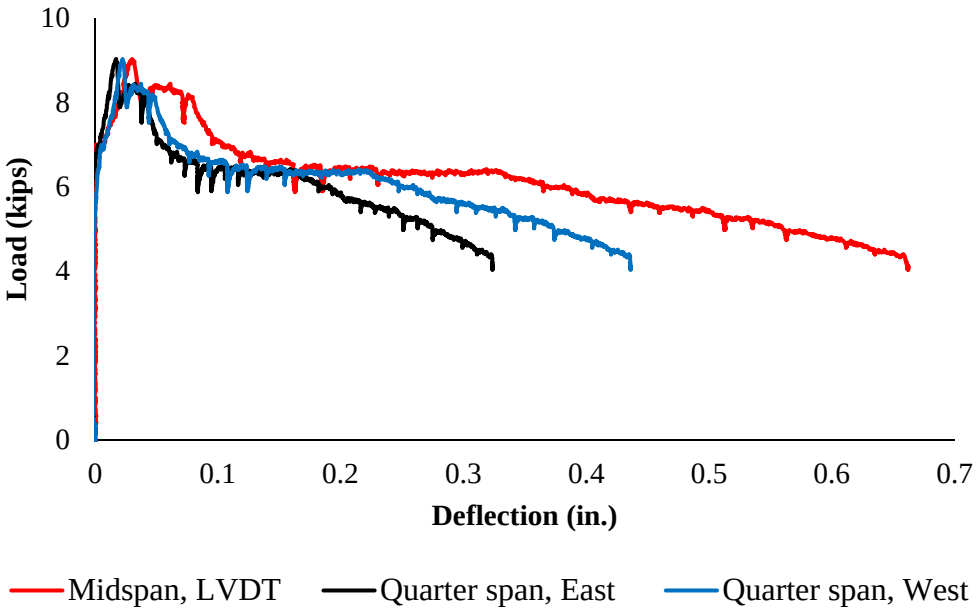

Figure A. 6 Load versus deflection for specimen B-4-C-N-A

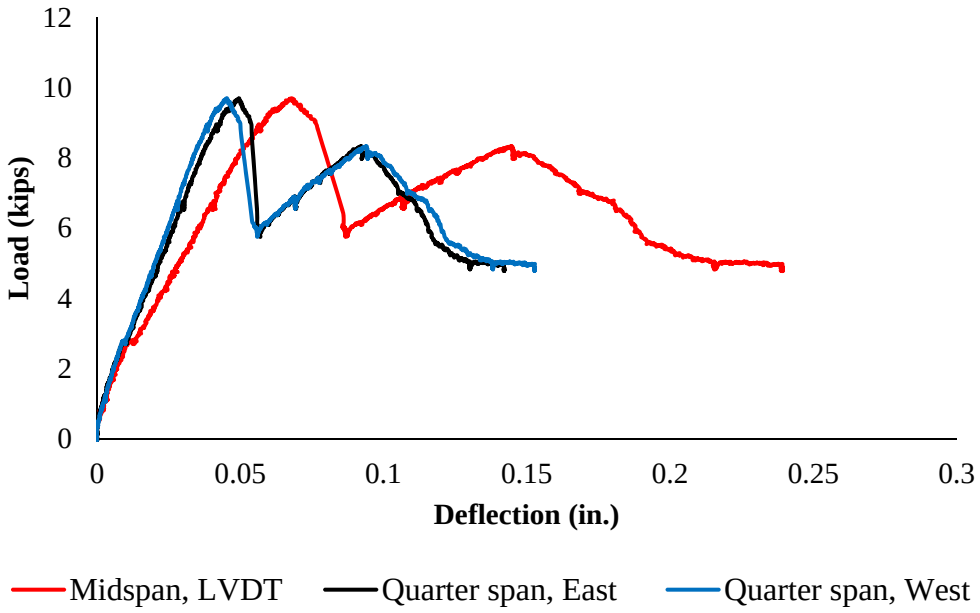

Figure A. 7 Load versus deflection for specimen B-5-H-N-S

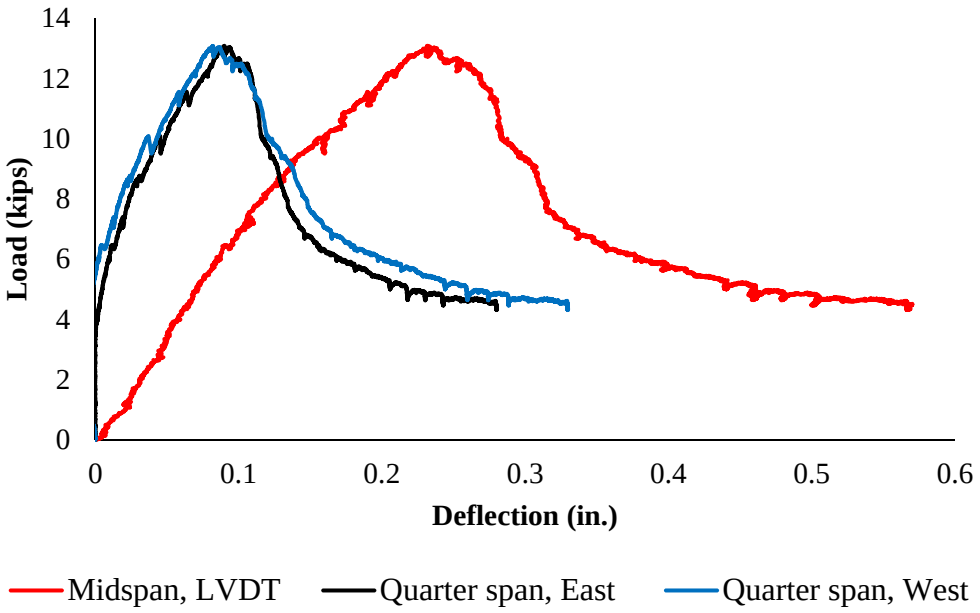

Figure A. 8 Load versus deflection for specimen B-6-H-N-H

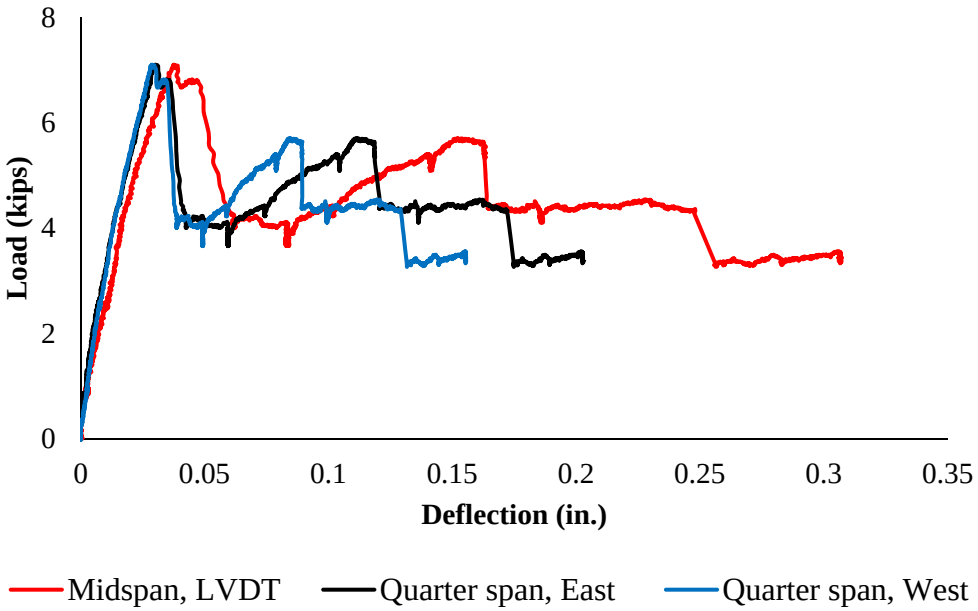

Figure A. 9 Load versus deflection for specimen B-7-H-N-A

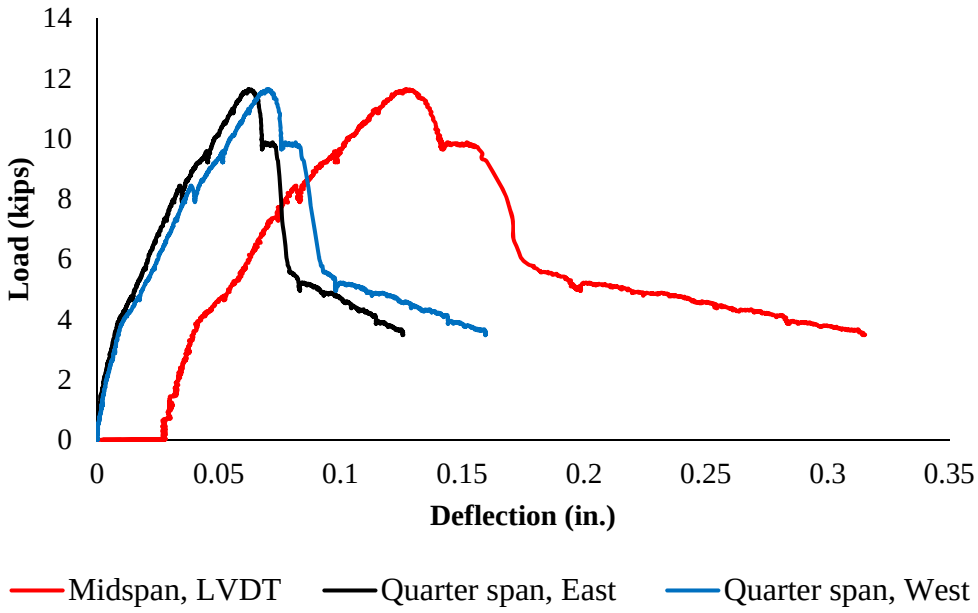

Figure A. 10 Load versus deflection for specimen B-8-H-R-S

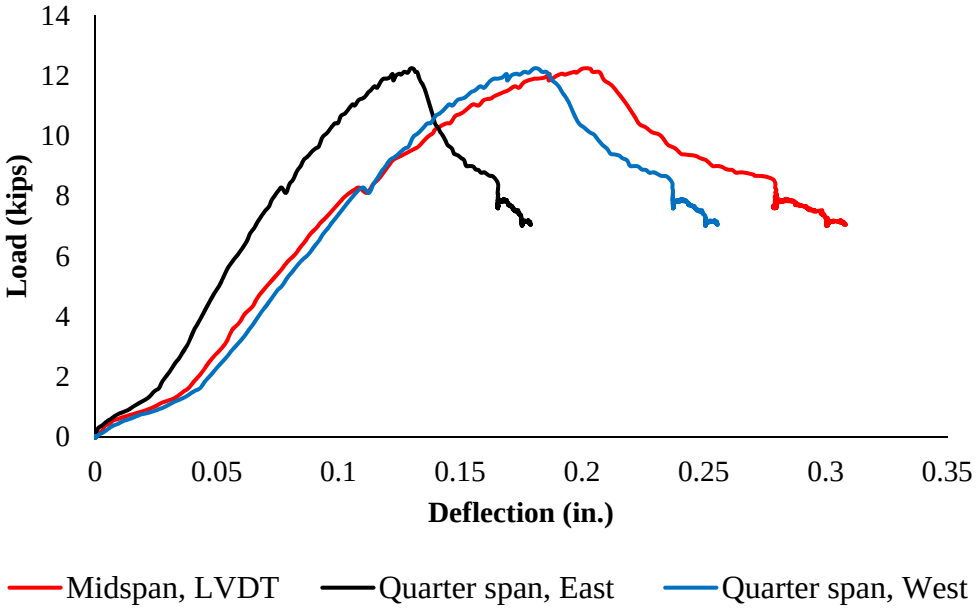

Figure A. 11 Load versus deflection for specimen B-9-H-R-H

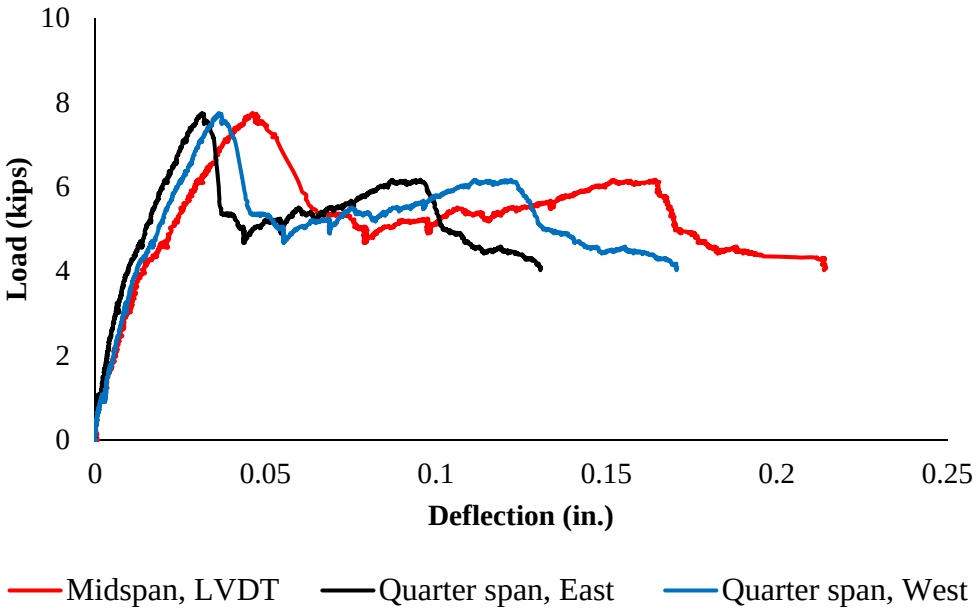

Figure A. 12 Load versus deflection for specimen B-10-H-R-A

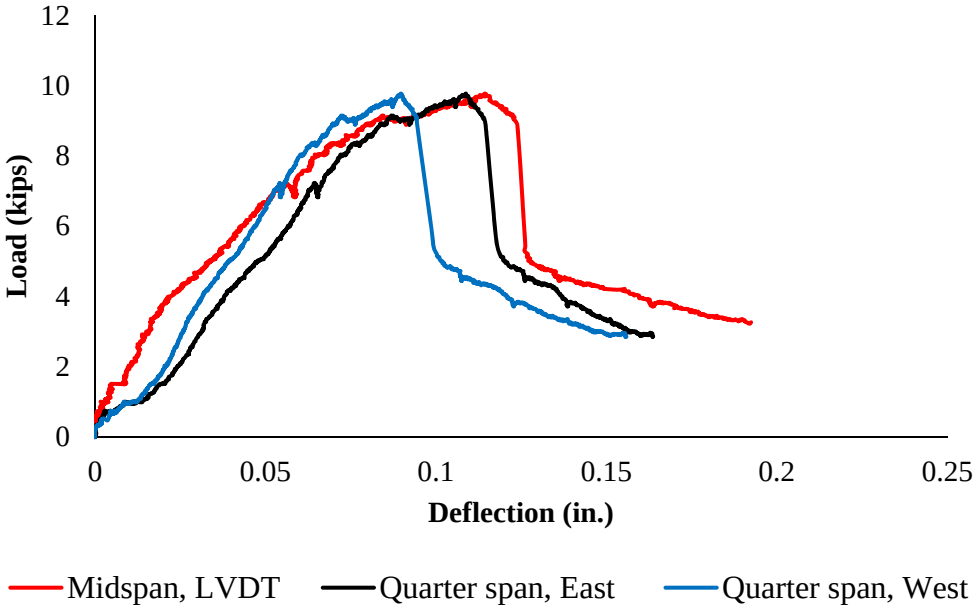

Figure A. 13 Load versus deflection for specimen B-11-H-S-S

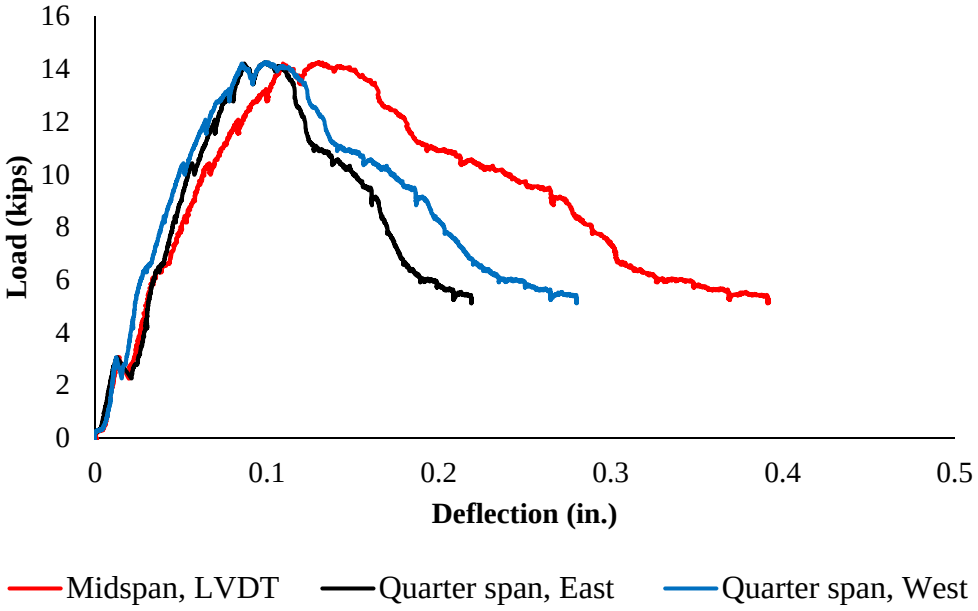

Figure A. 14 Load versus deflection for specimen B-12-H-S-H

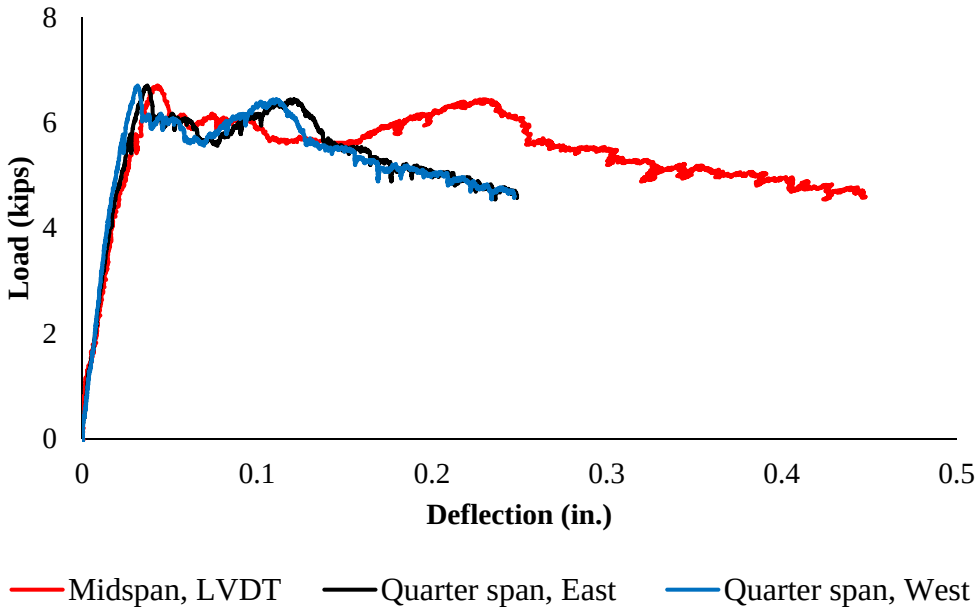

Figure A. 15 Load versus deflection for specimen B-13-H-S-A

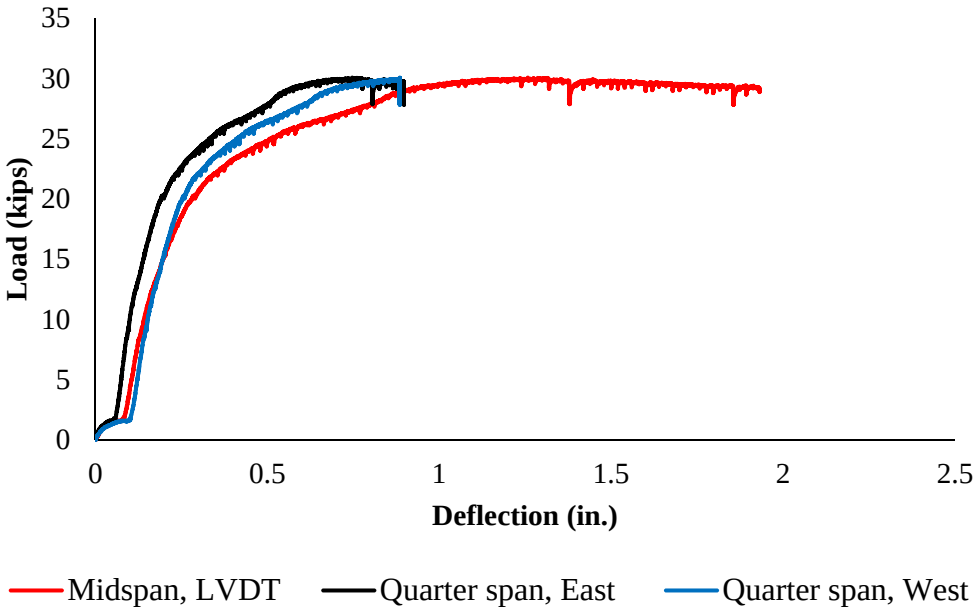

Figure A. 16 Load versus deflection for specimen B-14-U-N-S

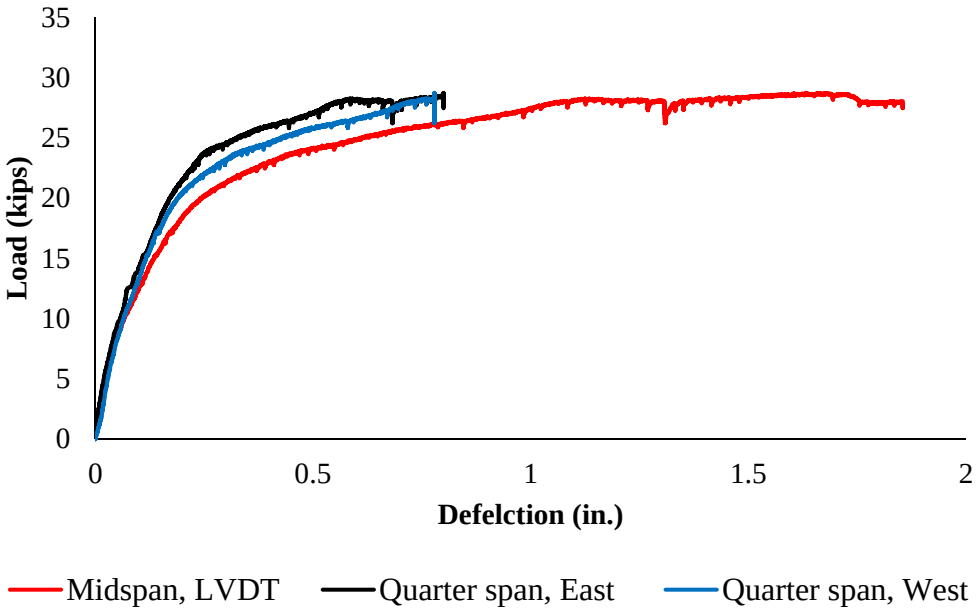

Figure A. 17 Load versus deflection for specimen B-15-U-N-H

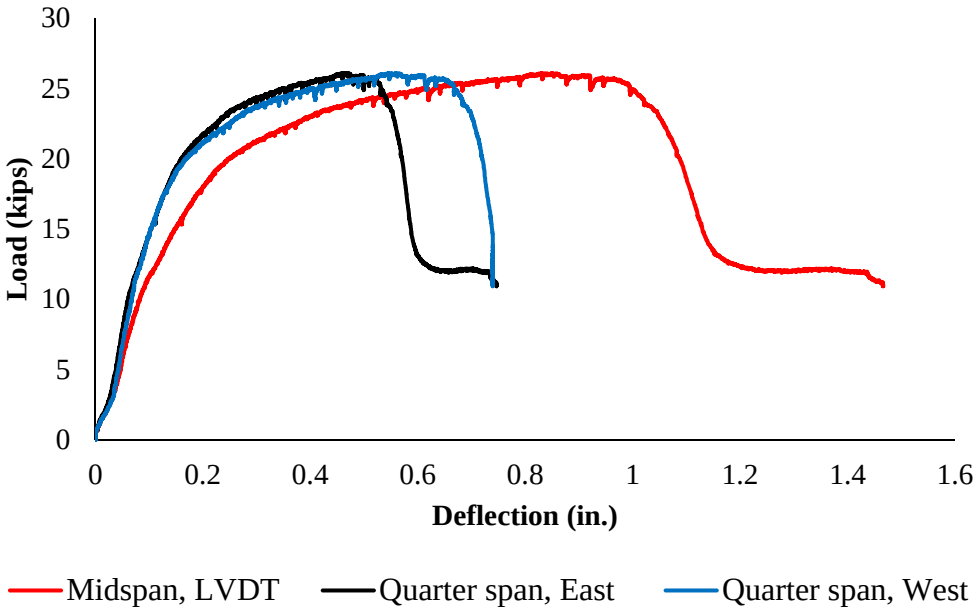

Figure A. 18 Load versus deflection for specimen B-16-U-N-A

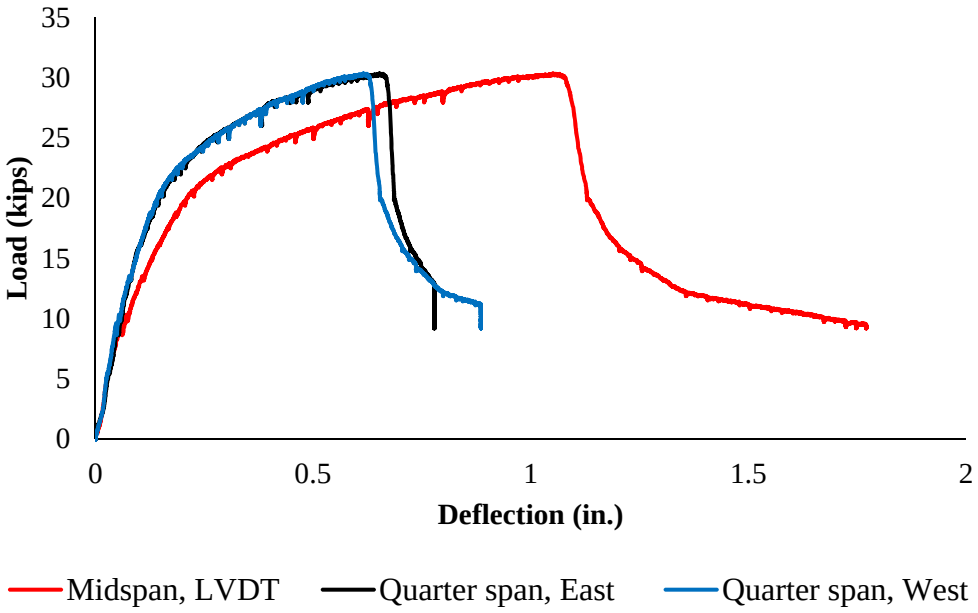

Figure A. 19 Load versus deflection for specimen B-17-U-R-S

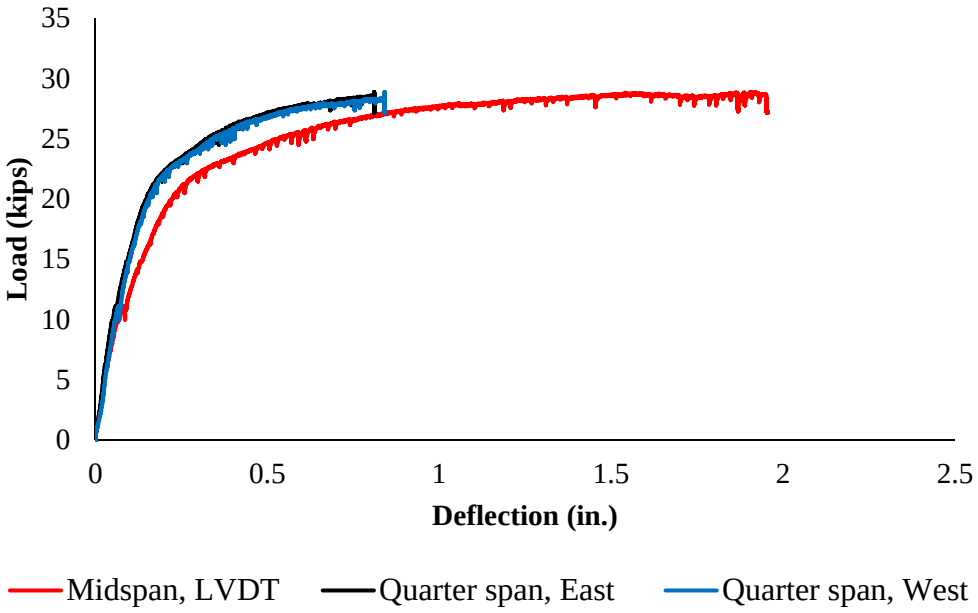

Figure A. 20 Load versus deflection for specimen B-18-U-R-H

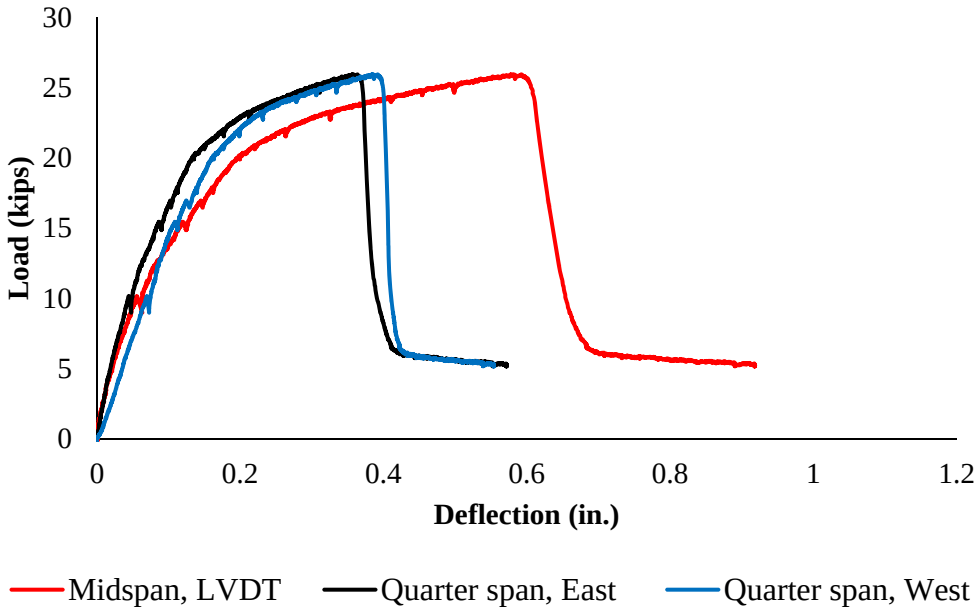

Figure A. 21 Load versus deflection for specimen B-19-U-R-A

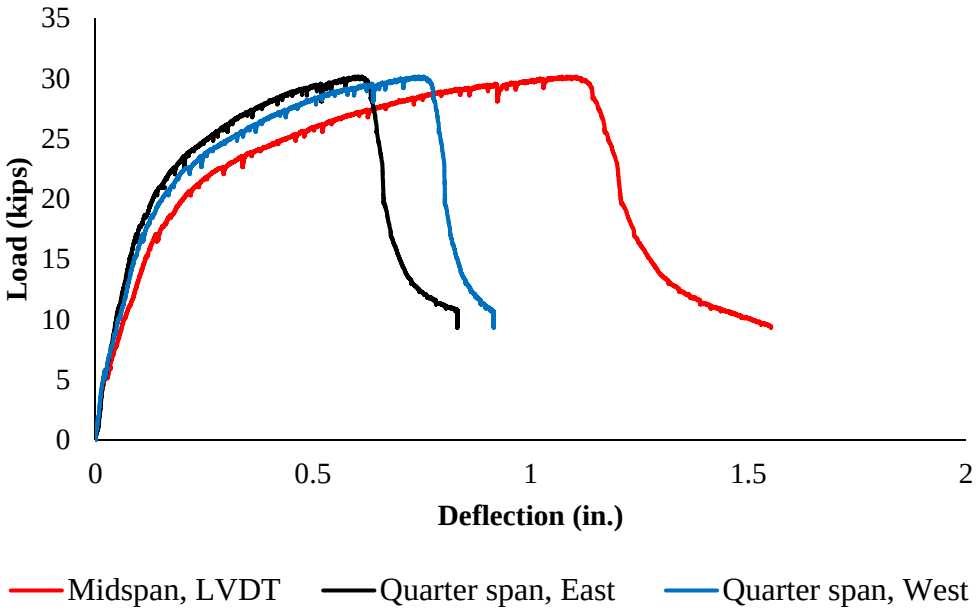

Figure A. 22 Load versus deflection for specimen B-20-U-S-S

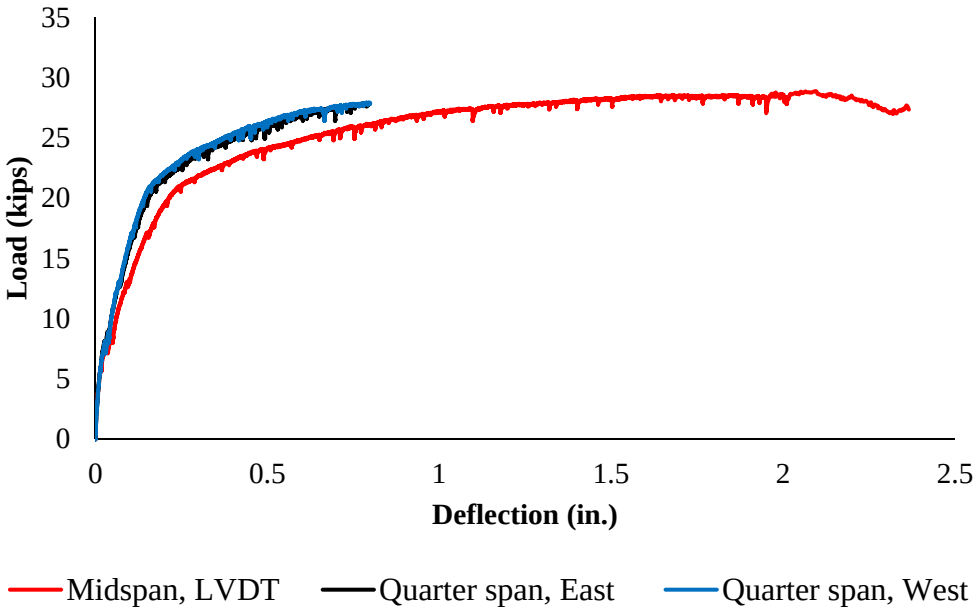

Figure A. 23 Load versus deflection for specimen B-21-U-S-H

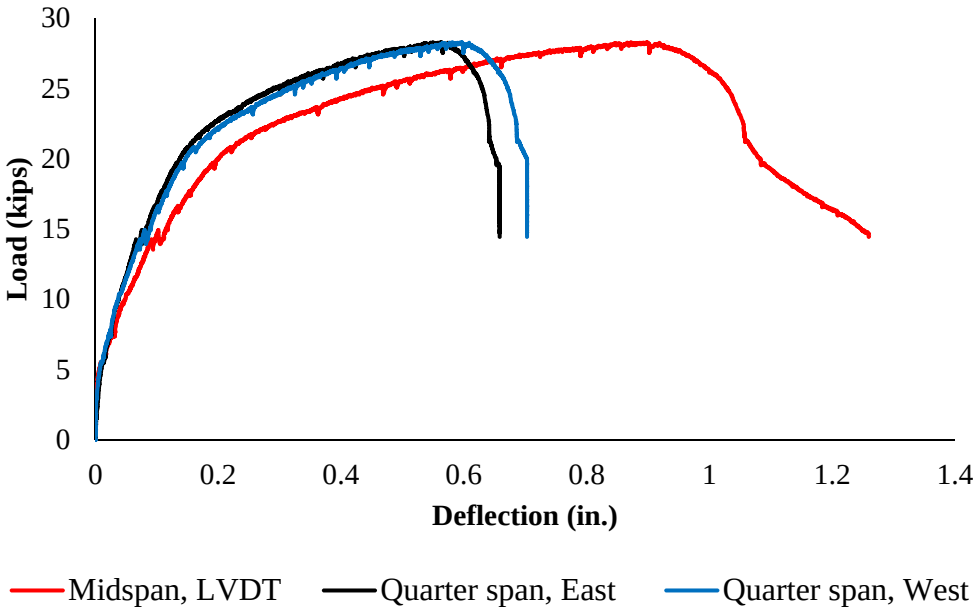

Figure A. 24 Load versus deflection for specimen B-22-U-S-A

PHASE TWO

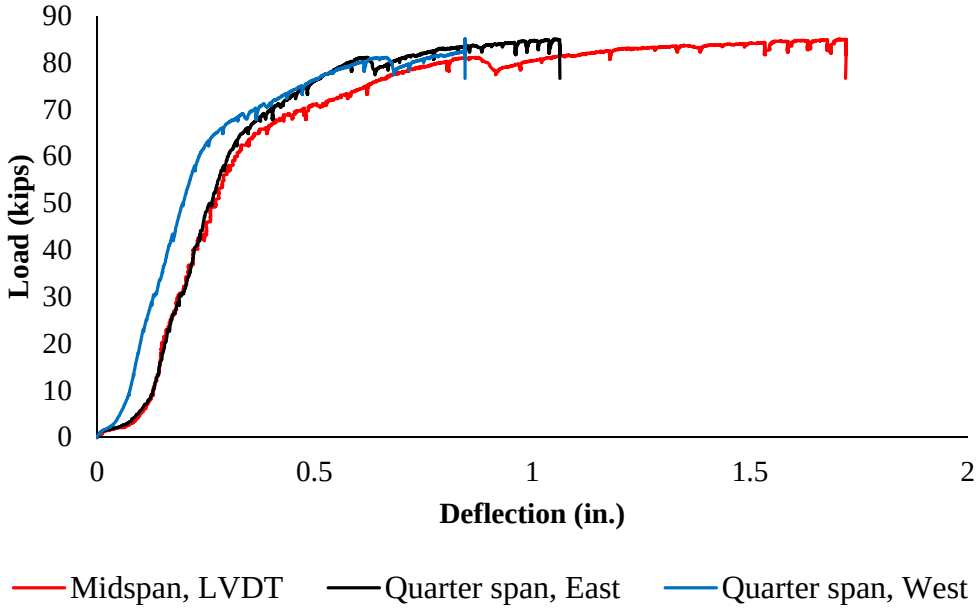

Figure A. 25 Load versus deflection for specimen B-1-C-C-N

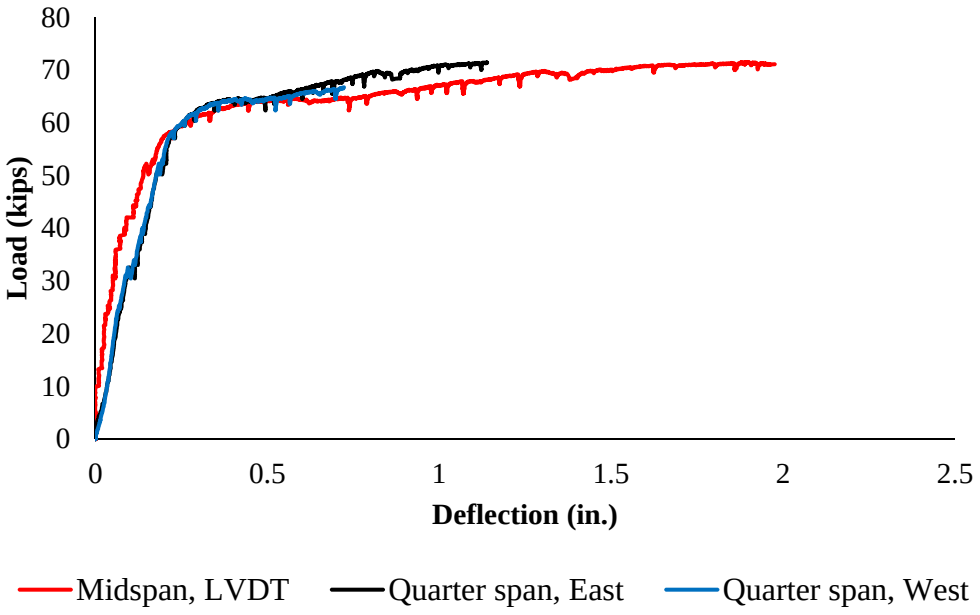

Figure A. 26 Load versus deflection for specimen B-2-C-C-M

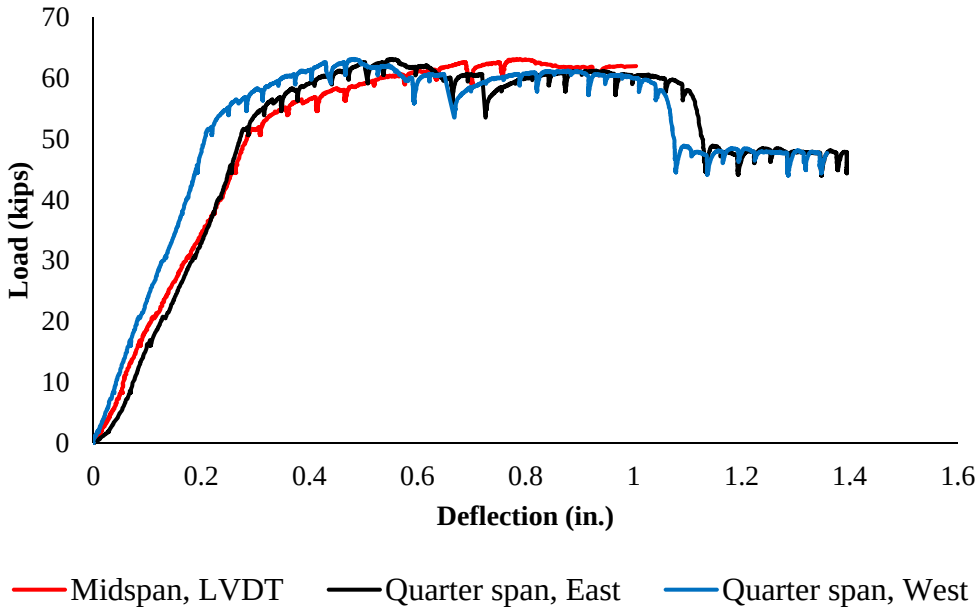

Figure A. 27 Load versus deflection for specimen B-3-MB-MB-M

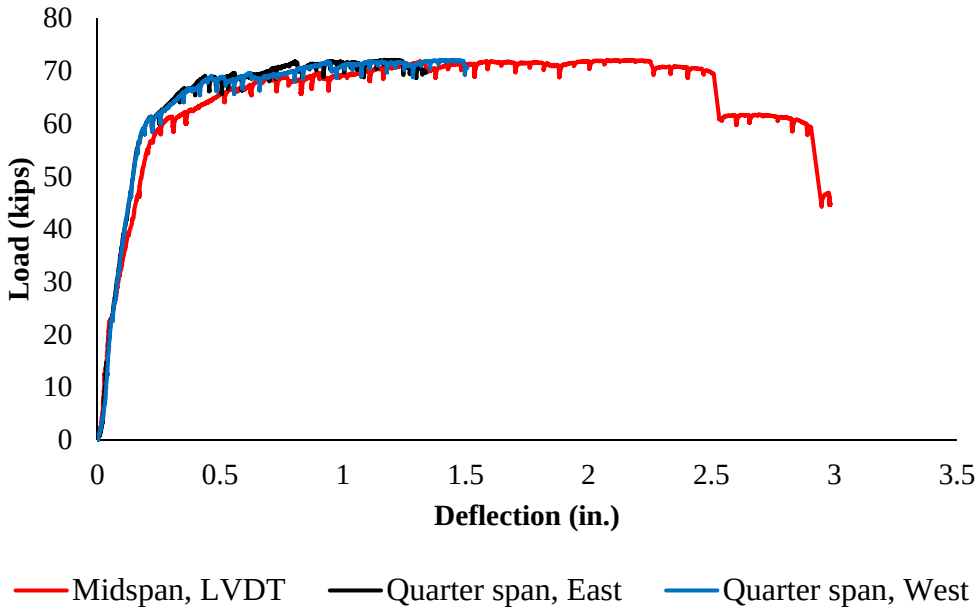

Figure A. 28 Load versus deflection for specimen B-4-U-MB-M

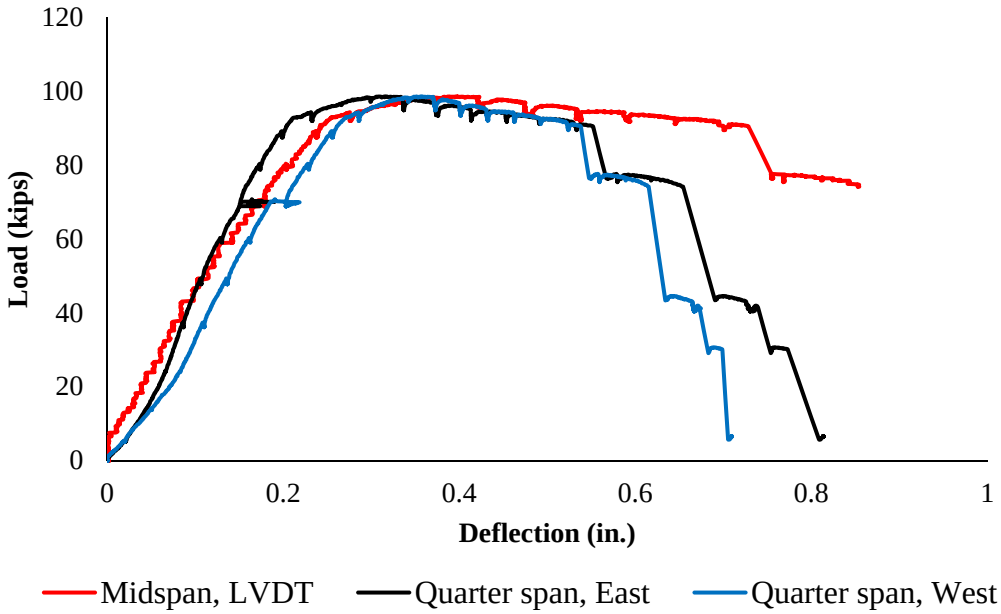

Figure A. 29 Load versus deflection for specimen B-5-U-U-M

APPENDIX B.
LOAD VERSUS STRAIN PLOTS

This appendix lists the load versus strain plots of all the specimens. Strain gages were installed on the top and bottom reinforcements and on the concrete surface of the specimens to study the strain behavior of the steel in the concrete and surface strain of the concrete at peak load. The location of strain gages is listed in Table B. 1 and shown in Figure B. 1 and Figure B. 2.

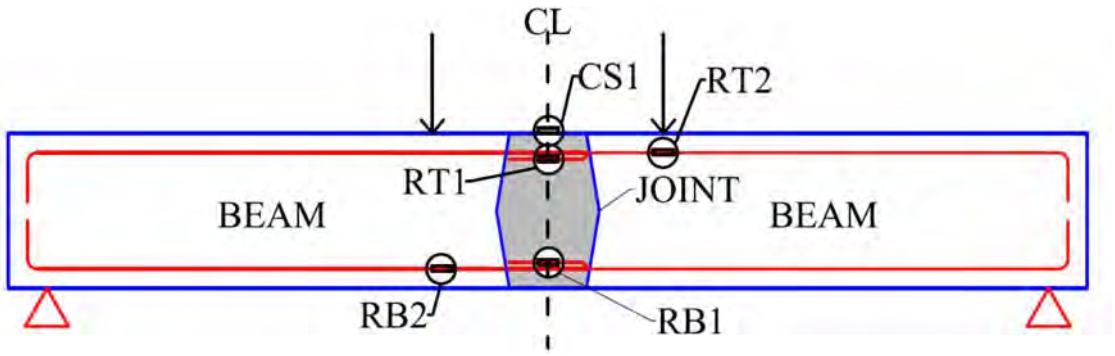

Figure B. 1 Location of strain gages in Phase one

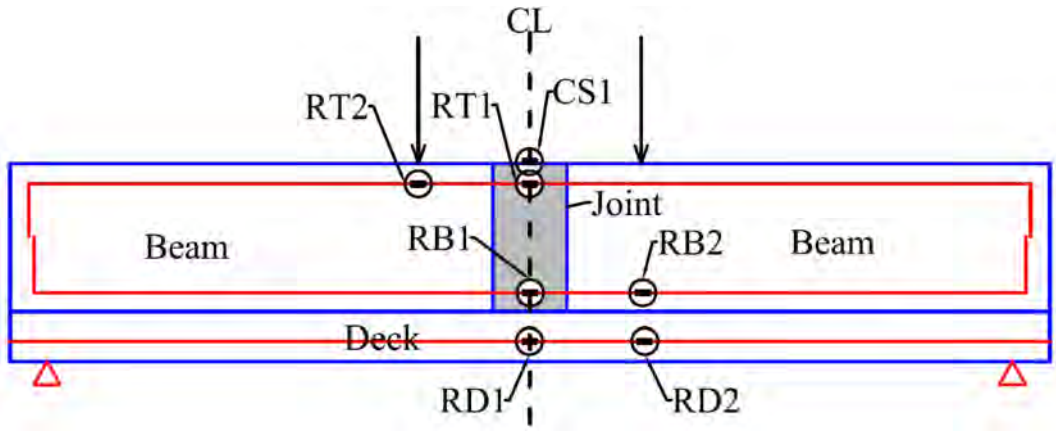

Figure B. 2 Location of strain gages in Phase two

Table B. 1 Location of Strain gages

Nomenclature	Color used in plots	Location of strain gauge
RB1	Red	On tensile reinforcement at midspan
RB2	Black	On tensile reinforcement under the load point
RT1	Blue	On compressive reinforcement at midspan
RT2	Purple	On compressive reinforcement under the load point
RD1	Green	On deck reinforcement at midspan
RD2	Magenta	On deck reinforcement under the load point
CS1	Yellow	On concrete surface

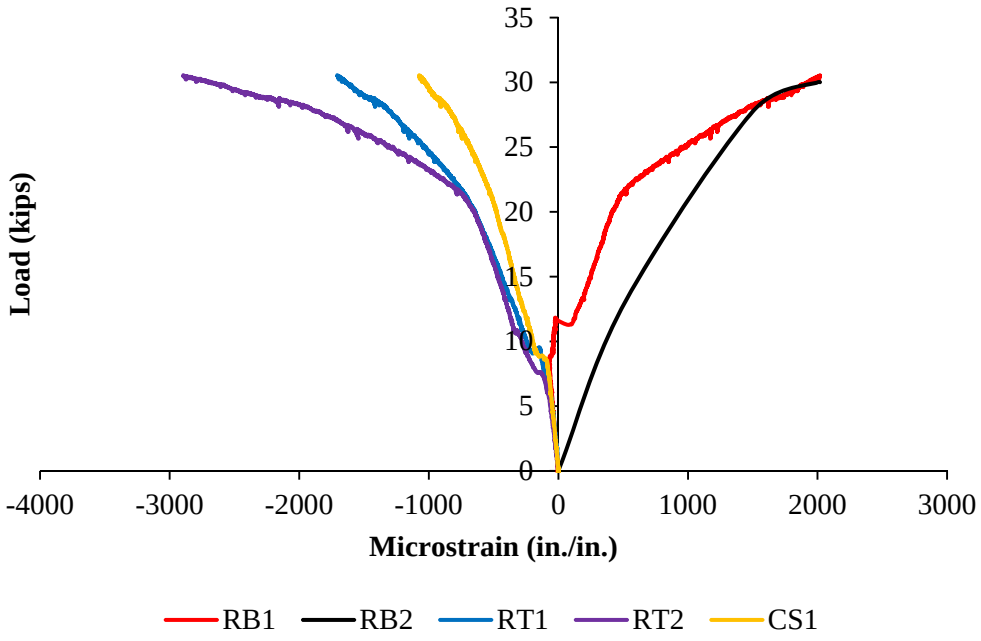

Figure B. 3 Load versus strain for specimen B-1-C-N-N

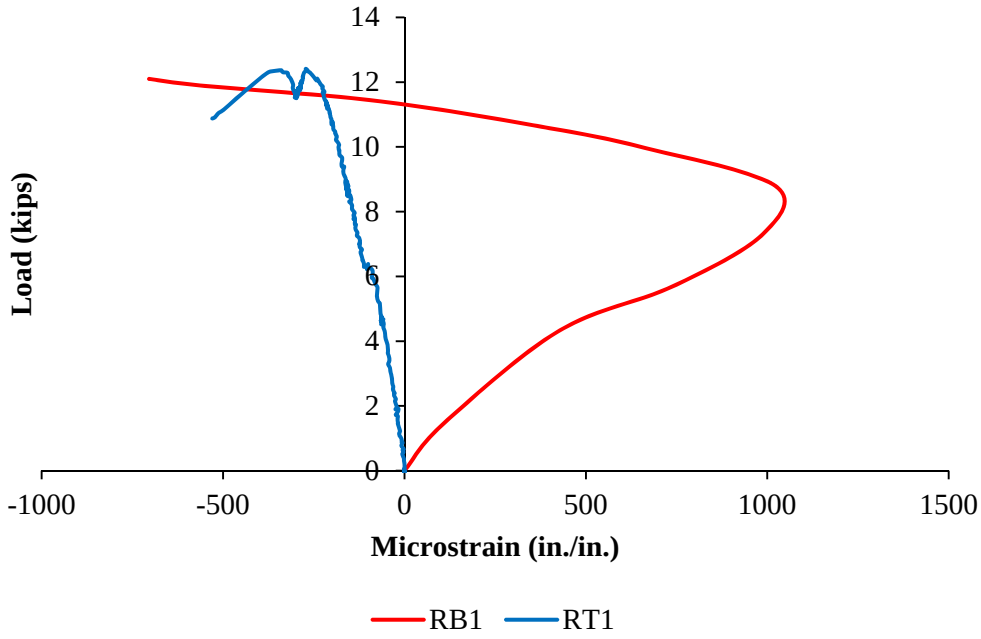

Figure B. 4 Load versus strain for specimen B-2-C-N-S

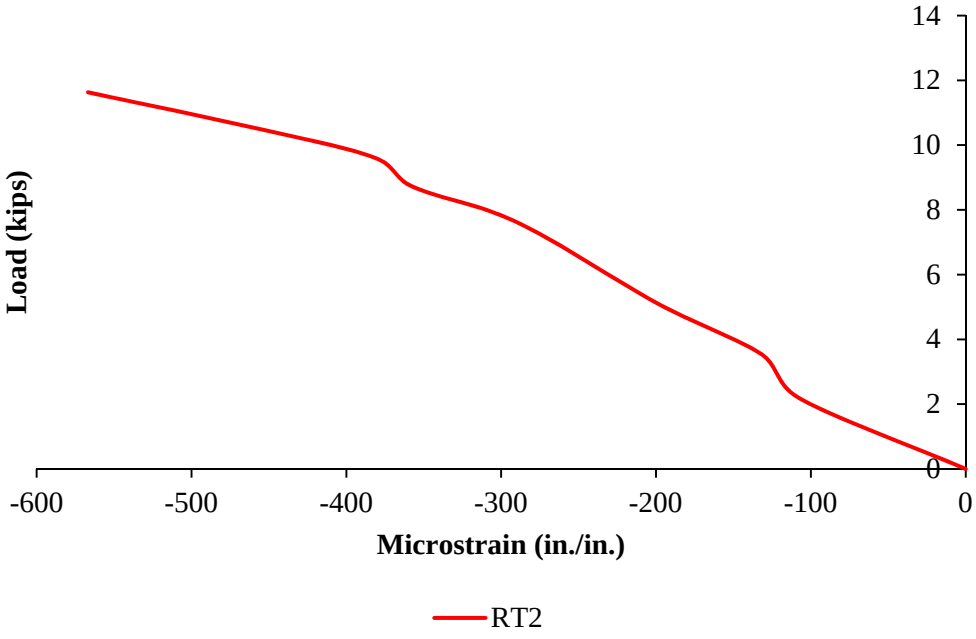

Figure B. 5 Load versus strain for specimen B-3-C-N-H

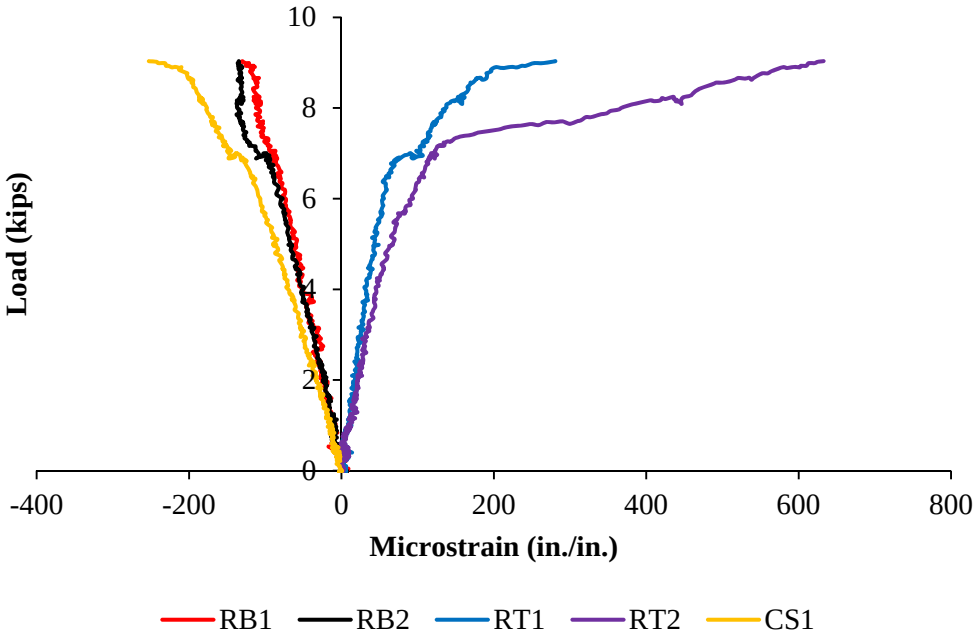

Figure B. 6 Load versus strain for specimen B-4-C-N-A

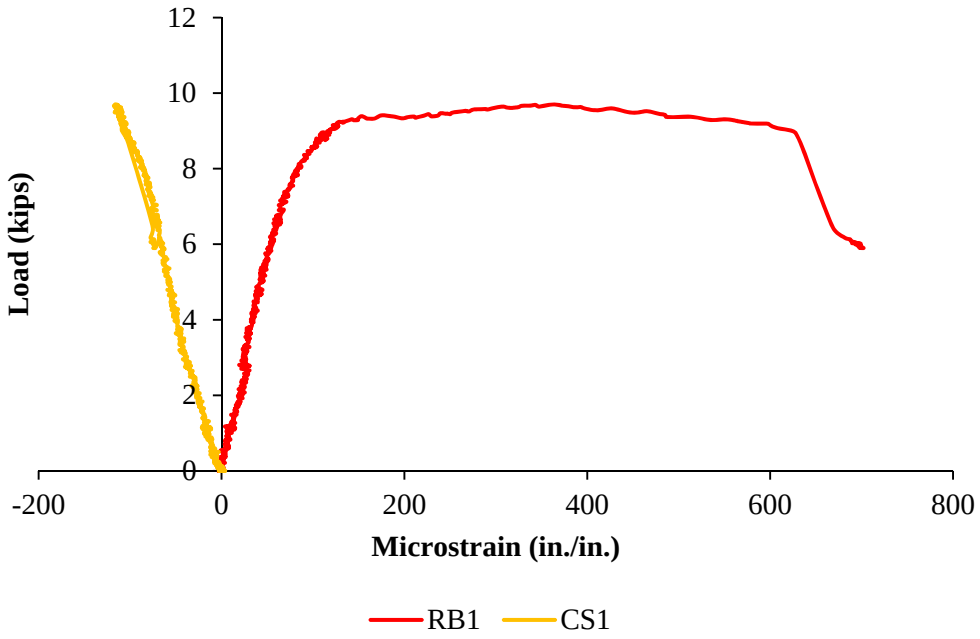

Figure B. 7 Load versus strain for specimen B-5-H-N-S

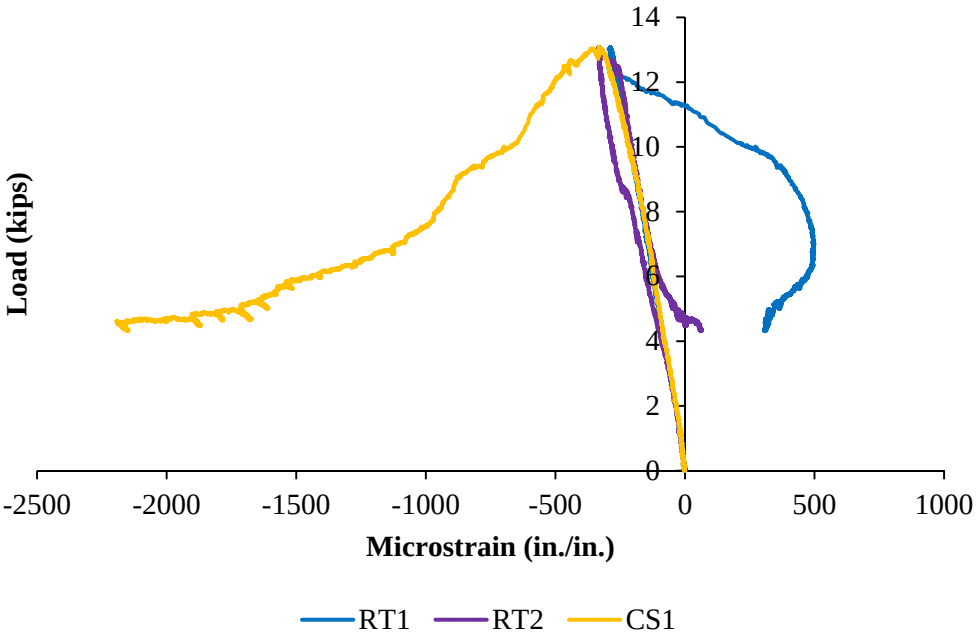

Figure B. 8 Load versus strain for specimen B-6-H-N-H

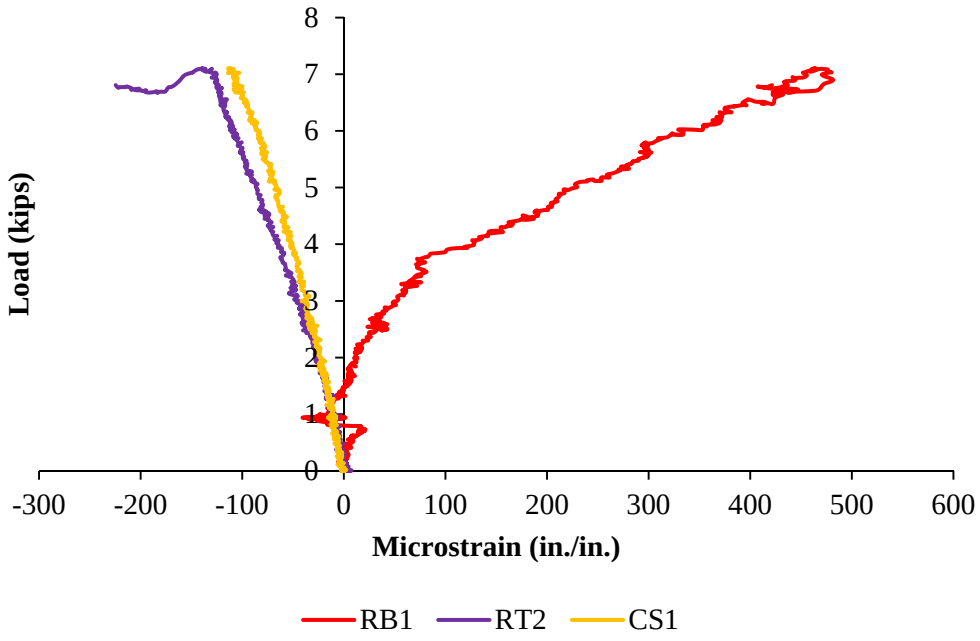

Figure B. 9 Load versus strain for specimen B-7-H-N-A

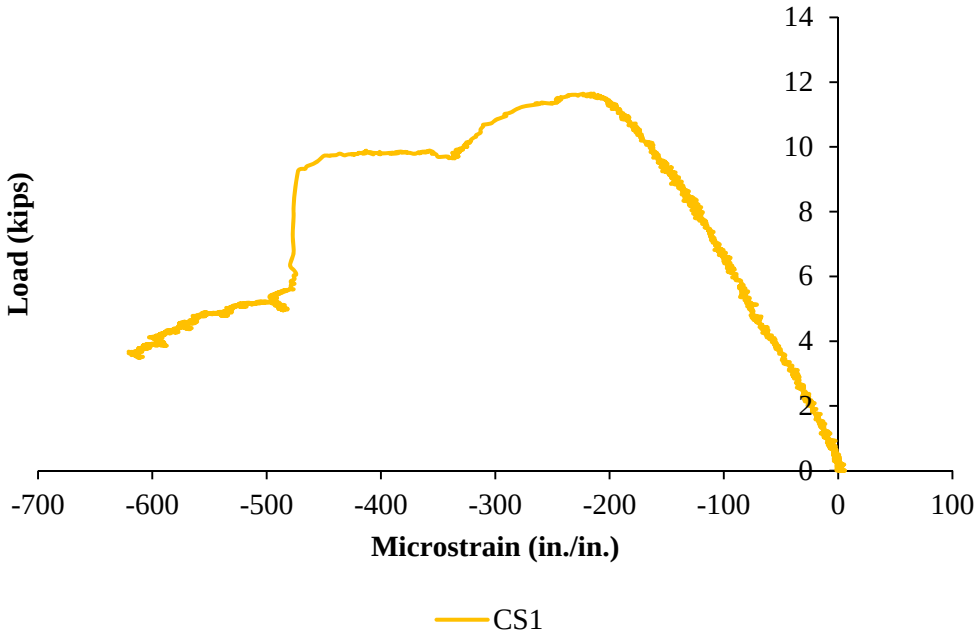

Figure B. 10 Load versus strain for specimen B-8-H-R-S

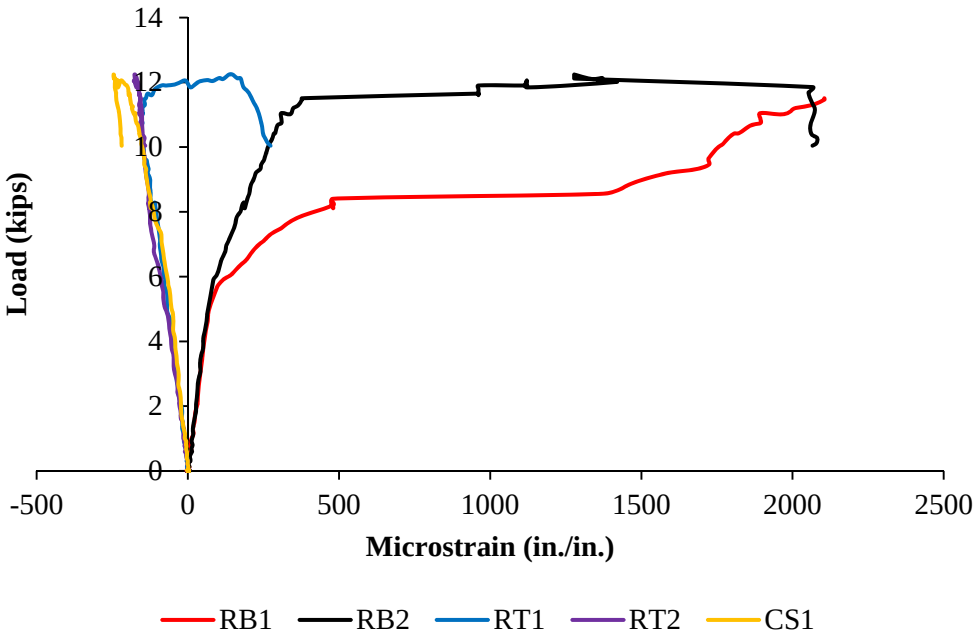

Figure B. 11 Load versus strain for specimen B-9-H-R-H

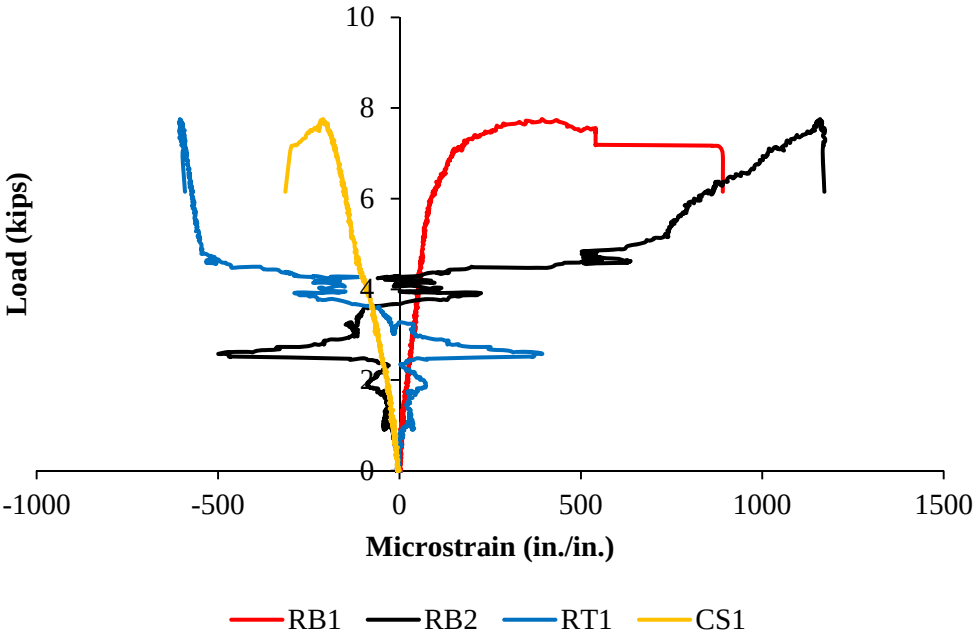

Figure B. 12 Load versus strain for specimen B-10-H-R-A

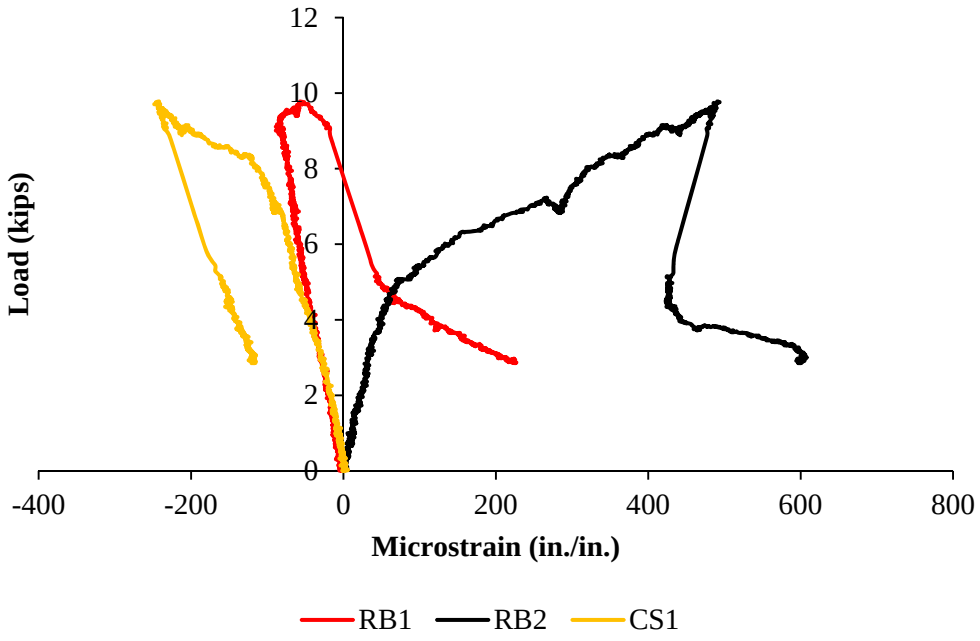

Figure B. 13 Load versus strain for specimen B-11-H-R-S

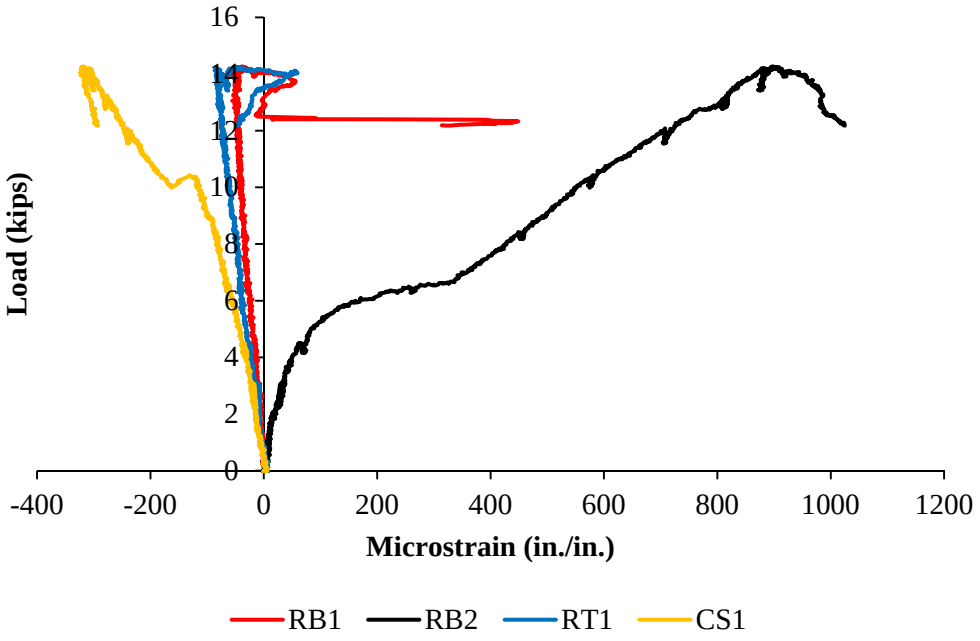

Figure B. 14 Load versus strain for specimen B-12-H-S-H

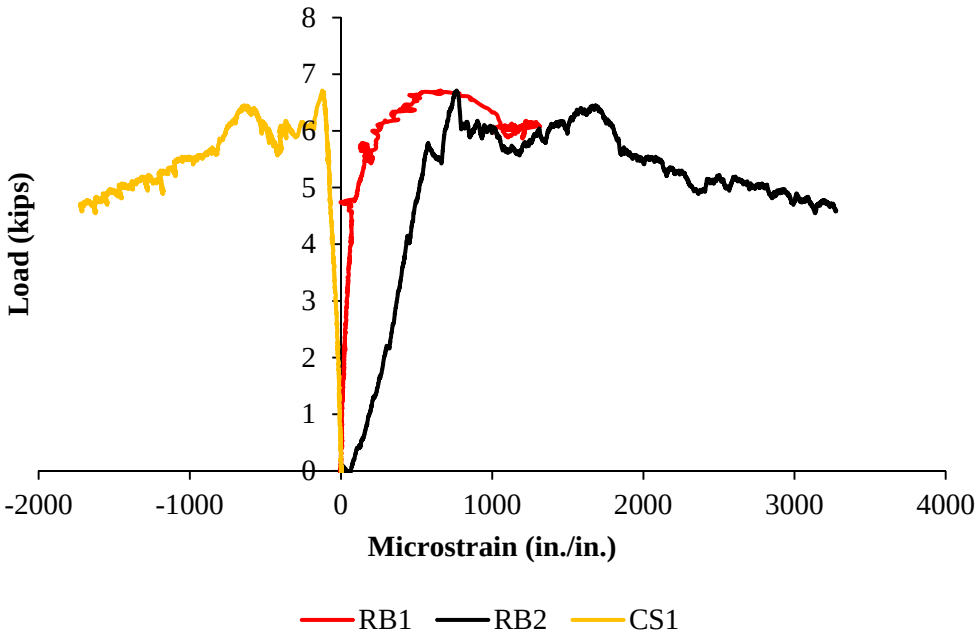

Figure B. 15 Load versus strain for specimen B-13-H-S-A

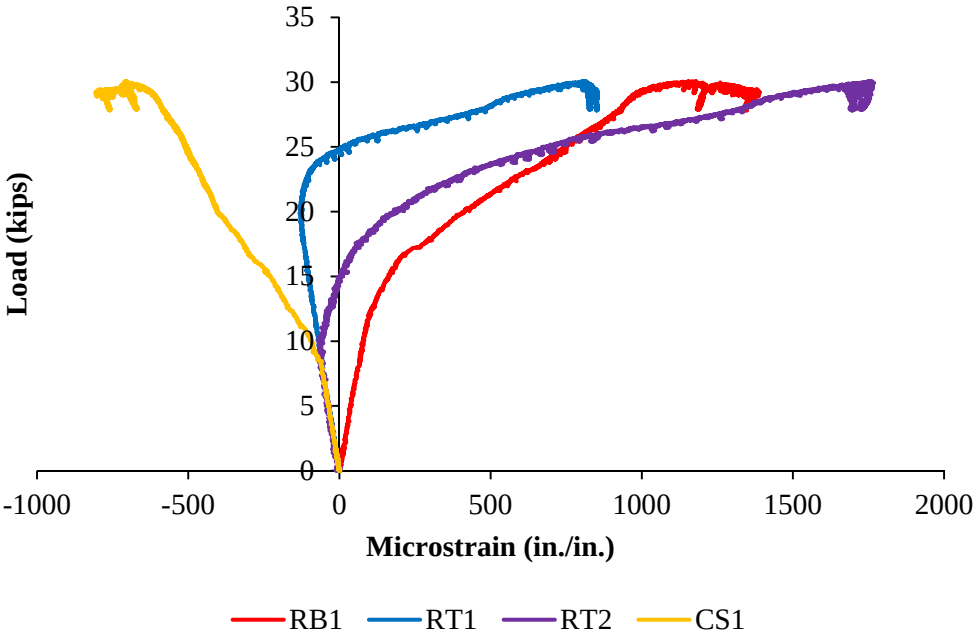

Figure B. 16 Load versus strain for specimen B-14-U-N-S

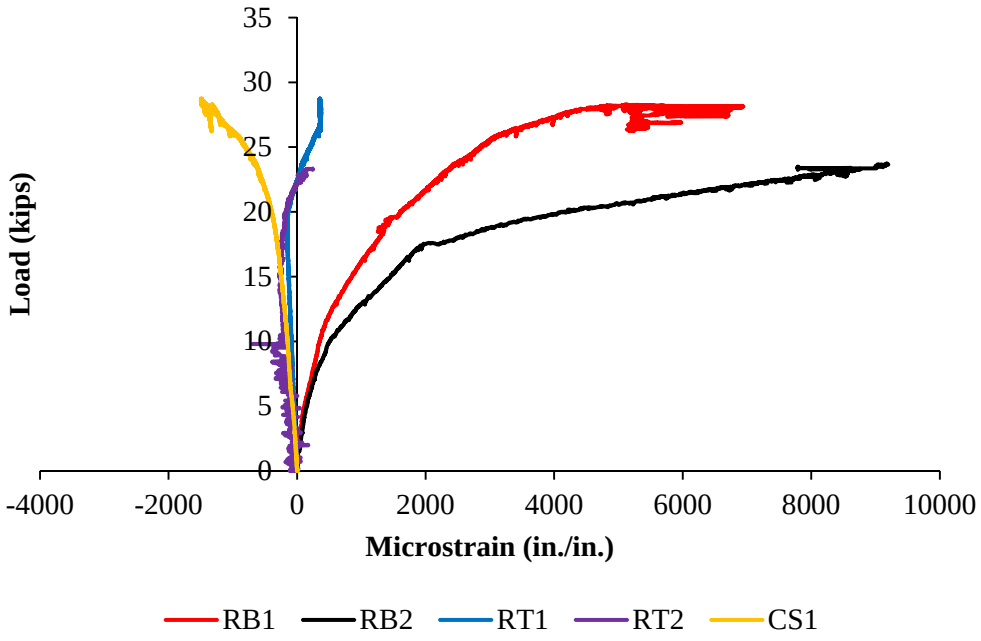

Figure B. 17 Load versus strain for specimen B-15-U-N-H

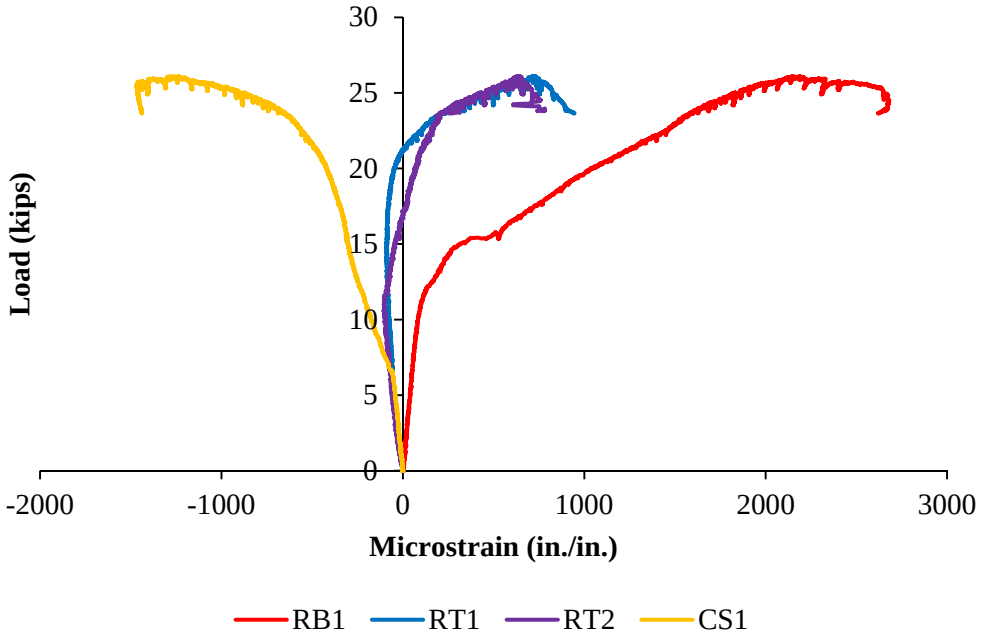

Figure B. 18 Load versus strain for specimen B-16-U-N-A

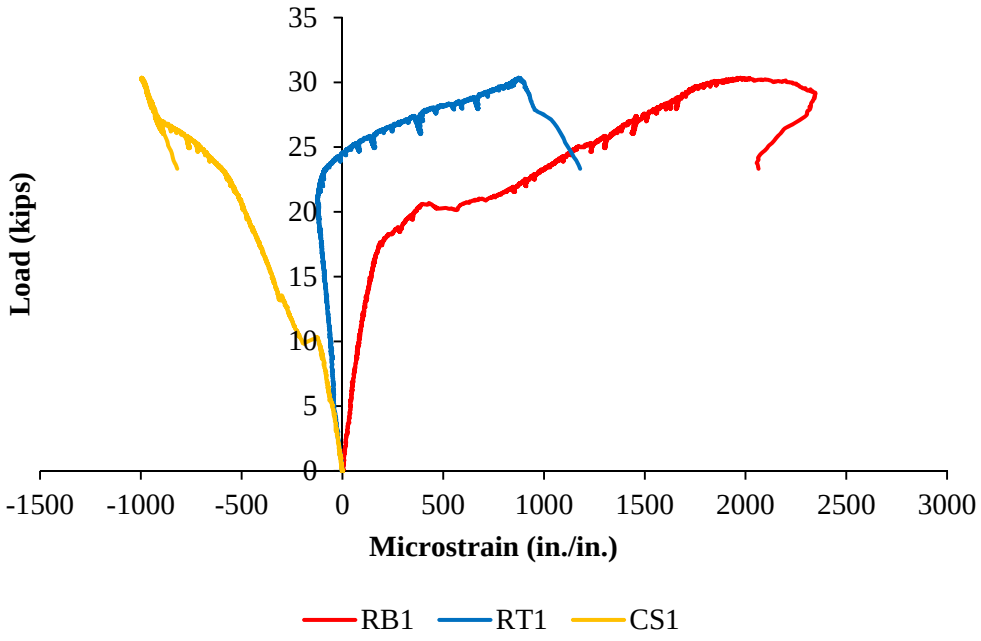

Figure B. 19 Load versus strain for specimen B-17-U-R-S

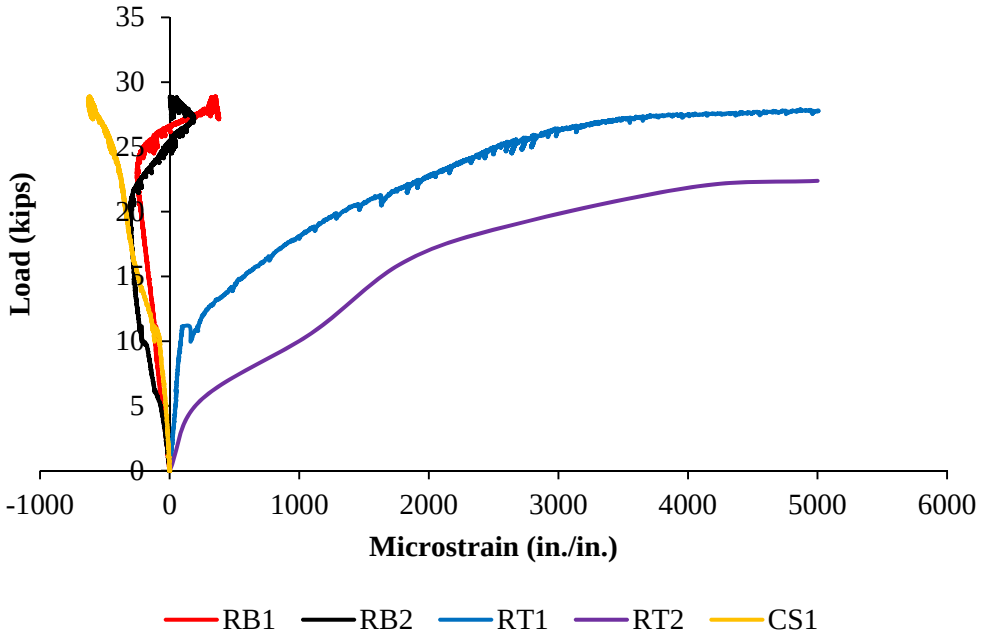

Figure B. 20 Load versus strain for specimen B-18-U-R-H

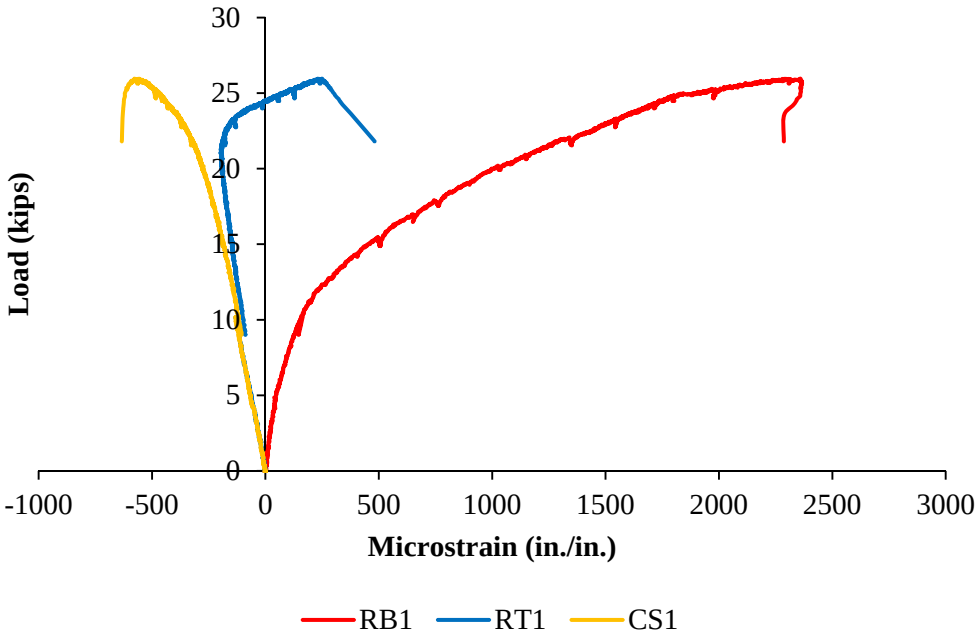

Figure B. 21 Load versus strain for specimen B-19-U-R-A

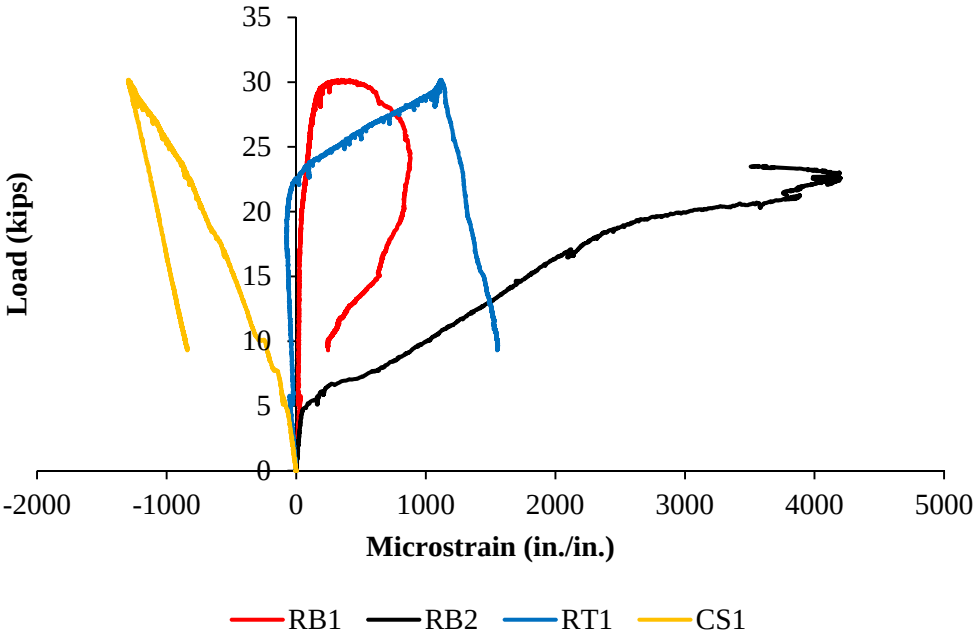

Figure B. 22 Load versus strain for specimen B-20-U-S-S

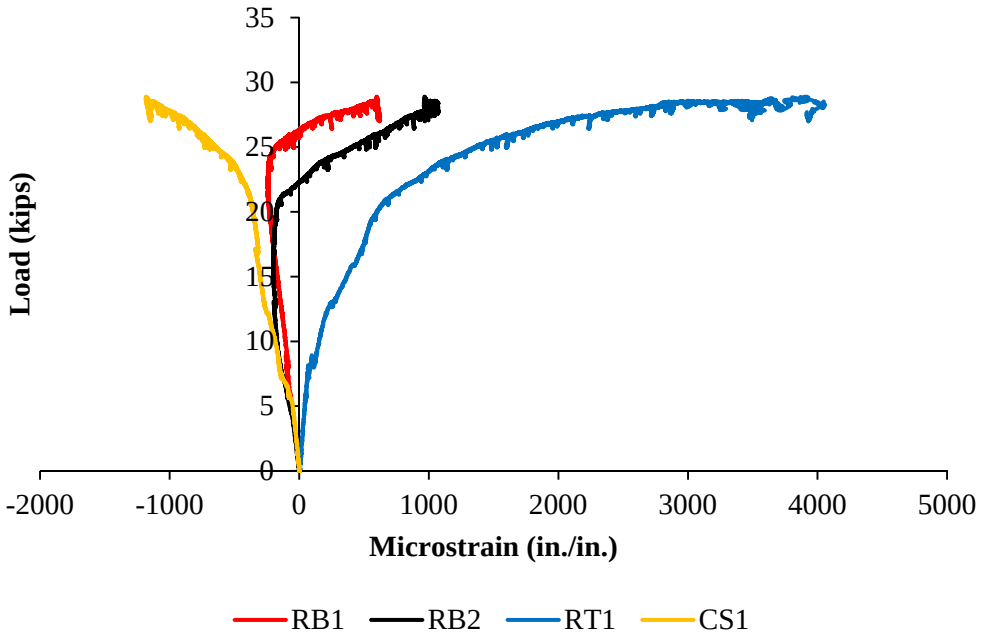

Figure B. 23 Load versus strain for specimen B-21-U-S-H

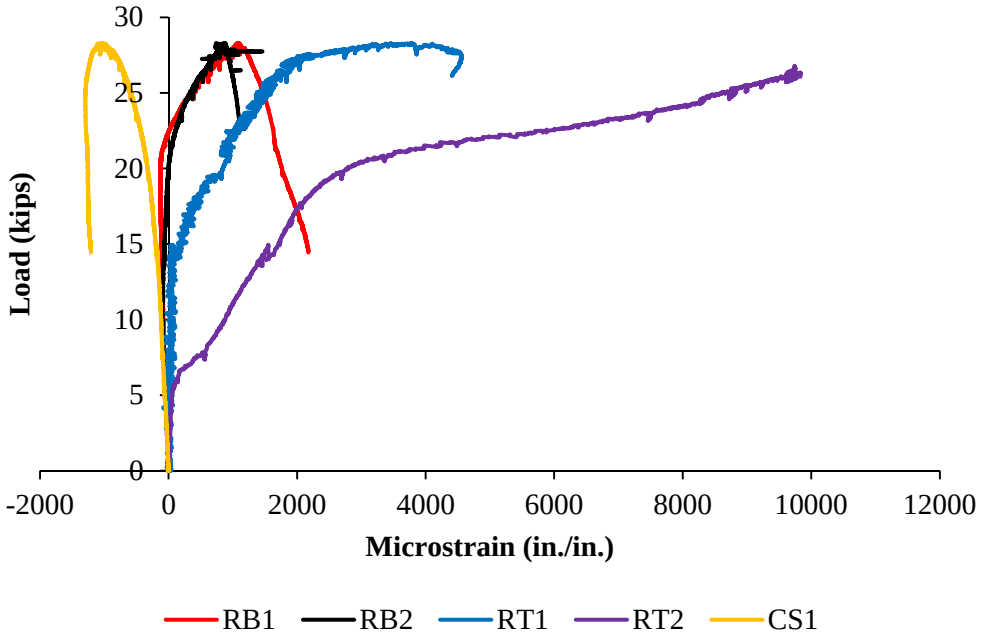

Figure B. 24 Load versus strain for specimen B-22-U-S-A

PHASE TWO

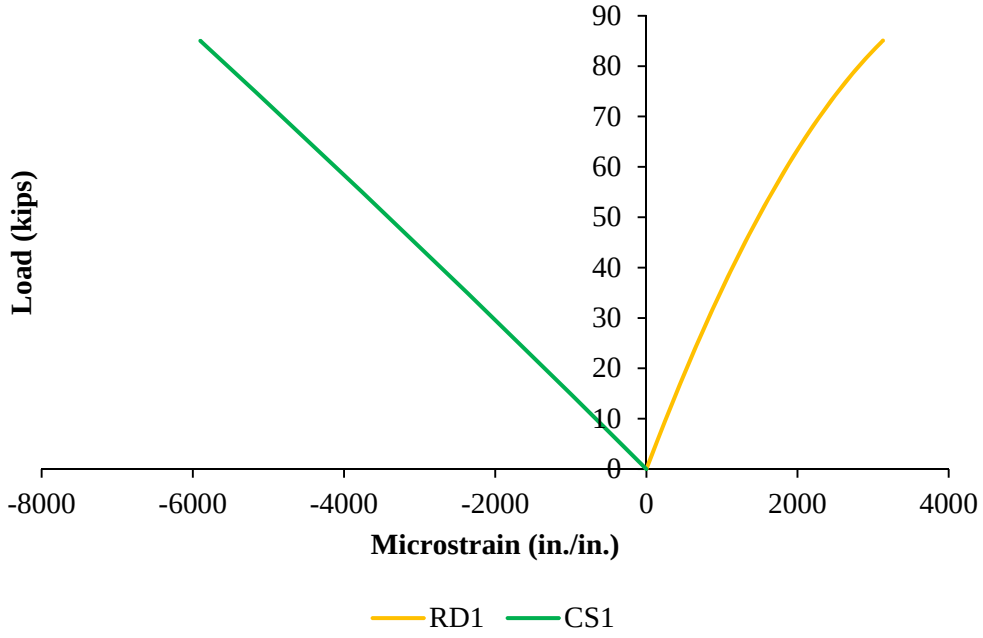

Figure B. 25 Load versus strain for specimen B-1-C-C-N

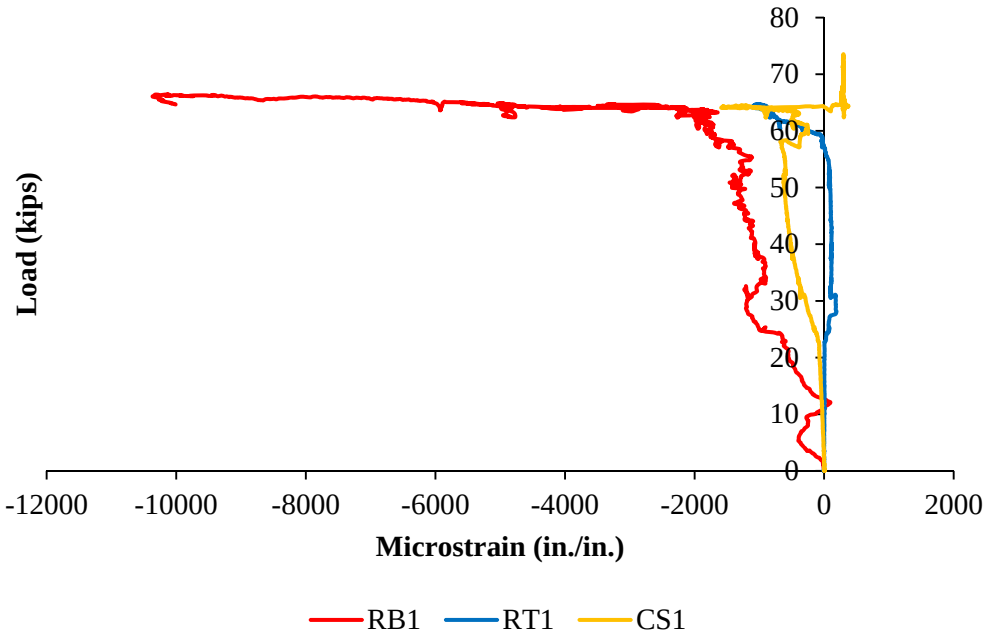

Figure B. 26 Load versus strain for specimen B-2-C-C-M

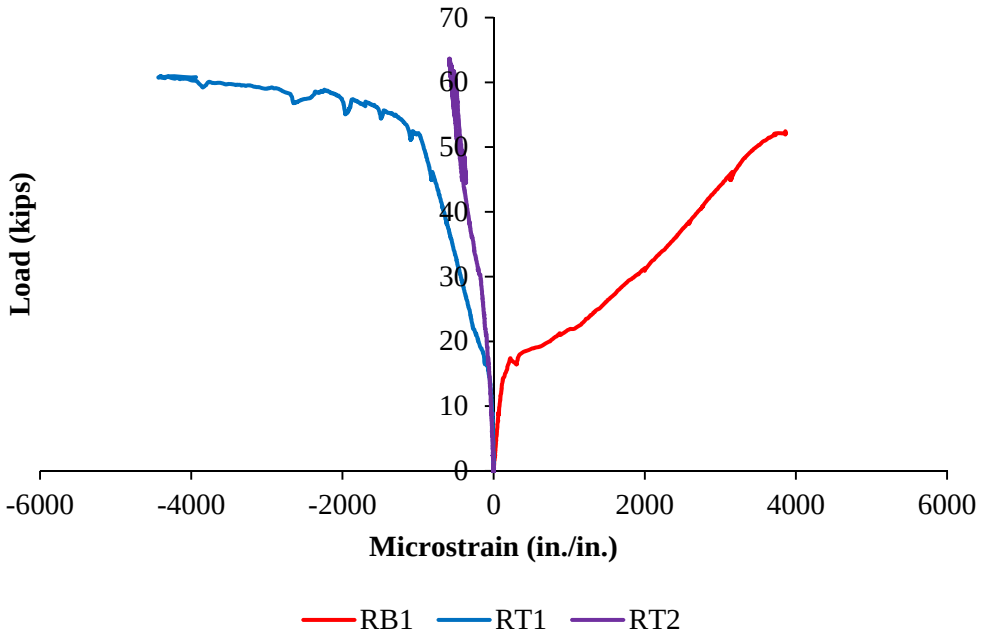

Figure B. 27 Load versus strain for specimen B-3-MB-MB-M

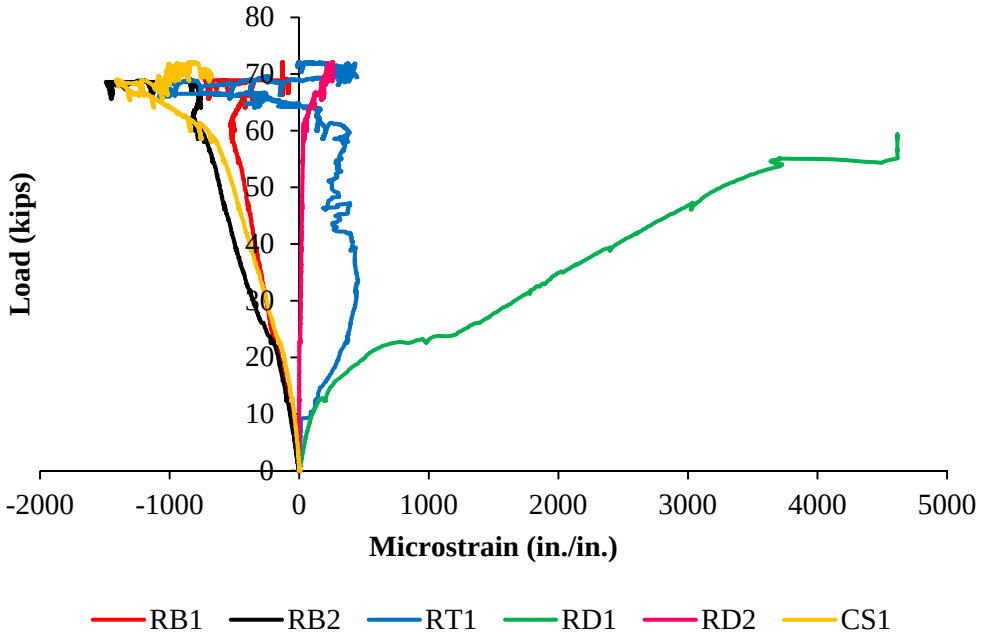

Figure B. 28 Load versus strain for specimen B-4-U-MB-M

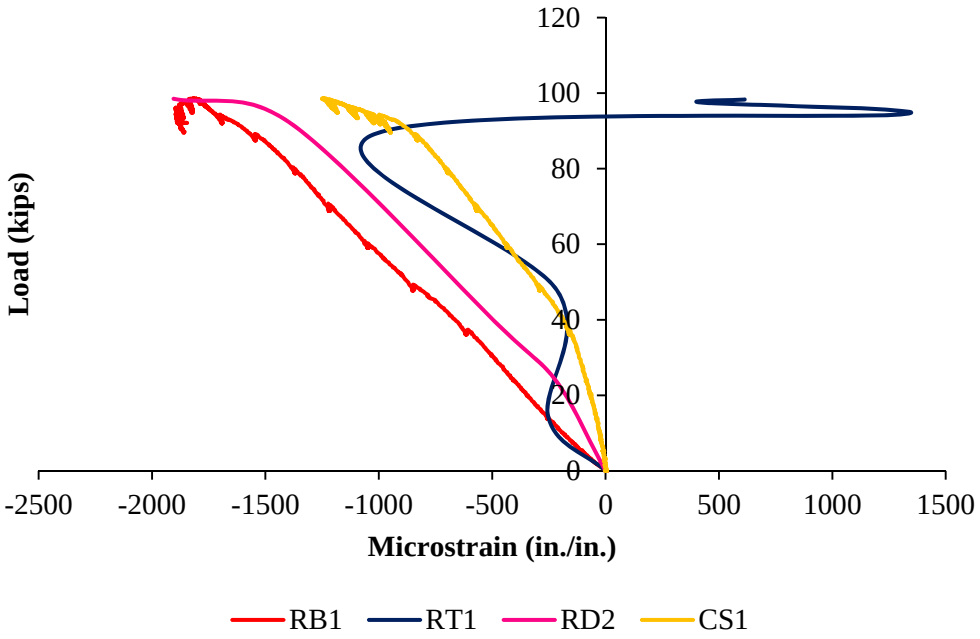

Figure B. 29 Load versus strain for specimen B-5-U-U-M

APPENDIX C.
AGGREGATE PROPERTIES

This appendix contains the materials properties such as gradation data of aggregates and design properties of aggregates like specific gravity, absorption, and moisture content. The specific gravity of aggregate tests are tabulated in the following table.

Table C. 1 Aggregate properties

Aggregate	Specific Gravity	Absorption (%)	DRUW
1-in. Stone	2.53	3.3	102.9 lb/ft^3
3/8-in.Crushed stone	2.61	1.5	-
River sand	2.62	0.5	-
Masonry sand	2.57	0.7	-

Gradation of aggregates can be used to determine the packing density of the concrete mix. Gradation was run for Fine aggregate (river sand), masonry sand, concrete stone (1-in.) and crushed stone (3/8-in.). The following tables give the gradations of the aggregates followed by a gradation plot.

Table C. 2 Missouri river sand gradation data

River Sand					
W_0= 4 lbs.					
Sieve		Sample Weight (lb.)	Retaining (%)	Accumulative Retaining (%)	Passing (%)
#4	4.75 mm	0.042	1.05	1.05	100
#8	2.36 mm	0.37	9.25	10.3	90
#16	1.18 mm	1.107	27.675	37.975	62.0
#30	0.6 mm	1.792	44.8	82.775	17.2
#50	0.3 mm	0.648	16.2	98.975	1.0
#100	0.15 mm	0.022	0.55	99.525	0.5
#200	0.075 mm	0.017	0.425	99.95	0
Pan		0.001	0.025	99.975	0
FM=3.306					

Conversion 1-in. = 25.4 mm

Table C. 3 Masonry sand gradation data

Masonry sand					
W_0= 2.2 lbs.					
Sieve		Sample Weight (lb.)	Retaining (%)	Accumulative Retaining (%)	Passing (%)
#4	4.75 mm	0	0	0	100
#8	2.36 mm	0	0	0	100
#16	1.18 mm	0	0	0	100
#30	0.6 mm	0.149	7	7	93
#50	0.3 mm	1.323	60	67	33
#100	0.15 mm	0.72	33	100	0
#200	0.075 mm	0	0	100	0
Pan		0.001	0.04543	100	0
FM= 1.73					

Conversion 1-in. = 25.4 mm

Table C. 4 Concrete stone gradation data

Stone					
W_0= 6.91 lbs.					
Sieve		Sample Weight (lb.)	Retaining (%)	Accumulative Retaining (%)	Passing (%)
1	25.4	0	0	0	100
3/4"	19	0.255	3.6903039	4	96
1/2"	12.5	1.112	16.092619	20	80
3/8"	9.5	1.917	27.742402	48	52
#4	4.75	3.154	45.643994	93	7
#8	2.36	0.049	0.7091172	94	6
#30	1.18	0.001	0.0144718	94	6
#100	0.149	0.001	0.0144718	94	6
#200	0.075	0.001	0.0144718	94	6.1
Pan		0.014	0.2026049	94	6
FM =4.260					

Conversion 1-in. = 25.4 mm

Table C. 5 Crushed stone gradation data

Crushed Stone 3/8"					
W0= 6.37 lbs.					
Sieve		Sample Weight (lb.)	Retaining (%)	Accumulative Retaining (%)	Passing (%)
3/4"	19 mm	0	0	0	100
1/2"	12.5 mm	0	0	0	100
3/8"	9.5 mm	0	0	0	100
#4	4.75 mm	3.152	49	49	51
#8	2.36 mm	2.857	45	94	6
#16	1.18 mm	0.186	3	97	3
#200	0.075 mm	0.152	2	100	0.39
Pan		0.015	0	100	0
FM=2.4					

Conversion 1-in. = 25.4 mm

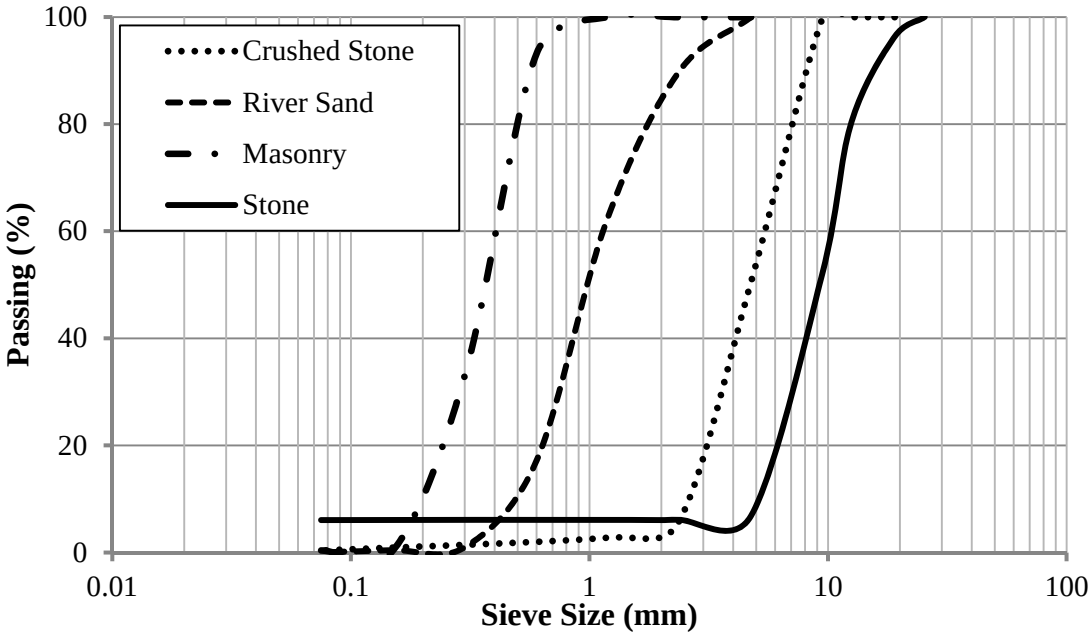

Figure C. 1 Gradation plot for all aggregates

APPENDIX D.
STRENGTH GAIN CURVES OF ALL MIX DESIGNS

This appendix contains the strength gain plots for all the mixes followed by the compressive strength f'c tabulated for each mix. In total, there were four CC, one HS-SCC, one MoDOT MB, and five UHSC castings for two Phases of the project.

In Phase one, CC was used to cast the beam specimens and also to cast the controls. Three castings took place.

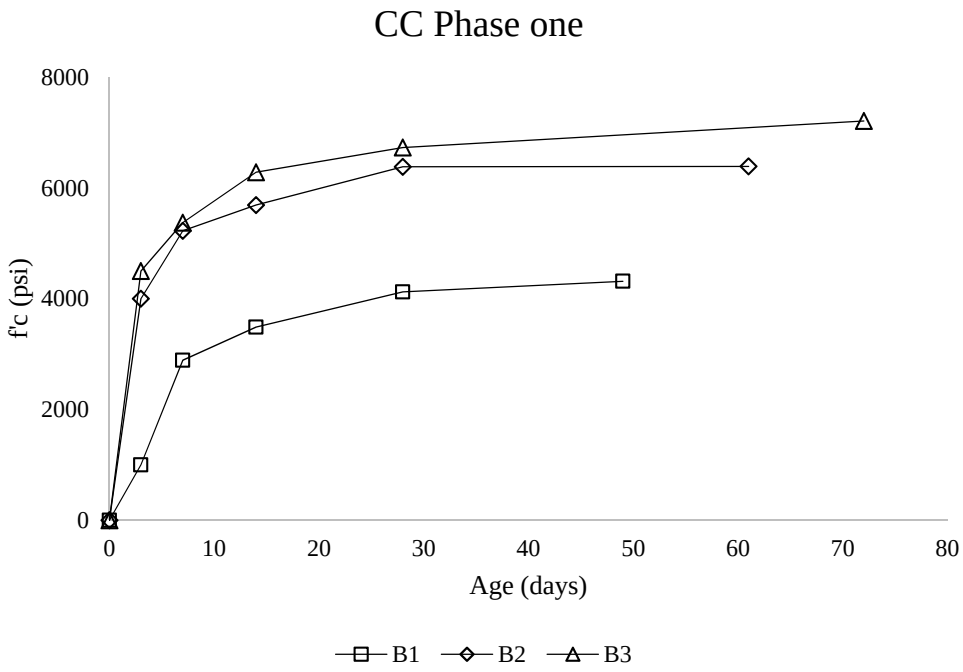

Figure D. 1 f'c curves for CC during Phase one

Table D. 1 f'c data for CC during Phase one

CC Phase one			
Mix name	B1	B2	B3
Age (days)	f'c (psi)		
3	1000	4000	4500
7	2890	5227	5375
14	3488	5692	6285
28	4123	6383	6731
Test	4315	6390	7210
Day of casting	4/1/2015	4/17/2015	5/4/2015
Day of testing	5/19/2015	6/16/2015	7/15/2015
Test age	49	61	72

Conversion 1 psi = 0.006895 MPa

In Phase two, CC was used to cast the controls and beam specimens.

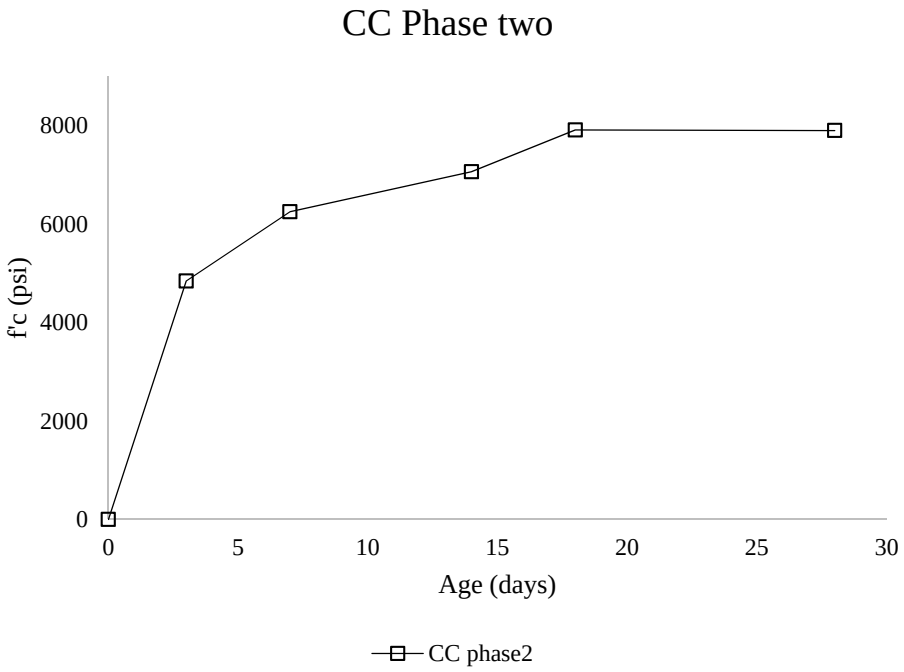

Figure D. 2 f’c curves for CC during Phase two

Table D. 2 f’c data for CC during Phase two

CC Phase two	
Age (days)	f'c (psi)
3	4844
7	6252
14	7064
28	7912
Test	7901
Day of casting	9/23/2015
Day of testing	10/27/2015
Test age	18

Conversion 1 psi = 0.006895 MPa

In Phase one, HS-SCC was used as one of the joint fillers.

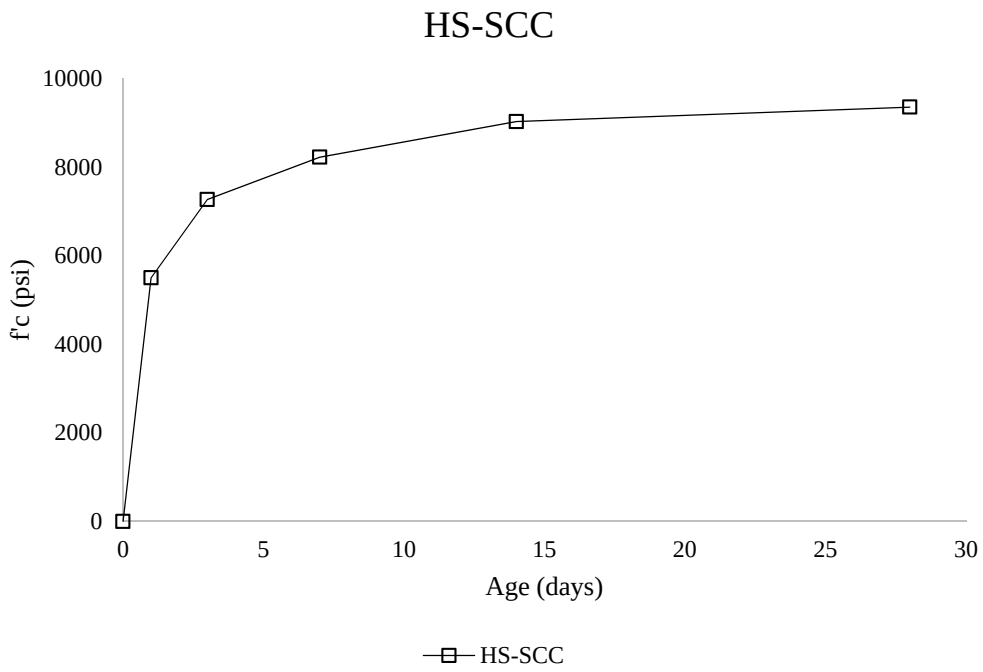

Figure D. 3 f’c curve for HS-SCC during Phase one

Table D. 3 f’c data for HS-SCC during Phase one

HS-SCC	
Age (days)	f'c (psi)
1	5500
3	7267
7	8222
14	9027
28/Test day	9353
Day of casting	5/22/2015
Day of testing	6/18/2015
Test age	28

Conversion 1 psi = 0.006895 MPa

This mix was developed as part of research project for Highway 50 and additional mix properties are given in report “Self-Consolidating Concrete (SCC) and High-Volume Fly-Ash Concrete (HVFAC) for Infrastructure Rehabilitation: Implementation, Myers et al., 2014”.

In Phase two, MoDOT B mix was used to cast the deck and joint in B-3-MB-MB-M and deck in B-4-U-MB-M.

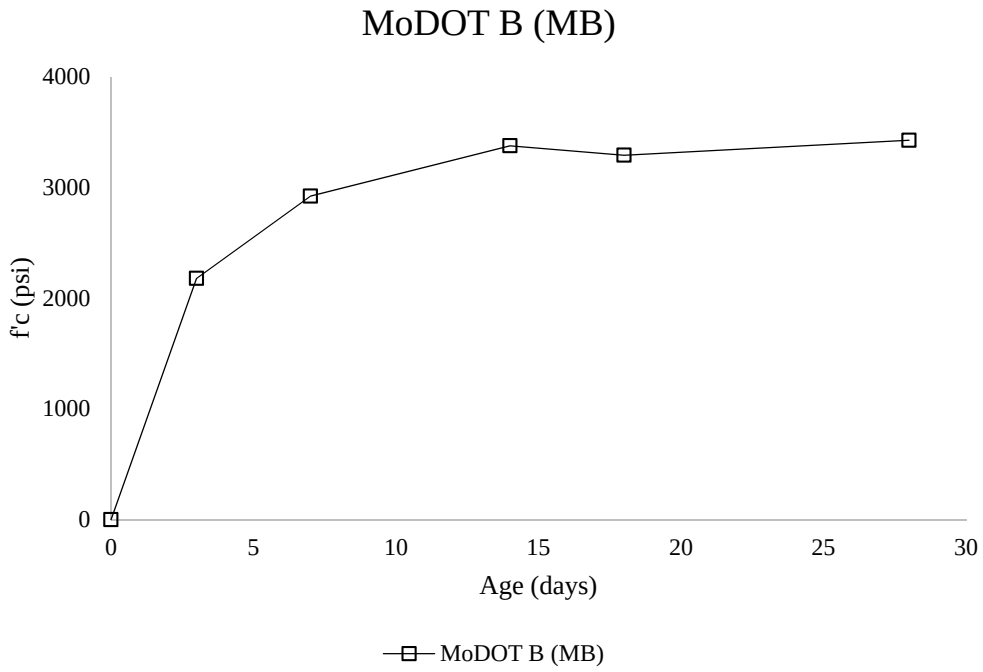

Figure D. 4 f’c curves for MoDOT B mix during Phase two

Table D. 4 f’c data for MoDOT B mix during Phase two

MoDOT B (MB)	
Age (days)	f'c (psi)
3	2178
7	2921
14	3375
28	3426
Test	3291
Day of casting	10/9/2015
Day of testing	10/27/2015
Test age	18

Conversion 1 psi = 0.006895 MPa

In Phase one, three batches of UHSC were mixed using the same mix and volume and same curing regime to maintain consistency.

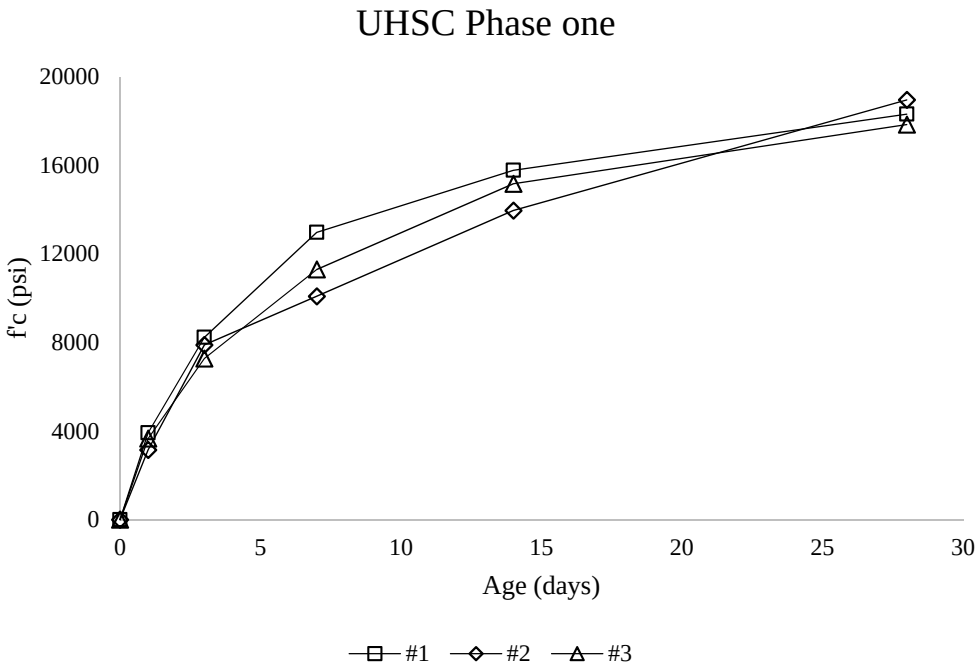

Figure D. 5 f’c curves for UHSC during Phase one

Table D. 5 f’c data for UHSC during Phase one

UHSC			
Mix name	#1	#2	#3
Age (days)	f'c (psi)		
1	3918	3146	3658
3	8233	7887	7274
7	12971	10083	11295
14/Test day	15772	13958	15163
28	18308	18950	17834
Day of casting	7/1/2015	7/1/2015	7/2/2015
Day of testing	7/15/2015	7/16/2015	7/17/2015
Test age	14	15	15

Conversion 1 psi = 0.006895 MPa

In Phase two, U#1 was used to cast the joint in B-4-U-MB-M. UD (UHSC deck) was used to cast the deck and joint in B-5-U-U-M.

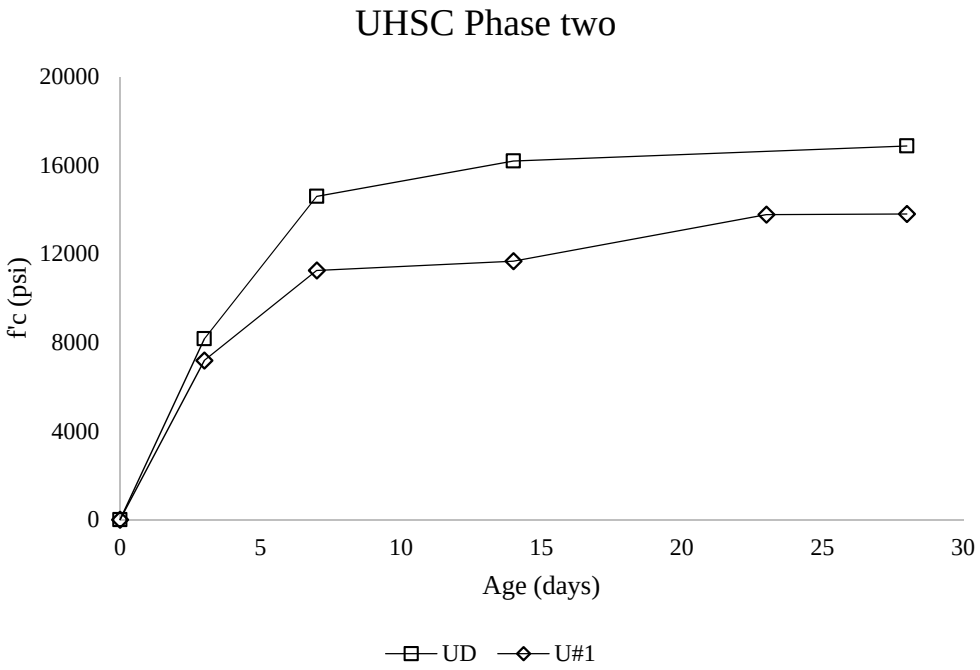

Figure D. 6 f’c curves for UHSC during Phase two

Table D. 6 f’c data for UHSC during Phase two

UHSC Phase two		
Mix name	U#1	UD
Age (days)	f'c (psi)	
3	7189	8165
7	11253	14594
14	11672	16192
28	13801	16871
Test	13772	16192
Day of casting	10/3/2015	10/5/2015
Day of testing	10/26/2015	10/19/2015
Test age	23	14

Conversion 1 psi = 0.006895 MPa

APPENDIX E.
MoDOT BRIDGE DESIGN DRAWING

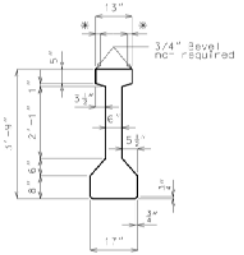

GIRDER DIMENSIONS

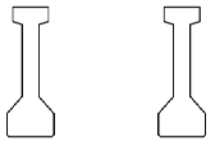

℄ GIRDER STRAND ARRANGEMENTS

END OF GIRDER STRAND ARRANGEMENTS

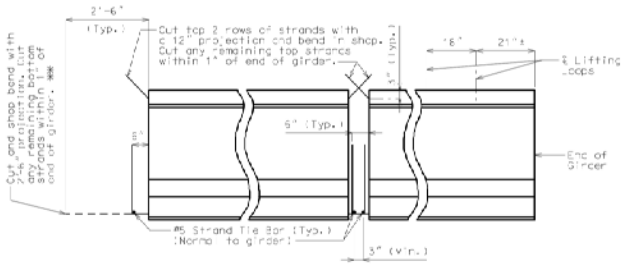

END BENT STRAND DETAILS AT GIRDER ENDS

Fabricator shall be responsible for location and design of lifting devices.

INTERMEDIATE BENT LOCATION OF LIFTING LOOPS

BILL OF REINFORCING STEEL – EACH GIRDER

NO.	TYPE & MARK	TOTAL LENGTH	SHAPE	BEND DIAGRAM
XXX	X 'A'	X'-X"	20	
XXX	X 'B'	X'-X"	11	
†6	6 B2	2'-6"	11	
XXX	4 'C'	13"	†0	
XXX	4 'D'	2'-6"	3	

SHAPE 'C' SHAPE 3 SHAPE 20 SHAPE 11 B1 B2

Concrete for prestressed girders shall be Class A-1 with f'c = psi and f'ci = psi.

(+) indicates prestressing strand.

Use strands with an initial prestress force of kips.

Prestressing tendons shall be uncoated, seven-wire, low-relaxation strands, ½ inch diameter in accordance with AASHTO M 203, Grade 270. Prestressed members shall be in accordance with Sec 1025.

* At contractor's option a 1 1/2" to 1 3/4" smooth finish strip is permitted to facilitate placement of preformed fiber expansion joint material or expanded or extruded polystyrene bedding material for the prestressed panels.

** At the contractor's option the location for bent-up strands may be varied from that shown for fully bonded strands only. The total number of bent-up strands shall not be changed. One strand tie bar is required for each layer of bent-up strands except on end bents which requires one bar on the bottom layer of strands only. No additional payment will be made for additional strand tie bars are required.

A dimensions are out to out.

Hooks and bends shall be in accordance with the CRSI Manual of Standard Practice for Detailing Reinforced Concrete Structures. Stirrup and Tie Dimensions.

Actual lengths are measured along centerline of bar to the nearest inch.

Minimum clearance to reinforcing shall be 1".

A reinforcement shall be Grade 60.

The two D1 bars may be furnished as one bar at the fabricator's option.

A B1 bars shall be epoxy coated.

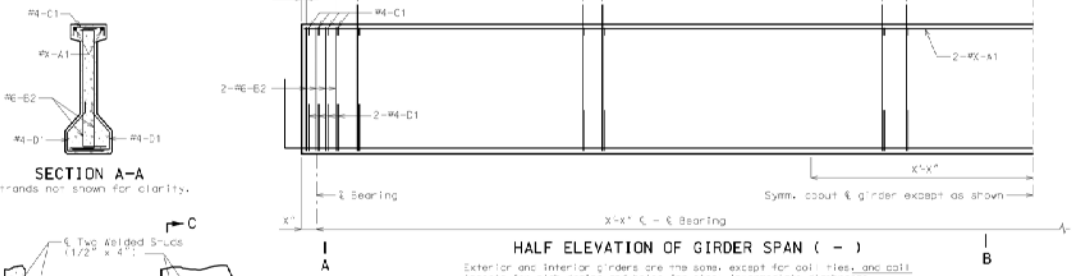

HALF ELEVATION OF GIRDER SPAN (–)

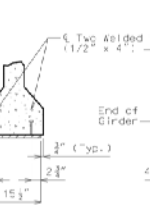

SECTION A-A
Strands not shown for clarity.

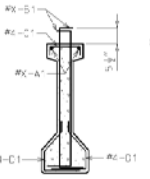

SECTION B-B
Strands not shown for clarity.

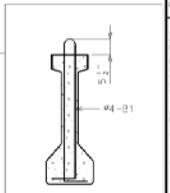

B1 BAR PERMISSIBLE ALTERNATE SHAPE

SECTION C-C PART ELEVATION AT END OF GIRDER

BEARING PLATE DETAILS

Galvanize the 1/2" bearing plate (ASTM A709 Grade 36) in accordance with ASTM A123.

Cost of furnishing, galvanizing, and installing the 1/2" bearing plate (ASTM A709 Grade 36) and welded studs in the prestressed girder will be considered completely covered by the contract unit price for Prestressed Concrete I-Girder.

Exterior and interior girders are the same, except for coil ties, and coil inserts for slab drains and holes for steel intermediate diaphragms.

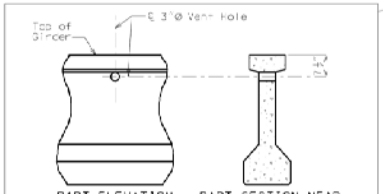

DETAILS OF VENT HOLE

Place vent holes at or near upgrade 1/3 point of girders and clear reinforcing steel or strands by 1" minimum and steel intermediate diaphragm by connectors by 6" minimum.

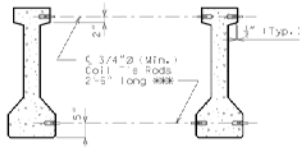

EXTERIOR GIRDERS AT INT. BENTS

EXTERIOR GIRDERS AT END BENTS INTERIOR GIRDERS AT ALL BENTS

DETAILS OF COIL TIES

*** Length of coil tie rods at exterior girders on end bents = 1'-7".

Cost of 3/4"Ø coil tie rods placed in diaphragms will be considered completely covered by the contract unit price for Prestressed Concrete I-Girder.

Coil ties shall be held in place in the forms by slotted wire-setting-studs projecting through forms. Studs are to be left in place or replaced with temporary plugs until girders are erected, then replaced by coil tie rods.

For location of coil inserts at slab drains, see Sheet No. .

For location of coil ties, see Sheets No. & .

The 1 1/2"Ø holes shall be cast in the web for steel intermediate diaphragms. Drilling is not allowed.

For details of diaphragms, see Sheet No. .

For Girder Camber Diagram, see Sheet No. .

Note: This drawing is not to scale. Follow dimensions. Sheet No. of

"THIS MEDIA SHOULD NOT BE CONSIDERED A CERTIFIED DOCUMENT."

DATE PREPARED 11/23/2015

ROUTE	STATE
*	VO
DISTRICT	SHEET NO.
BR	*

COUNTY *

JOB NO. *

CONTRACT ID.

PROJECT NO.

BR DGN NO. GDR 3

DESCRIPTION	DATE

MISSOURI HIGHWAYS AND TRANSPORTATION COMMISSION

MoDOT

105 WEST CAPITOL
JEFFERSON CITY, MO 65102
1-888-ASK-MODOT (1-888-275-6636)

gdr3_type4_3-9.dgn 1:37:33 PM 9/23/2015

APPENDIX F.
MOMENT CURVATURE ANALYSIS

This appendix contains the Moment versus curvature plots for the primary control specimen of Phase one generated using the experimental data and by analyzing the section using Response 2000. It can be observed that the experimental behavior of specimen surpassed the analytical behavior as seen by increased moment capacity. This follows the regular code convention where safety factors are usually used to under estimate the final behavior.

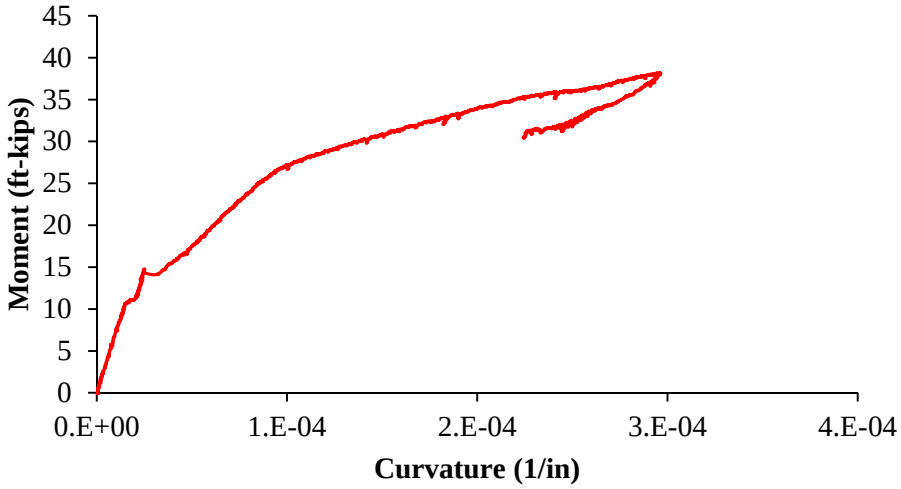

Figure F. 7 Moment versus curvature analysis of experimental data

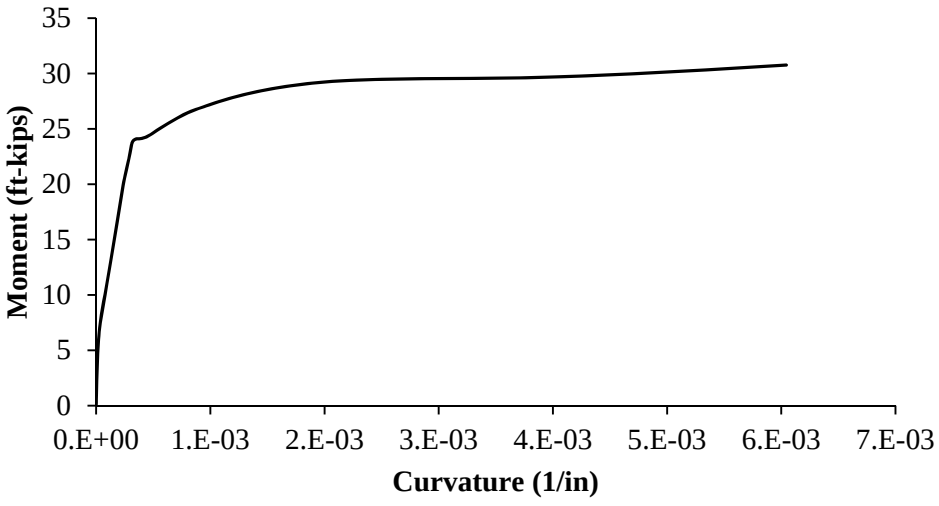

Figure F. 2 Moment versus curvature generated by Response-2000

BIBLIOGRAPHY

AASHTO (American Association of State Highway and Transportation Officials), 2012, LRFD Bridge Design Specifications, 6th edition, Washington, DC.

ACI 318-11, “Building Code Requirements for Structural Concrete and Commentary,” 2011.

ACI Committee 239, “Ultra-High Performance Concrete,” 2011.

ASTM C29, “Standard Test Method for Bulk Density (“Unit Weight”) and Voids in Aggregate,” American Society for Testing and Materials Standard Practice C39, Philadelphia, PA, 2016.

ASTM C39, “Standard Test Method for Compressive Strength of Cylindrical Concrete Specimens,” American Society for Testing and Materials Standard Practice C39, Philadelphia, PA, 2016.

ASTM C70, “Standard Test Method for Surface Moisture in Fine Aggregate,” American Society for Testing and Materials Standard Practice C70, Philadelphia, PA, 2016.

ASTM C117, “Standard Test Method for Materials Finer than 75-µm (No. 200) Sieve in Mineral Aggregates by Washing,” American Society for Testing and Materials Standard Practice C117, Philadelphia, PA, 2016.

ASTM C127, “Standard Test Method for Relative Density (Specific Gravity) and Absorption of Coarse Aggregate,” American Society for Testing and Materials Standard Practice C127, Philadelphia, PA, 2016.

ASTM C128, “Standard Test Method for Relative Density (Specific Gravity) and Absorption of Fine Aggregate,” American Society for Testing and Materials Standard Practice C128, Philadelphia, PA, 2016.

ASTM C136, “Standard Test Method for Sieve Analysis of Fine and Coarse Aggregates,” American Society for Testing and Materials Standard Practice C136 , Philadelphia, PA, 2016.

ASTM C143,”Standard Test Method for Slump of Hydraulic-Cement Concrete,” American Society for Testing and Materials Standard Practice C143, Philadelphia, PA, 2016.

ASTM C230 “Standard specification for Flow Table for Use in Tests of Hydraulic Cement,” American Society for Testing and Materials Standard Practice C230, Philadelphia, PA 2016.

ASTM C469, “Standard Test Method for Static Modulus of Elasticity and Poisson’s Ratio of Concrete in Compression,” American Society for Testing and Materials Standard Practice C469, Philadelphia, Pennsylvania, 2016.

ASTM C566, “Standard Test Method for Total Evaporable Moisture Content of Aggregate by Drying,” American Society for Testing and Materials Standard Practice C566, Philadelphia, Pennsylvania, 2016.

ASTM C496, “Standard Test Method for Splitting Tensile Strength of Cylindrical Concrete Specimens,” American Society for Testing and Materials Standard Practice C496, Philadelphia, Pennsylvania, 2016.

ASTM C1437, “Standard Test Method for Flow of Hydraulic Cement Mortar,” American Society for Testing and Materials Standard Practice C1437, Philadelphia, Pennsylvania, 2016.

ASTM C1611 “Standard Test Method for Slump Flow of Self-Consolidating Concrete,” American Society for Testing and Materials Standard Practice C1611, Philadelphia, PA 2016.

ASTM C1621 “Standard Test Method for Passing Ability of Self-Consolidating Concrete by J-Ring,” American Society for Testing and Materials Standard Practice C1621, Philadelphia, PA 2016.

DiPaolo, B., “Ultra-High Performance Concrete Information and Literature Search -2011 (UHPC I&LS-2011),” Geotechnical and Structures Laboratory, ERDC/GSL SR-11-1, US Army Corps of Engineers, 2011.

Hernandez, E.S., Griffin, A., Myers, J.J., “Construction and Monitoring of sustainable Concrete bridgeA7957 in Missouri, USA,” 23rd Australasian Conference on the Mechanics of Structures and Materials (ACMSM23) Byron Bay, Australia, 9-12 December 2014, S.T. Smith (Ed.).

Federal Highway Administration, list of UHPC Bridges, accessed 2014, https://www.fhwa.dot.gov/research/resources/uhpc/bridges.cfm.

Federal Highway Administration, publications, accessed 2014, https://www.fhwa.dot.gov/research/resources/uhpc/publications.cfm.

Graybeal, B., "Behavior of Field-Cast Ultra-High Performance Concrete Bridge Deck Connections under Cyclic and Static Structural Loading," FHWA, U.S. Department of Transportation, Report No. FHWA-HRT-11-023, National Technical Information Service Accession No. PB2011-101995, 2010.

Graybeal, B., "Development of Non-Proprietary Ultra-High Performance Concrete for Use in the Highway Bridge Sector," FHWA, U.S. Department of Transportation, Report No. FHWA-HRT-13-100, National Technical Information Service Accession No. PB2013-110587, 2010.

Graybeal, B., "Field-Cast UHPC Connections for Modular Bridge Deck Elements," Report no. FHWA-HRT-11-022. Washington, DC: Federal Highway Administration, 2010.

Graybeal, B., "Design and Construction of Field-cast UHPC Connections," Report no. FHWA-HRT-14-084. Washington, DC: Federal Highway Administration, 2014.

Graybeal, B., "Ultra-High Performance Concrete," Report no. FHWA-HRT-06-038. Washington, DC: Federal Highway Administration, 2011.

Graybeal, B., "Ultra-High Performance Concrete connections for precast concrete bridge decks," PCI Journal, 2014.

Graybeal, B., "Construction of Field-Cast Ultra-High Performance Concrete Connections," Report no. FHWA-HRT-12-038. Washington, DC: Federal Highway Administration, 2012.

Griffin, A., Myers, J.J., "Shear Behavior of High-Strength Self-Consolidating Concrete in NU Bridge Girders," Thesis report, Missouri University of Science and Technology, 2014.

Hunt, T., "Sandblasting of Concrete Surfaces," article from Concrete construction.net, The Aberdeen Group, publication #C680449, 1968.

Lafarge North America, Product Data Sheet: Ductal® JS1000, 2009, www.imagineductal.com, accessed 2014.

Lafarge North America, Ductal® Bridge Portfolio of 2011, www.ductal.com, accessed 2014.

Meng, W., Khayat, K., "Experimental and Numerical Studies on Flexural Behavior of Ultra-High Performance Concrete Panels Reinforced with Embedded Glass Fiber-Reinforced Polymer Grids," Transportation Research Record Journal, 2016.

Myers, J.J., Hernandez, E.S., Griffin, A., Hayder, A., “Self-Consolidating Concrete (SCC) and High-Volume Fly Ash (HVFAC) for Infrastructure Elements: Implementation,” Bridge A7957-ROUTE 50, Osage County, Missouri, MoDOT Project TRyy1236, 2014.

Missouri Department of Transportation (MoDOT), Bridge Connection Detail Manual, Jefferson City, Missouri, 2014.

Missouri Department of Transportation (MoDOT), Bridge Standard Drawings http://www.modot.org/business/consultant_resources/bridgestandards.htm, accessed 2014.

Perry, V., and Royce M., “Innovative Field-Cast UHPC Joints for Precast Bridge Decks(Full depth precast panels), Oneonta, NY- Design, Prototype Testing and Construction,” CBC, 2010.

Perry, V., Krisciunas, R., and Stofko. B., “Mackenzie River Twin Bridges North America’s Largest Field-Cast Ultra-High Performance Concrete Connections Project,” PCI Journal, 2014.

Royce, M., “Implementing Ultra-High Performance Concrete for Accelerated bridge Construction in New York,” PCI Journal, 2014.

Russel, H., Graybeal, B., “Ultra-High Performance Concrete: A State-of-the-Art Report for the Bridge Community,” Report no. FHWA-HRT-13-060. Washington, DC: Federal Highway Administration, 2013.

Willey, J., Myers, J.J., “Use of Ultra-High Performance Concrete to Mitigate Impact and Explosives Threats,” CIES Report, Missouri University of Science and Technology, 2013.

Yin, L., “Continuity of Bridge Composed of Simple Span Precast Prestressed Concrete Girders made Continuous,” New Jersey’s Science and Technology University, 2004.